NASA TECHNICAL NOTE

NASA TN D-7744

NASA TN D-7744

AN EXPERIMENTAL AND NUMERICAL STUDY OF WAVE MOTION AND UPSTREAM INFLUENCE IN A STRATIFIED FLUID

by David A. Hurdis

Goddard Space Flight Center
Greenbelt, Md. 20771

NATIONAL AERONAUTICS AND SPACE ADMINISTRATION • WASHINGTON, D. C. • AUGUST 1974

1. Report No.	2. Government Accession No.	3. Recipient's Catalog No.
D-7744		

4. Title and Subtitle	5. Report Date
An Experimental and Numerical Study of Wave Motion and Upstream Influence in a Stratified Fluid	AUGUST 1974
	6. Performing Organization Code: 322
7. Author(s): David A. Hurdis	8. Performing Organization Report No.: G-7440
9. Performing Organization Name and Address: Goddard Space Flight Center, Greenbelt, Maryland 20771	10. Work Unit No.: 502-21-28-01
	11. Contract or Grant No.
	13. Type of Report and Period Covered: Technical Note
12. Sponsoring Agency Name and Address: National Aeronautics and Space Administration, Washington, D.C. 20546	14. Sponsoring Agency Code

15. Supplementary Notes

16. Abstract

A system consisting of two superimposed layers of liquid of different densities, with a thin transition layer at the interface, provides a good laboratory model of an ocean thermocline or of an atmospheric inversion layer. The object of this research was to gain knowledge about the propagation of disturbances within these two geophysical systems. The technique used was to observe the propagation of internal waves and of upstream influence within the density-gradient region between the two layers of liquid. The disturbances created by the motion of a vertical flat plate, which was moved longitudinally through this region, were examined both experimentally and numerically. An upstream influence, which resulted from a balance of inertial and gravitational forces, was observed, and it was possible to predict the behavior of this influence with the numerical model. The prediction included a description of the propagation of the upstream influence to steadily increasing distances from the flat plate and the shapes and magnitudes of the velocity profiles.

17. Key Words (Selected by Author(s)): Fluid mechanics; Stratified fluids; Mathematics/computer programs

18. Distribution Statement: Unclassified–Unlimited

CAT. 12

19. Security Classif. (of this report)	20. Security Classif. (of this page)	21. No. of Pages	22. Price*
Unclassified	Unclassified	88	$4.00

*For sale by the National Technical Information Service, Springfield, Virginia 22151.

PREFACE

The work presented here was completed while the author, now an assistant professor of mechanical engineering at the University of Maryland, was an employee at Goddard Space Flight Center. The material was submitted in May, 1973, to the faculty of the School of Engineering and Architecture, at the Catholic University of America, as a doctoral dissertation.

The author wishes to express his gratitude to Professor H. P. Pao of Catholic University for his guidance throughout the course of this work. In addition thanks are due to Professors Timothy W. Kao and H. Bulent Atabek, also of Catholic University, for their helpful comments. The author's supervisors at GSFC, William W. Auer and Henry Maurer, Jr., showed continuing interest and helpfulness throughout his doctoral studies.

CONTENTS

AN EXPERIMENTAL AND NUMERICAL STUDY OF WAVE MOTION AND UPSTREAM INFLUENCE IN A STRATIFIED FLUID

David A. Hurdis
Goddard Space Flight Center

INTRODUCTION

Wave Propagation in Nonhomogeneous Fluids

The earliest significant study of waves in a nonhomogeneous fluid was that of Stokes (1847), who developed the theory of the propagation of infinitesimal waves in a two-layer fluid system. The excitation of waves in two fluid layers is discussed also by Lamb (1932, Section 231). In essence, it has been shown that for a two-layer fluid, two possible wave systems can exist for any given period of oscillation. One propagates at the free surface of the upper layer, while the other propagates at the interface of the two-layer fluid. Similarly, it can be shown for a three-layer fluid that three wave systems can exist, one for each surface of density discontinuity. In this context, a fluid with a continuous density stratification can be considered to be the limit of an n-layer fluid system as $n \to \infty$; internal waves can be propagated at all levels in such a fluid. A semantic distinction is usually made between waves propagating at the interfaces of a multilayer system and those propagating through a continuously stratified fluid. The former are called interfacial waves, while the latter are referred to as internal waves.

Internal wave propagation in a continuously stratified fluid is characterized by the local Brunt-Vaisala frequency $N = (-g/\rho\ d\rho/dz)^{1/2}$. (For stably stratified fluids, $d\rho/dz \leqslant 0$.) No waves can propagate with frequencies higher than the local value of N, and the direction of propagation of a wave of frequency σ is $\cos^{-1}(\sigma/N)$ from the vertical.

The earliest important experimental work on wave propagation in a nonhomogeneous fluid was published by Ekman (1904), who sought to explain the abnormally high resistance experienced by ships in the mouths of some Norwegian fjords where there is a layer of fresh water over salt water. Ekman demonstrated that the phenomenon is due to increased wave drag resulting from the ship's exciting of waves not only at the free surface but also at the interface of the two layers.

Upstream Influence

Density stratification affects the flow of an inviscid, incompressible fluid in two ways. First, a change in density causes a change in the inertia per unit volume of the fluid. Second, in a gravitational field, a density change causes a change in the body force per

unit volume of the fluid. Since, in general, the body force is not the only force acting on the fluid, these two effects will not nullify each other, and the flow pattern of a nonhomogeneous fluid may differ considerably from that of a homogeneous fluid even though the boundary conditions are the same.

One flow phenomenon exhibited by stratified fluids is upstream influence. This phenomenon occurs during the flow of a stratified fluid past an obstacle, and consists of the propagation of a disturbance upstream from the obstacle. It is especially strong when the obstacle is so wide, in comparison with its height, that the flow past the obstacle is essentially two-dimensional. Upstream influence is also called forward influence or upstream wake in the literature. The limiting case and strongest manifestation of upstream influence occurs in the slow flow of a continuously stratified fluid past an obstacle, and is called blocking. Blocking is the stagnation with respect to an obstacle of the fluid within a horizontal slab containing the obstacle and having the same height as the obstacle. Closed streamline recirculation may occur within the slug of blocked fluid being pushed ahead of the obstacle (Janowitz 1971; Browand and Winant 1972). For very low flow speeds, blocking occurs both upstream and downstream of the obstacle. At higher speeds, the downstream blocking is replaced by a wake and lee waves, and as the speed increases still more, the upstream blocking becomes incomplete and is therefore more properly referred to as upstream influence.

Qualitative explanations for upstream influence may be given from two viewpoints, the buoyancy viewpoint and the internal wave viewpoint.

Buoyancy Viewpoint

As a two-dimensional body moves through a stably stratified fluid, it is necessary for the fluid to be displaced vertically to get by the body. Because of the stable stratification, however, the fluid is reluctant to be displaced vertically, and tends to pile up in front of the body, thus accounting for the upstream influence.

Internal Wave Viewpoint

The upstream influence may also be regarded as the propagation of an internal wave of zero frequency. From the above discussion of internal waves, it is clear that such a wave can propagate from the disturbance source only in a horizontal direction, and that as the wave does so, it causes the presence of the disturbance to be felt far upstream.

Investigations of Upstream Influence

Experimental

The fundamental experiment which established the existence of the phenomenon of upstream blocking in stratified flows was conducted by Long (1955). He studied the flow of a linearly stratified salt solution over a two-dimensional barrier which was towed along

the bottom of a channel. He observed that for values of the internal Froude number ($F_i = U/(g\,\Delta\rho/\rho\,H)^{1/2}$) less than $1/\pi$, a disturbance was propagated upstream from a barrier moving through a fluid of depth H. He noted that for this case his analytical flow predictions became invalid, since they were dependent upon the assumption of undisturbed upstream flow.

More recent experiments have been performed by Pao (1967, 1968), Martin and Long (1968), Debler and Daily (1971), Browand and Winant (1972), and Laws and Stevenson (1972). The common features of these experiments are the use of a linearly stratified salt solution for the working fluid, and use of very slow obstacle speeds. All these investigators have reported upstream influence with a wavy velocity profile, thus confirming the early observations of Long (1955), who reported an upstream velocity profile consisting of alternate jets and stagnation regions.

Theoretical

The problem of stratified flow about an obstacle has also been studied analytically by several investigators. These studies generally have taken one of three theoretical approaches.

The first approach assumes inviscid steady flow everywhere and a uniform velocity profile upstream, includes nonlinear effects, and is generally based on the use of Long's equation; for example, Long (1953). For internal Froude numbers greater than $1/\pi$, good agreement is obtained between theoretical and experimental results. For lower internal Froude numbers, the experiment shows upstream blocking, a condition which violates the theoretical assumption of undisturbed upstream flow. It is therefore not surprising that this approach fails to predict the upstream flow conditions for $F_i < 1/\pi$.

By using the formulation of an inviscid, linearized initial value problem, the second approach permits study of the formation of the blocking column. However, introduction of viscosity into this formulation requires the assumption of a Schmidt number ($Sc = \nu/D$) equal to unity, which is far from accurate for the usual experimental conditions involving salt solutions for which $Sc \approx 800$. This approach is the one used by Bretherton (1967).

The third approach is a steady viscous formulation for very slow, low Reynolds number flows. The fluid is assumed to be nondiffusive, and the low velocity assumption allows the nonlinear inertial terms to be neglected in the flow equations. This formulation is thus a balance of the gravitational and viscous forces. This approach was used by Pao (1967, 1968), who used two-parameter perturbation expansions to solve for the flow field in front of and above a horizontal flat plate. He obtained good agreement with his experiment. Martin and Long (1968) and Brown (1968) have also arrived at solutions that predict upstream disturbance for slow stratified flow past a horizontal flat plate. Graebel (1969) solved for the flow field about a vertical flat plate by means of matched-asymptotic-expansion theory. His solution also predicts the existence of an upstream influence. Janowitz (1971) used an integral transform approach to examine the low Reynold's number flow of a linearly stratified fluid about a vertical flat plate. His solution predicts the existence of

an upstream blocking column within which the fluid recirculates in closed streamlines. The experimental work of Browand and Winant (1972) appears to confirm this result.

In a separate class of theoretical papers, Benjamin (1970), Keady (1971), and McIntyre (1972) have examined the phenomenon of upstream influence from a more abstract viewpoint to determine whether Long's hypothesis of no disturbance far upstream is ever strictly correct. Benjamin concludes that an upstream disturbance exists in the form of a uniform, long wave extending to steadily increasing distances ahead of the body whenever lee waves are present downstream. Keady extended Benjamin's work to the case of interfacial waves in a two-fluid system. McIntyre, whose paper is still the subject of considerable controversy, discusses a kind of upstream influence different from that considered here. His theory predicts an upstream influence related to the formation of lee waves and manifested by an increase in upstream velocity with respect to the body rather than a decrease.

Geophysical Implications

The flow of a stratified ocean or atmosphere over a barrier such as a mountain ridge usually will produce lee waves downstream and blocking upstream. The prevailing west wind flowing over the San Gabriel Mountains east of Los Angeles, for example, produces blocking which makes it more difficult for the region's pollutants to be dispersed.

Background of This Study

Previous studies have dealt with the slow flow about a two-dimensional body of either a linearly stratified fluid or of a two-layer fluid. The linear-density model is an idealization which has proven to be very useful in studies of atmospheric and oceanic flows. In the real atmosphere, however, the near-linear density gradient may be interrupted by one or more inversions; and in the real ocean, a thermocline of one or more sheets is usually present. At these locations, the density undergoes a sudden but nevertheless continuous change, for which neither the linear nor the two-layer model is a valid representation. The real condition is somewhere between these two extremes.

Long referred to this situation in Part III of his well-known trilogy on stratified flows (1955). He suggested that for strong inversions the shock-wave type of phenomena (hydraulic jumps and drops), such as exhibited in the flow of a two-layer fluid over a barrier (Long 1954), would dominate. For weak inversions, he proposed that the flow would behave like the linear model. He concluded, however, that the intermediate case would be highly nonlinear and therefore difficult to solve analytically.

Davis (1967), while doing research for his doctoral dissertation on the stability of oscillatory internal waves, used an experimental model consisting of a layer of fresh water on top of a layer of salt water, with a thin transition region at the interface. He recognized, within the transition layer, the propagation of a new type of solitary wave which had not been reported in the literature. This type of solitary wave was new, in that it could be propagated in a fluid of infinite depth, whereas internal solitary waves were known previously

only as shallow-water phenomena. Davis added an investigation of this new wave to his dissertation (see also Davis and Acrivos 1967). Independently and at about the same time, Benjamin completed a theoretical study in which he predicted the existence of such waves (1967).

Davis's experience suggests that the flow behavior of a stratified fluid in which the density changes suddenly over a short distance cannot necessarily be inferred from previous work on linearly stratified or two-layer fluids. In view of the importance of sudden density changes in geophysical fluids (atmospheric inversions and ocean thermoclines), it was decided to undertake a study of flow about an obstacle by a fluid with a sudden but continuous density change.

Outline of This Study

Experimental

A laboratory flow model consisting of a layer of fresh water on top of a layer of salt water with a thin transition region at the interface was used for this study. A vertical flat plate of 2.54-cm height was towed through the interfacial layer at various speeds and for various density profiles. Upstream and downstream velocity profiles were measured by a flow visualization technique. A conductivity probe was used to determine the density profile before and after each run. In addition to the shape of the density profile, the present work differs from that of most previous experiments in another respect. Those workers whose theoretical work depended upon neglecting the inertial terms in the momentum equation considered only very slow flow speeds in their experiments. The top speed considered by Laws and Stevenson (1972), for example, was only 0.07 mm/s, corresponding to a Reynolds number of O(1) and a Richardson number ($Ri = -g/\rho\, d\rho/dz/(dU/dz)^2$) of $O(10^4)$. For the present study, flow speeds as high as 4 cm/s were examined. The corresponding dimensionless parameters were $Re = O(10^3)$ and $Ri = O(1)$.

Theoretical

The flow conditions described above were formulated as a nonlinear initial-value problem in a viscous diffusive medium. The Boussinesq approximation, which neglects the effect of density variation on the nonlinear inertial terms, was not used. The initial density profile was expressed mathematically by fitting experimental measurements to the equation $\rho = \bar{\rho}\,(1 - \bar{\omega} \tanh \alpha z)$, where $\bar{\omega}$ is a dimensionless constant and α^{-1} is a measure of the thickness of the density-gradient region. Formulation as an initial-value problem permitted theoretical study of the development of the upstream influence. The formulation is analytically intractable, and the problem was therefore solved numerically. Comparison of theoretical upstream velocity profiles with those measured experimentally shows good agreement, but the theory fails to predict the existence of the reverse lee jet which was observed downstream in the density-gradient layer.

THEORETICAL STUDY

Formulation

Dimensionless-flow equations will now be developed for the case of a vertical flat plate of height 2b moving to the right with velocity U through the density-gradient layer of a viscous, diffusive, stably stratified fluid whose initial density profile is of the form $\rho = \bar{\rho}(1 - \bar{\omega} \tanh \alpha z)$. The flow is viewed from a Cartesian coordinate system attached to the plate (see figure 1), and the plate is of infinite extent in the y direction.

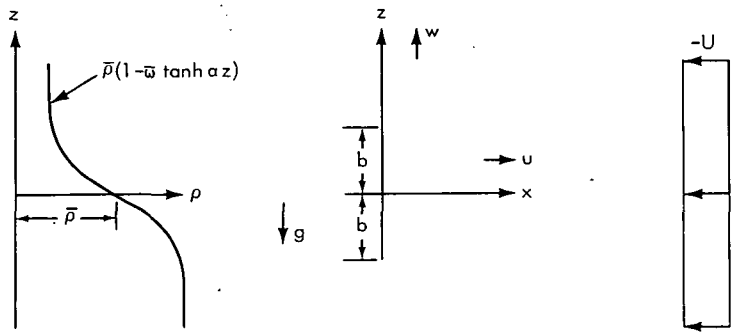

Figure 1. Geometry of the Flow Field

The continuity equation for a diffusive medium is

$$\frac{\partial \rho}{\partial t} + \frac{\partial}{\partial x}(u\rho) + \frac{\partial}{\partial z}(w\rho) = D\nabla^2\rho . \tag{1}$$

The incompressibility equation is

$$\frac{\partial u}{\partial x} + \frac{\partial w}{\partial z} = 0 . \tag{2}$$

Since this equation is not quite correct for the case of a diffusive fluid such as salt water (see Phillips 1969, p. 15), it introduces a slight error to the formulation. The momentum equations are

$$\rho \frac{Du}{Dt} = -\frac{\partial p}{\partial x} + \mu\nabla^2 u \tag{3a}$$

$$\rho \frac{Dw}{Dt} = -\frac{\partial p}{\partial z} - \rho g + \mu\nabla^2 w \tag{3b}$$

where

$$\frac{D}{Dt} \equiv \frac{\partial}{\partial t} + u\frac{\partial}{\partial x} + w\frac{\partial}{\partial z} \qquad \nabla^2 \equiv \frac{\partial^2}{\partial x^2} + \frac{\partial^2}{\partial z^2} .$$

The stream function ψ is defined by

$$u = \frac{\partial \psi}{\partial z}, w = -\frac{\partial \psi}{\partial x} \tag{4}$$

and the y component of the vorticity $\vec{\omega} = \nabla \times \vec{q} = (\xi, \eta, \zeta)$ is

$$\eta = \frac{\partial u}{\partial z} - \frac{\partial w}{\partial x}, \tag{5a}$$

so that by combining (4) and (5a)

$$\nabla^2 \psi = \eta. \tag{5b}$$

Subtracting the x derivative of (3b) from the z derivative of (3a) yields

$$\frac{\partial \rho}{\partial z}\frac{Du}{Dt} - \frac{\partial \rho}{\partial x}\frac{Dw}{Dt} + \rho\left[\frac{\partial \eta}{\partial t} + \frac{\partial}{\partial x}(u\eta) + \frac{\partial}{\partial z}(w\eta)\right] = g\frac{\partial \rho}{\partial x} + \mu\nabla^2\eta. \tag{6}$$

The Boussinesq approximation, which will *not* be made here, consists of neglecting the first two terms on the left side of (6), and replacing the factor ρ in the third term by the average density $\bar{\rho}$.

The boundary conditions for the system (1), (4), (5b), and (6) for $t > 0$ are

$$\text{as } |x|, |z| \to \infty,\ \rho \to \bar{\rho}\ (1 - \bar{\omega}\tanh \alpha z),\ \psi \to -Uz \tag{7a}$$

$$\text{and at } x = 0,\ |z| \leqslant b,\ \frac{\partial \rho}{\partial x} = 0 \tag{7b}$$

$$\frac{\partial \psi}{\partial x} = 0,\ \frac{\partial \psi}{\partial z} = 0. \tag{7c}$$

Since u, w, and η are defined in terms of ψ by (4) and (5b), no independent boundary conditions are possible for these quantities. Although (4), (5b), and (6) can be easily combined into one unwieldy equation, this is not done here, to retain clarity and manipulative ease. The initial conditions are

$$\rho = \bar{\rho}\,(1 - \bar{\omega}\tanh \alpha z) \qquad \text{everywhere at } t = 0 \tag{8a}$$

and

$$\frac{\partial \psi}{\partial x} = \frac{\partial \psi}{\partial z} = 0 \qquad \text{everywhere at } t = 0\,. \tag{8b}$$

With the use of the density scale-length α^{-1} as a characteristic length, U as a characteristic velocity, and $\bar{\rho}$ as a characteristic density, these equations can be put into dimensionless form. Thus

$$(\tilde{x}, \tilde{z}) \equiv \alpha (x, z), \qquad (\tilde{u}, \tilde{w}) \equiv \frac{1}{U} (u, w), \qquad \tilde{\rho} \equiv \frac{\rho}{\bar{\rho}}$$

$$\tilde{t} \equiv U\alpha t, \qquad \tilde{\eta} \equiv \frac{1}{U\alpha} \eta, \qquad \tilde{\psi} \equiv \frac{\alpha}{U} \psi . \tag{9}$$

Equation (1) then becomes

$$\frac{\partial \tilde{\rho}}{\partial \tilde{t}} + \frac{\partial}{\partial \tilde{x}} (\tilde{u} \tilde{\rho}) + \frac{\partial}{\partial \tilde{z}} (\tilde{w} \tilde{\rho}) = \frac{1}{Sc \cdot Re} \tilde{\nabla}^2 \tilde{\rho} \tag{10}$$

where

Sc, Schmidt number = ν/D
Re, Reynolds number = $(U/\alpha\nu)$.

Equation (6) becomes

$$\frac{\partial \tilde{\rho}}{\partial \tilde{z}} \frac{D\tilde{u}}{D\tilde{t}} - \frac{\partial \tilde{\rho}}{\partial \tilde{x}} \frac{D\tilde{w}}{D\tilde{t}} + \tilde{\rho} \left[\frac{\partial \tilde{\eta}}{\partial \tilde{t}} + \frac{\partial}{\partial \tilde{x}} (\tilde{u} \tilde{\eta}) + \frac{\partial}{\partial \tilde{z}} (\tilde{w} \tilde{\eta}) \right] = \frac{1}{F^2} \frac{\partial \tilde{\rho}}{\partial \tilde{x}} + \frac{1}{Re} \tilde{\nabla}^2 \tilde{\eta}, \tag{11}$$

where

F, Froude number = $U/(g/\alpha)^{1/2}$.

Similarly, (4) and (5b) become

$$\tilde{u} = \frac{\partial \tilde{\psi}}{\partial \tilde{z}}, \quad w = \frac{-\partial \tilde{\psi}}{\partial \tilde{x}} \tag{12}$$

and

$$\tilde{\nabla}^2 \tilde{\psi} = \tilde{\eta} . \tag{13}$$

Note that the Froude number appearing in (11) is of the overall form, and is not the internal Froude number, $F_i = U/(g \Delta\rho/\rho H)^{1/2}$, that commonly appears in the formulation of stratified flow problems. This is a result of treating density in the present time-dependent problem as a separate unknown with a separate governing equation rather than combining the density profile into the momentum equation. To facilitate comparison of previous work with the results of this study, internal Froude numbers were computed for the conditions of the experimental runs.

The dimensionless form of the boundary conditions for $\tilde{t} > 0$ is

$$\text{as } |\tilde{x}|, |\tilde{z}| \to \infty, \quad \tilde{\rho} \to (1 - \bar{\omega} \tanh \tilde{z}), \quad \tilde{\psi} \to -\tilde{z} \tag{14a}$$

$$\text{and at } \tilde{x} = 0, \qquad |\tilde{z}| \leq \alpha b, \qquad \frac{\partial \tilde{\rho}}{\partial \tilde{x}} = 0 \tag{14b}$$

$$\frac{\partial \tilde{\psi}}{\partial \tilde{x}} = 0, \qquad \frac{\partial \tilde{\psi}}{\partial \tilde{z}} = 0. \tag{14c}$$

The initial conditions become

$$\tilde{\rho} = (1 - \bar{\omega} \tanh \tilde{z}) \qquad \text{everywhere at } \tilde{t} = 0 \tag{15a}$$

and

$$\frac{\partial \tilde{\psi}}{\partial \tilde{x}} = \frac{\partial \tilde{\psi}}{\partial \tilde{z}} = 0 \qquad \text{everywhere at } \tilde{t} = 0. \tag{15b}$$

Henceforth, the tildes ($\tilde{}$) will be omitted and all variables will be understood to be dimensionless.

Numerical Solution

Algorithm for Solution

The solution of a modified form of (10) through (15) was accomplished by writing them as finite difference equations and solving these on a digital computer according to the following algorithm:

(a) At $t = 0$, the initial conditions (15a) and (15b) exist.

(b) At $t = 0^+$, the flow is irrotational, with $\eta = 0$. The solution for the ψ field is accomplished by making an initial guess of $\psi = -z$ everywhere and then converging to the correct result by overrelaxation of (13), subject to the boundary conditions (14a) and (14c).

(c) The u and w velocity fields at $t = 0^+$ are computed from (12).

(d) Equation (10), subject to the boundary conditions (14a) and (14b), is used to make a time step in the density field.

(e) Equation (11) is used to make a time step in the vorticity field. [The boundary conditions on ψ result in the following conditions on η: as $|x|, |z| \to \infty$, $\eta \to 0$; and at $x = 0$, $|z| \leq \alpha b$, $(u = \partial\psi/\partial z = 0) \Rightarrow \eta = \partial^2 \psi/\partial x^2$].

(f) With the new result for the vorticity field, a new value for the ψ field is computed by overrelaxing (13), subject to (14a) and (14c).

(g) The u and w velocity fields are computed from (12). Steps d, e, f, and g are repeated until a specified time $t = t_f$ has been reached. The computer can be

requested to print out the ρ, ψ, η, u, and w fields at $t = 0^+$, $t = t_f$, and at intermediate times, so that the time development of the flow field can be studied.

As mentioned above, the numerical solution is accomplished with a *modified* form of (10) through (15). The nature of these modifications will now be discussed.

Modification of Nonlinear Boussinesq Terms

Numerical evaluation of nonlinear terms was accomplished by a technique called the special three-point noncentral differences method (Torrance and Rockett 1969). To use this method, it is necessary that nonlinear terms be of the form $\partial (fg)/\partial x$ rather than of the form $g (\partial f/\partial x)$. This is accomplished in the case of the first two terms on the left side of (11) by recalling (2) and adding $u (\partial u/\partial x + \partial w/\partial z)$ to the factor Du/Dt and $w (\partial u/\partial x + \partial w/\partial z)$ to the factor Dw/Dt. Equation (11) then becomes

$$\frac{\partial \rho}{\partial z}\left[\frac{\partial u}{\partial t} + \frac{\partial}{\partial x}(u^2) + \frac{\partial}{\partial z}(uw)\right] - \frac{\partial \rho}{\partial x}\left[\frac{\partial w}{\partial t} + \frac{\partial}{\partial x}(uw) + \frac{\partial}{\partial z}(w^2)\right]$$

$$+ \rho\left[\frac{\partial \eta}{\partial t} + \frac{\partial}{\partial x}(u\eta) + \frac{\partial}{\partial z}(w\eta)\right] = \frac{1}{F^2}\frac{\partial \rho}{\partial x} + \frac{1}{Re}\nabla^2 \eta \,. \tag{16}$$

Stretching the Coordinate System

Previous attempts at numerical solution of similar problems have had difficulty with the application of boundary conditions at infinity. A dilemma is posed by the conflicting requirements of keeping the finite-difference grid mesh fine in the vicinity of the body where the gradients are largest, and at the same time having the last grid point be far enough away from the body that it is an accurate approximation of infinity. One is forced to choose among an overly coarse mesh near the body, or prohibitively large computer core requirements, or an infinity so close to the body that errors are introduced. This problem was circumvented by writing (10) and (12) through (16) with respect to a coordinate system such that its mapping to real-world coordinates has a fine-grid mesh near the origin, a coarser mesh farther away, and a last grid point as close to infinity as desired. This mapping, which involves the hyperbolic tangent function, will now be developed.

The coordinate system sought $(\bar{x}, \bar{z})$ is one whose mapping to ordinary Cartesian coordinates (x, z) is such that as $\bar{x}$ and $\bar{z}$ vary from -1 to $+1$, x and z vary from $-\infty$ to $+\infty$. The transformation for such a system is given by

$$\bar{x} = \tanh ax, \quad \bar{z} = \tanh cz \tag{17}$$

where

$$\frac{d\bar{x}}{dx} = a \cdot \operatorname{sech}^2 ax = a(1 - \tanh^2 ax) = a(1 - \bar{x}^2) \tag{18a}$$

and

$$\frac{d\bar{z}}{dz} = c(1 - \bar{z}^2). \tag{18b}$$

Therefore, for any arbitrary function f,

$$\frac{\partial f}{\partial x} = \frac{d\bar{x}}{dx}\frac{\partial f}{\partial \bar{x}} = a(1 - \bar{x}^2)\frac{\partial f}{\partial \bar{x}} \tag{19a}$$

and

$$\frac{\partial f}{\partial z} = c(1 - \bar{z}^2)\frac{\partial f}{\partial \bar{z}}, \tag{19b}$$

so that from (12)

$$u = \frac{\partial \psi}{\partial z} = c(1 - \bar{z}^2)\frac{\partial \psi}{\partial \bar{z}} = c(1 - \bar{z}^2)\bar{u} \tag{19c}$$

and

$$w = -\frac{\partial \psi}{\partial x} = -a(1 - \bar{x}^2)\frac{\partial \psi}{\partial x} = a(1 - \bar{x}^2)\bar{w}. \tag{19d}$$

Finally

$$\frac{\partial^2 f}{\partial x^2} = a\frac{\partial}{\partial x}\left[(1 - \bar{x}^2)\frac{\partial f}{\partial \bar{x}}\right] = a^2(1 - \bar{x}^2)^2\frac{\partial^2 f}{\partial \bar{x}^2} - 2a^2\bar{x}(1 - \bar{x}^2)\frac{\partial f}{\partial \bar{x}} \tag{19e}$$

and

$$\frac{\partial^2 f}{\partial z^2} = c^2(1 - \bar{z}^2)^2\frac{\partial^2 f}{\partial \bar{z}^2} - 2c^2\bar{z}(1 - \bar{z}^2)\frac{\partial f}{\partial \bar{z}}. \tag{19f}$$

At this point, it is useful to restate the untransformed dimensionless governing equations.

$$\frac{\partial \rho}{\partial t} + \frac{\partial}{\partial x}(u\rho) + \frac{\partial}{\partial z}(w\rho) = \frac{1}{Sc \cdot Re}\nabla^2 \rho \tag{20a}$$

$$\frac{\partial \rho}{\partial z}\left[\frac{\partial u}{\partial t} + \frac{\partial}{\partial x}(u^2) + \frac{\partial}{\partial z}(uw)\right] - \frac{\partial \rho}{\partial x}\left[\frac{\partial w}{\partial t} + \frac{\partial}{\partial x}(uw) + \frac{\partial}{\partial z}(w^2)\right]$$

$$+ \rho\left[\frac{\partial \eta}{\partial t} + \frac{\partial}{\partial x}(u\eta) + \frac{\partial}{\partial z}(w\eta)\right] = \frac{1}{F^2}\frac{\partial \rho}{\partial x} + \frac{1}{Re}\nabla^2 \eta \tag{20b}$$

$$u = \frac{\partial \psi}{\partial z}, \quad w = -\frac{\partial \psi}{\partial x} \tag{20c}$$

$$\nabla^2 \psi = \eta. \tag{20d}$$

Boundary conditions for $t > 0$ are

$$\text{as } |x|, |z| \to \infty, \ \rho \to (1 - \bar{\omega} \tanh z), \ \psi \to -z \tag{20e}$$

$$\text{and at } x = 0, \ |z| \leqslant \alpha b, \qquad \frac{\partial \rho}{\partial x} = 0 \tag{20f}$$

$$\frac{\partial \psi}{\partial x} = 0, \qquad \frac{\partial \psi}{\partial z} = 0. \tag{20g}$$

Initial conditions are

$$\rho = (1 - \bar{\omega} \tanh z) \qquad \text{everywhere at } t = 0 \tag{20h}$$

$$\frac{\partial \psi}{\partial x} = \frac{\partial \psi}{\partial z} = 0 \qquad \text{everywhere at } t = 0. \tag{20i}$$

Substitution of the transformation (19) into the governing equations (20) results in a system of equations which can be put into finite-difference form and solved numerically by the algorithm discussed above. The transformed equations are so lengthy that their presentation has been deferred to appendix 1. The finite-difference form of these equations is given in appendix 2, and the computer program is presented in appendix 3.

At this point, it is appropriate to mention another approximation necessitated by numerical modeling. Although the vertical flat plate used in the experimental study was very thin in the x-direction compared to its height, it was necessary that the numerical model of the plate be at least two x-grid widths thick to avoid instability in the solution caused by singularities at (0, b) and (0, -b). This approximation is not believed to have significantly affected theoretical results upstream, but was found to be responsible for the discrepancy between theoretical and experimental results downstream.

Numerical Results

Figure 2 presents a typical theoretical result for the velocity profiles at four upstream locations at some time, $t = t_1$. Figure 3 shows a typical theoretical prediction for the variation of center line velocity with upstream distance at $t = t_1$. Further information on numerical results will be presented in the section, Discussion of Results, where they are interpreted in the light of experimental findings.

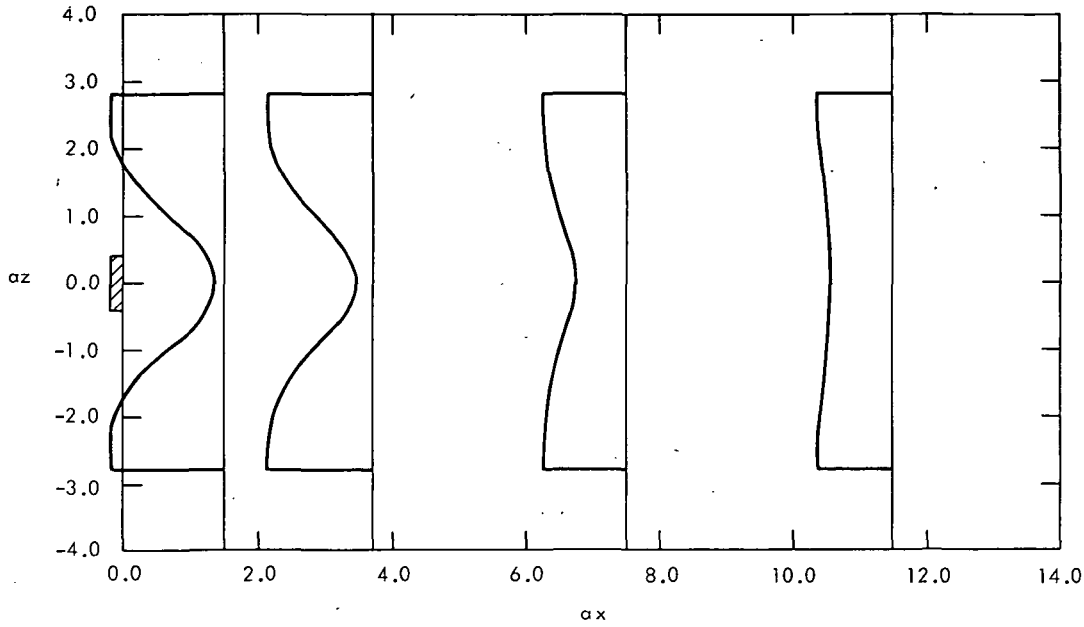

Figure 2. Typical Theoretical Result for Upstream Velocity Profiles

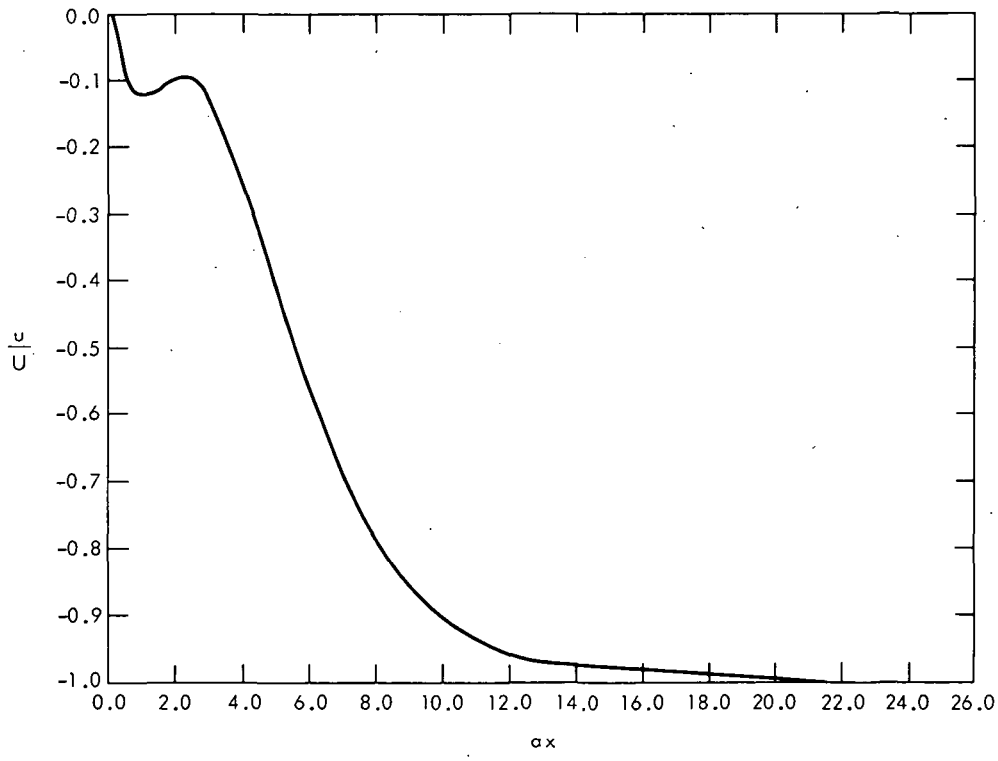

Figure 3. Typical Theoretical Prediction for the Variation of Centerline Velocity with Upstream Position

EXPERIMENTAL STUDY

Description of Experiments

Filling the Channel

The experiments were carried out in a Plexiglass channel 10 m long, 60 cm deep, and 35.5 cm wide. On the day before a set of experimental runs, the channel would be filled to a depth of 23 cm with a uniform salt water solution lightly tinted with nigrosine. To ensure its uniformity, the solution in the channel was thoroughly agitated and then allowed to sit for at least 12 hours. Two salt solution densities were used during this study, 1.013 g/cm^3 and 1.026 g/cm^3. On the day of the experimental runs, a layer of fresh water was slowly floated onto the salt solution until the total fluid depth was 46 cm. This was accomplished by letting the fresh water from the filling hose flow into a sponge rubber basin which was floating on a Styrofoam raft. The water seeped through the sponge, thereby dissipated most of its momentum, and floated with little mixing onto the salt solution. Gradient-layer thicknesses of the order of 4 cm were achieved by this method.

By making certain that the temperature of the inflowing fresh water differed by no more than 2° C from that of the salt water onto which it was floated, convective fluid motions were reduced. These small secondary motions could not be entirely eliminated, however.

Measurement of Density Profiles

Density profiles were measured before and after each run with a conductivity probe. The probe was calibrated with standard salt solutions whose densities had been measured by a hydrometer to an accuracy of ±0.0005 g/cm^3. Density measurements made with the probe are estimated to be accurate to ±0.0005 g/cm^3, while the z elevations for these density measurements have an estimated accuracy of ±0.2 cm. The resulting density profiles were fitted to Benjamin's expression (1967), $\rho = \bar{\rho}\,(1 - \bar{\omega}\tanh \alpha z)$, where $\bar{\rho} = 1/2\,(\rho_u + \rho_\ell)$ = average density of upper and lower layers; $\bar{\omega} = (\rho_\ell - \rho_u)/(\rho_\ell + \rho_u)$; α is a number determined by least-squares fit whose reciprocal is a measure of the gradient thickness, and z is the height above the level at which $\rho = \bar{\rho}$. Figure 4 shows a typical experimentally-measured density profile and the function to which it was fitted. Interestingly enough, it was found that the increase in the gradient layer thickness α^{-1} was very nearly a linear function of the number of transits made through the layer by the vertical flat plate. This relationship is illustrated in figure 5. Since the diffusivity of salt in water is very low, the thickening is almost entirely due to mixing.

Typically, about four experiment runs and four subsequent retrievals of the plate could be made during the course of a day. Approximately an hour was allowed between runs for residual fluid motions to dampen out.

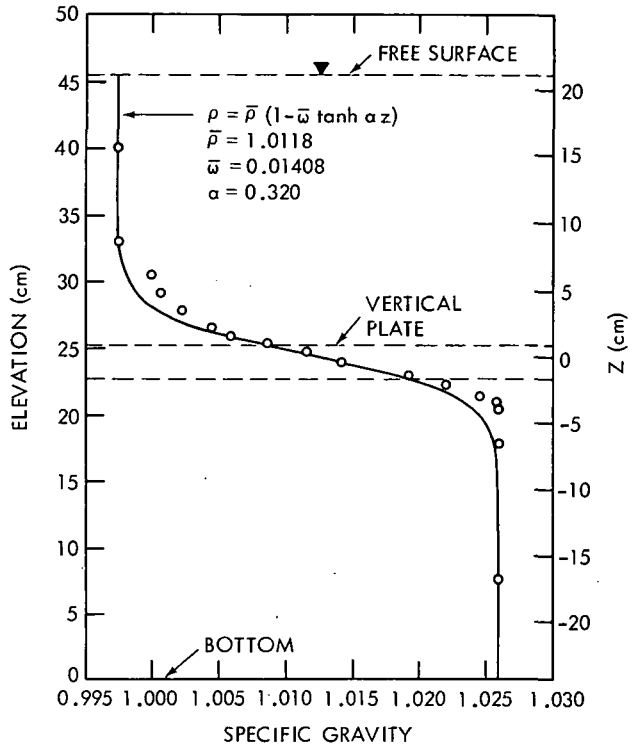

Figure 4. Typical Density Profile—Theoretical and Experimental

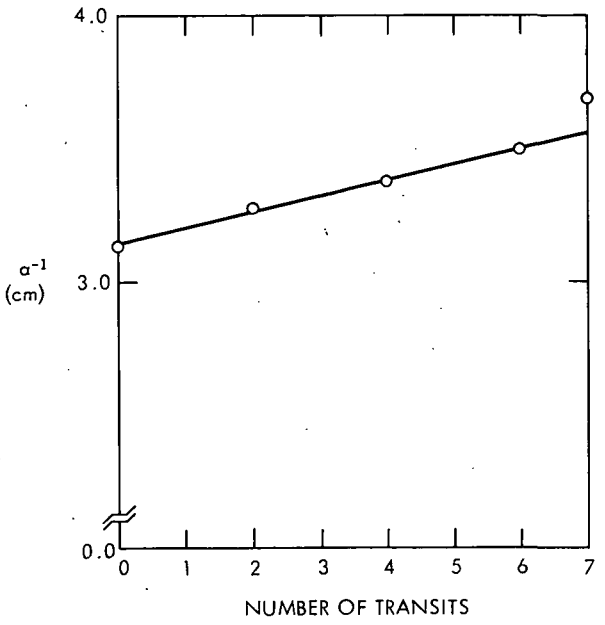

Figure 5. Thickening of the Gradient Layer Caused by Transits of the Vertical Flat Plate

Plate and Towing System

The vertical flat plate was a Plexiglass strip 2.54 cm high, 35.0 cm wide, and 2 mm thick. This was suspended below a carriage by two Plexiglass struts which had been machined to an easy shape to minimize their effect on the flow. The carriage rolled on four double-race ball-bearing roller skate wheels along rails made from aluminum angle. The towing mechanism consisted of a variable-speed motor at one end of the channel and a system of counterweights at the other end. The motor and the counterweights were connected to the carriage over pulleys by size 20 Hygrade flexible fiberglass cord.* Of several types of cords and cables tried, this material proved to be the most satisfactory for minimizing jerkiness in the towing motion. Considerable time was spent in trial and error with the towing system in an attempt to achieve smooth towing motion. Although towing motion was made adequately smooth for the range of plate speeds considered in this study, it was less than adequate at very slow speeds. During an experimental run, the motor was reversed so that the cord unwound from the motor pulley and the counterweight pulled the carriage along the rails. After each run, the plate was retrieved to its original starting position in preparation for the next run. Figure 6 is a schematic drawing of the plate and towing system.

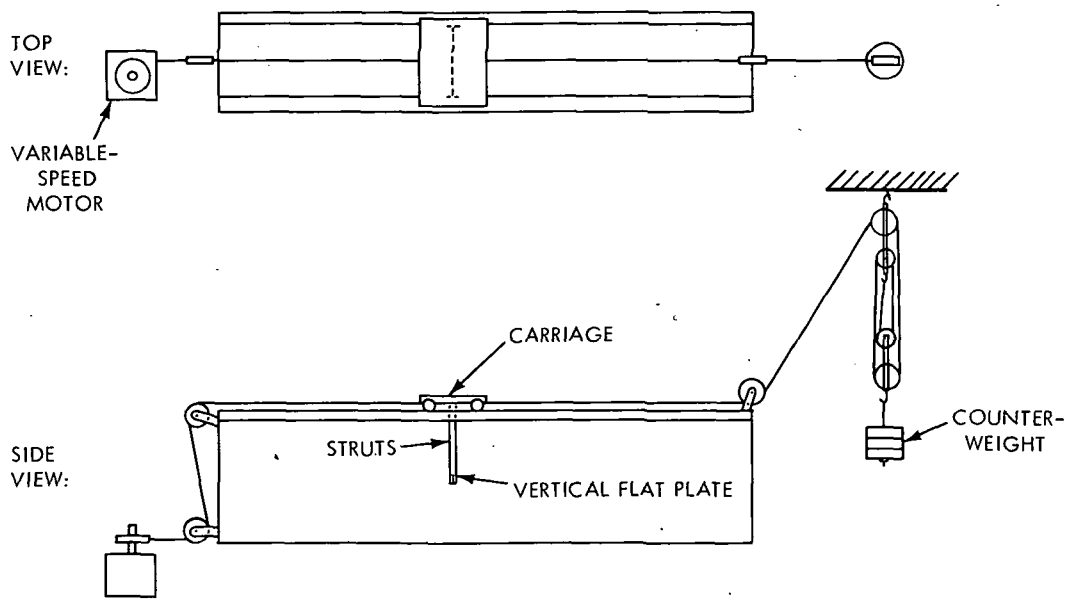

Figure 6. Plate and Towing System

Early in the study, some qualitative experiments were run with two other body shapes: a 2.54 cm-diameter circular cylinder, and a 2.54 cm-thick lenticular cylinder. The vertical flat plate was chosen for all quantitative experiments, because it produced the strongest upstream influence.

* The cord is manufactured by Markel & Sons of Norristown, Pa.

Flow Visualization

Visualization of fluid motion in the gradient layer was aided by injecting droplets of a mixture of carbon tetrachloride, mineral oil, and oil red dye into the upper layer with a syringe and hypodermic needle. The density of the mixture was such that the droplets were neutrally buoyant at the middle of the gradient layer. The syringe and hypodermic needle were required both to control droplet size and to prevent the mixture from being held at the free surface by surface tension. Droplets of a mixture containing toluene instead of mineral oil were tried earlier in the study. That mixture was rejected because of the toxicity of toluene fumes, high volatility of the toluene which made it difficult to control the mixture density, and the mixture's tendency to dissolve and permanently discolor the Plexiglass channel.

In addition to the droplets in the gradient layer, upstream flow visualization was accomplished by the use of vertical dye lines. These dye lines were created by dropping nigrosine dye crystals upstream of the approaching body. Arrival of the upstream disturbance was made visible by the horizontal displacement of the dye lines. When the first set of dye lines became so distorted that accurate measurement of their displacement was no longer possible, a second group of dye crystals was dropped. The second drop created dye lines which made it possible to evaluate the flow in the near upstream vicinity of the plate. Figure 7 is a photograph showing the displacement of dye lines due to the arrival of an upstream disturbance.

Measurement of Upstream Velocity Profiles

Upstream velocity profiles were evaluated by photographing the droplets and dye lines at known time intervals and measuring the displacement which they experienced during those intervals. As figure 7 shows, the displacements were measured with respect to a rectangular grid fixed to the rear wall of the channel. Also visible in the figure is one of the three stopclocks used. These clocks were started simultaneously with the start of the plate towing motor so that they measured the total duration of the run as well as the time intervals between photographs. The clock shown, an Aristo stopclock, measures time in minutes and seconds. Also used, but not shown in the figure, was a larger stopclock (manufactured by the A. W. Haydon Co.) which measures time in seconds and hundredths of seconds. The time intervals between photographs were measured with an accuracy of ± 0.01 seconds.

As shown schematically in figure 8, two cameras with overlapping fields of view were used so that detailed photographs were made of a section of the channel about 125 cm long. Nikon-F cameras were used with 135 mm Nikkor telephoto lenses. Each camera had a motorized shutter release and film advance which made possible short time intervals between successive exposures. Camera motors were connected in parallel to a single switch so that the cameras made simultaneous exposures. The cameras were focused on the midplane of the channel, so that both the rectangular grid and the clocks were in focus.

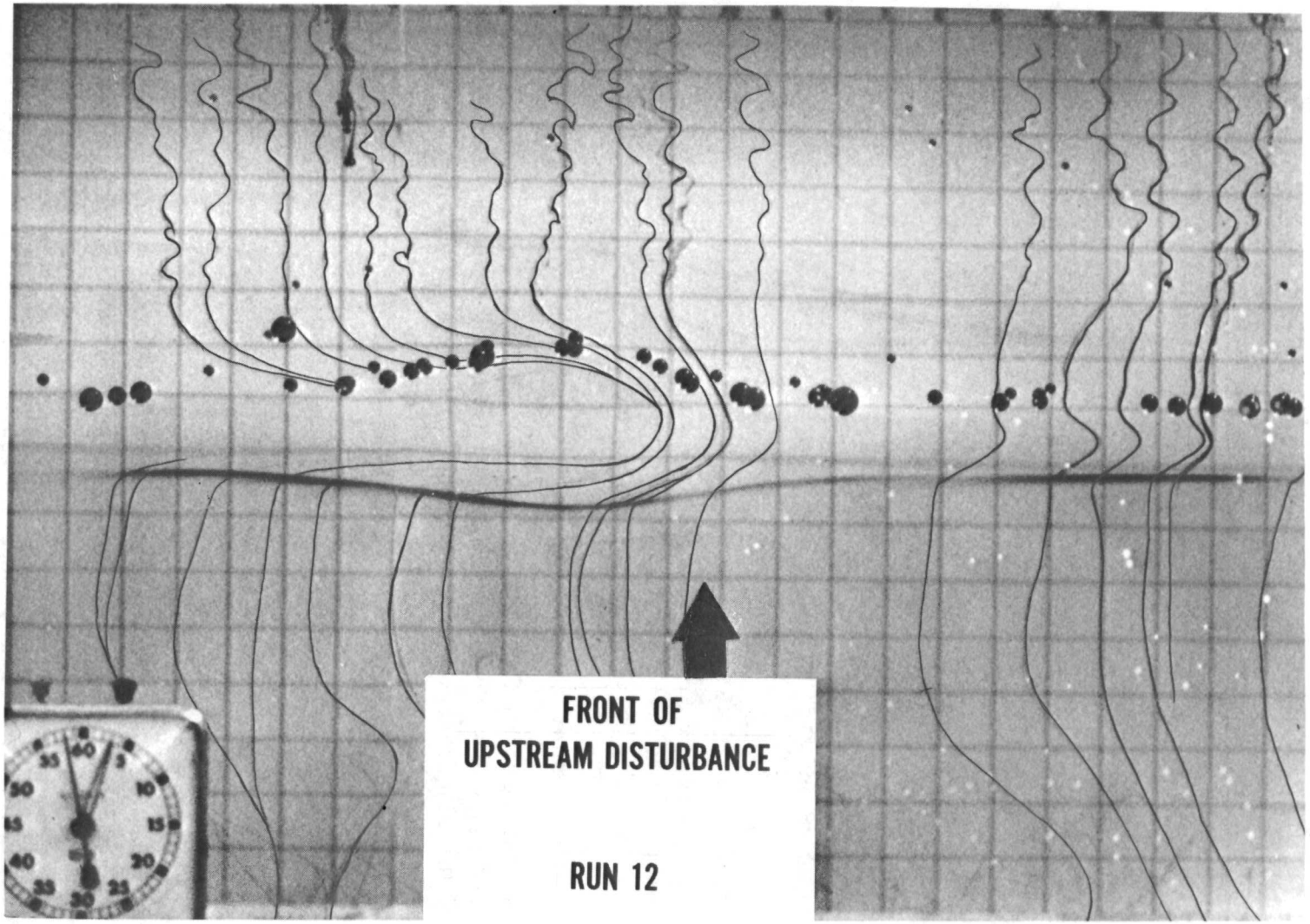

Figure 7. Displacement of Vertical Dye Lines Caused by the Arrival of an Upstream Disturbance

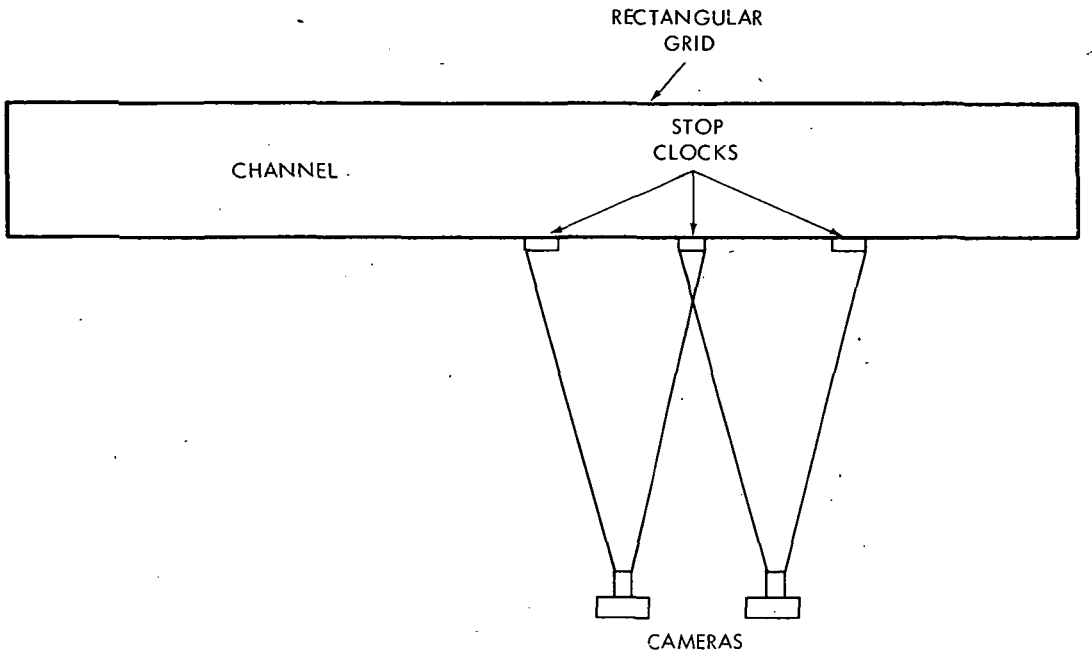

Figure 8. Placement of the Cameras

Typical shutter and aperture settings were 1/250 second at *f*/4.0, using Hi-Speed Ektachrome color film developed for an effective film speed of ASA 400.

Measurement of Downstream Velocity Profiles

The measurement of downstream velocity profiles was considerably less accurate, not only because no dye crystals were dropped there, but also because the mixing in the wake combined with the sudden change of index of refraction in the gradient region to cause such optical distortion that accurate displacement measurements were impossible. By observing the motion of the oil droplets, however, qualitative assessments of the downstream flow could be made. The most striking feature of the downstream flow was the presence of a reverse jet in the gradient layer, which carried oil droplets about 75 cm downstream with respect to the fixed cameras before dissipating. This reverse jet is discussed in the section, Discussion of Results.

Measurement of Body Speed

The speed of the vertical flat plate was determined by two methods. By stopping the towing motor and the clocks simultaneously at the completion of a run, the body speed could be computed directly from the length and duration of the run. Secondly, the body speed could be computed as the slope of a straight line determined from a least-squares fit of photographically recorded body positions and elapsed times. Excellent agreement was obtained between the two methods.

Measurement of Speed of Disturbance Front

The least-squares method was also used to determine the propagation speed of the front of the upstream disturbance.

Parameters for Experimental Runs

Table 1 lists values of the density and flow parameters for the ten quantitative experimental runs. Data from the last six runs are considered most reliable.

Table 1

Flow Parameters for Experimental Runs

Run	Density Profile $\rho = \bar{\rho}(1 - \bar{\omega}\tanh\alpha z)$				Body Speed	Reynolds Number	Froude Number	Brunt-Vaisala Frequency at z=0	Richard-son Number at z=0	Internal Froude Number
	$\bar{\rho}$	$\bar{\omega}$	α	α^{-1}	U	Re	F	N	Ri	F_i
	(g/cm^3)	$\frac{\rho_\ell - \rho_\mu}{\rho_\ell + \rho_\mu}$	(cm^{-1})	(cm)	(cm/s)	$\frac{U}{\alpha\nu}$	$\frac{U}{(g/\alpha)^{1/2}}$	(s^{-1})	$\frac{N^2}{(U\alpha)^2}$	$\frac{1}{(Ri)^{1/2}}$
13	1.0053	0.00771	0.50	2.00	3.18	672.	0.0718	1.94	1.49	0.818
14	1.0053	0.00771	0.48	2.07	1.95	429.	0.0432	1.90	4.14	0.492
16	1.0127	0.01417	2.44	0.41	1.94	84.	0.0968	5.82	1.51	0.813
17	1.0127	0.01417	1.09	0.92	3.80	368.	0.1268	3.89	0.88	1.065
19	1.0127	0.01417	0.73	1.37	2.60	376.	0.0710	3.18	2.81	0.596
20	1.0127	0.01417	0.65	1.54	2.60	422.	0.0670	3.00	3.16	0.563
21	1.0118	0.01408	0.32	3.13	3.31	1092.	0.0598	2.10	3.94	0.504
22	1.0118	0.01408	0.31	3.28	3.16	1094.	0.0558	2.05	4.53	0.470
23	1.0118	0.01408	0.30	3.38	4.08	1456.	0.0709	2.02	2.80	0.598
24	1.0118	0.01408	0.29	3.51	4.15	1538.	0.0708	1.98	2.81	0.597

DISCUSSION OF RESULTS

Qualitative Description of Observed Flow

Figure 9 is a schematic drawing which shows the type of flow observed to be caused by the motion of a vertical flat plate in a region of sudden density variation.

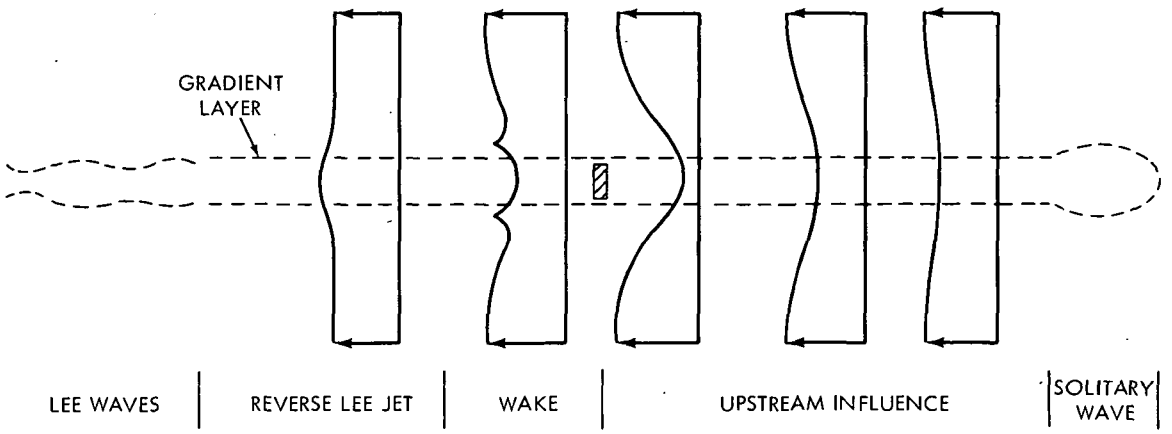

Figure 9. Schematic Drawing of the Type of Flow Phenomena Induced by the Motion of a Vertical Flat Plate in a Region of Sudden Density Variation

At the front of the upstream disturbance an internal solitary wave of the type predicted by Benjamin (1967) and observed by Davis (1967) was always present. Behind the solitary wave was a region of upstream influence. This upstream influence did not take the form of complete blocking such as has been observed in the very slow motion of bodies through stratified fluids. Nevertheless, a strong upstream wake was observed in the gradient layer. (The solitary wave and the upstream influence when discussed together are called here the upstream disturbance.) Both the solitary wave and the upstream influence propagated upstream to steadily increasing distances in front of the plate. This is consistent with the internal wave concept of upstream influence, discussed in the Introduction. The connection, if any, between the upstream influence and the solitary wave is not entirely clear. Present indications are, however, that the solitary wave is a distinct phenomenon generated by the impulsive start of plate motion.

As shown also in figure 9, the upstream flow in the fresh- and salt-water layers was opposite in direction to that in the gradient layer.

The downstream flow observed in the gradient layer was somewhat surprising. Nearby the body, the flow looked like ordinary wake flow. About 10 cm downstream, however, a reverse jet was observed to carry oil droplets downstream not only with respect to the moving plate, but also with respect to the fixed cameras. The following explanation is suggested: The observed upstream influence did not take the form of complete blocking, and some upstream fluid was sufficiently displaced vertically that it cleared the plate. After passing the plate, the stratified fluid rushed back to its position of neutral buoyancy.

In doing so, it accumulated a residual rearward momentum manifested in the form of the observed lee jet.

The reverse lee jet dissipated about a meter downstream where it was replaced by a system of lee waves in which the oil particles, as seen by the fixed cameras, simply orbited in closed paths.

Examination of the Internal Solitary Wave

Figure 10 is a photograph showing the propagation of an internal solitary wave from left to right ahead of the upstream influence which is in turn ahead of the vertical flat plate.

Comparison With Theory

The solitary waves which were observed in this study to head the upstream disturbance have been examined in the light of the work of Benjamin (1967) and Davis and Acrivos (1967).

Benjamin predicted that for a region whose density profile is described by $\rho = \bar{\rho}\ (1 - \bar{\omega}\ \tanh \alpha z)$, an infinitesimal solitary wave of the first mode would propagate with the speed $c_{sw}^0 = (g\bar{\omega}/2\alpha)^{1/2}$. A wave with finite amplitude a is predicted to propagate with the speed

$$c_{sw} = c_{sw}^0 \left(1 + \frac{3}{5}\alpha a\right)^{1/2}. \tag{21}$$

In the present study, the speed c_{sw} could be determined accurately from photographs by the least-squares method (see the section, Experimental Study). Thus, it was possible to compare Benjamin's theory with experimental results by measuring the observed solitary wave amplitudes, using (21) to predict wave speeds, and comparing these predictions with experiment. For the purpose of these measurements, the amplitude was defined as the maximum vertical displacement of the streamline at $z = \alpha^{-1}$. The results of the comparison are presented in table 2.

Considering the crudeness of the experimental amplitude measurements, the agreement between the last two columns of table 2 is quite good.

A correlation between the dimensionless amplitude, $a\alpha$, and the dimensionless group $\lambda = g/2\alpha c_{sw}^2\ \ell n\ (\rho_\ell/\rho_u)$ is predicted by Davis's theory. Moreover, for small values of $a\alpha$, the relation $\lambda = 2.0 - 1.2\ a\alpha$ is predicted to be a good approximation to this correlation. Figure 11 is a plot of λ vs $a\alpha$ for the solitary waves observed in the present study. The theoretical predictions of both Davis and Benjamin are plotted in the same figure. The agreement between these theories and the results of the present experiment is quite good. Since the theories have nothing to do with upstream influence, this agreement indicates that the observed solitary waves are generated by the impulsive start of plate motion and are independent of the existence of upstream influence.

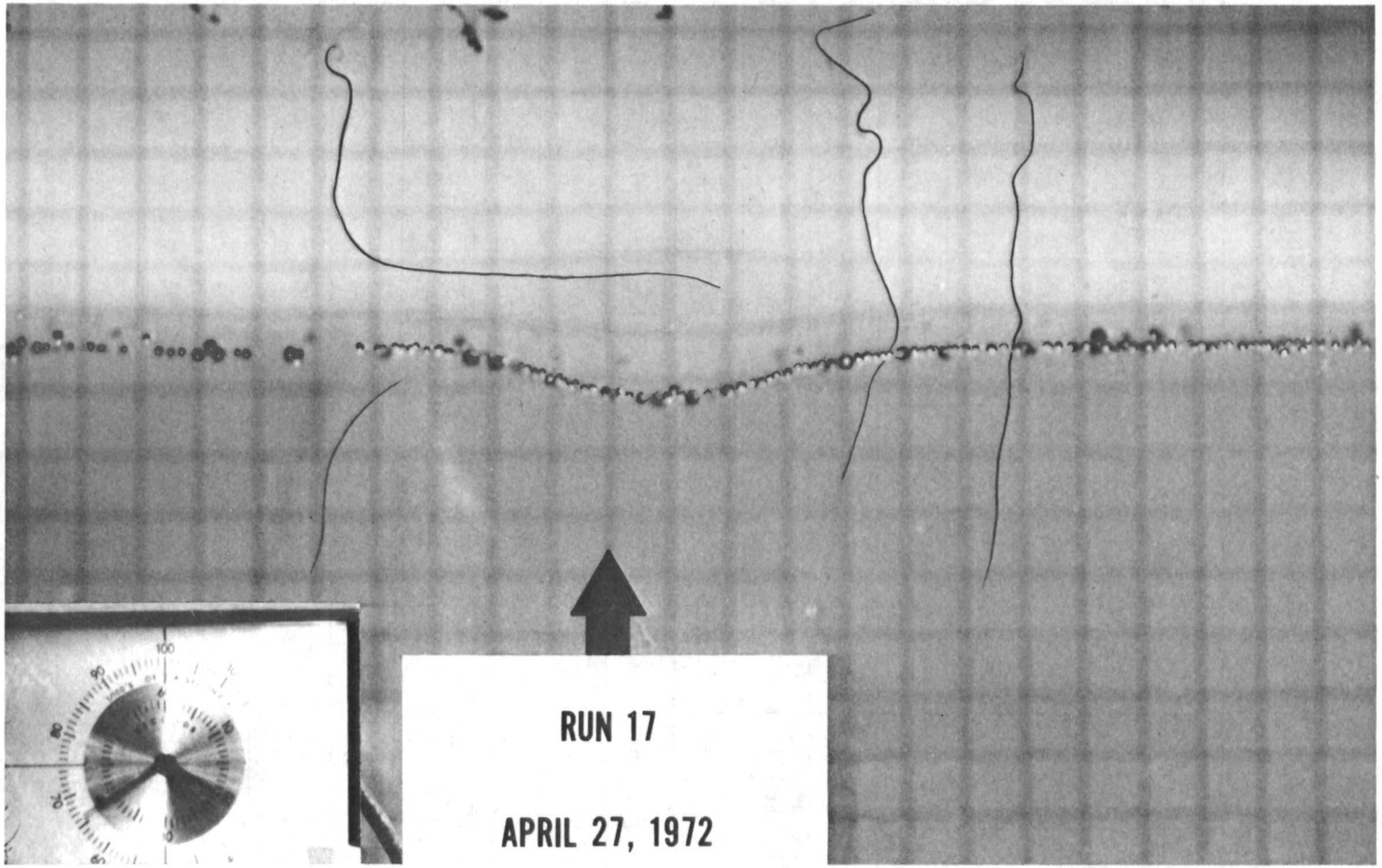

Figure 10. Propagation of an Internal Solitary Wave from Left to Right Ahead of the Vertical Flat Plate

Table 2

Comparison of Benjamin's Predictions for
Internal Solitary-Wave Speed With
Experimental Measurements

Run	$\bar{\omega}$	α (cm^{-1})	$c_{sw}^0 = \left(\frac{g\bar{\omega}}{2\alpha}\right)^{1/2}$ (cm/s)	Measured Amplitude a (cm)	Measured Wave Speed c_{sw} (cm/s)	Calculated Wave Speed c_{sw} [Equation (21)] (cm/sec)
13	0.00771	0.50	2.75	2.5	3.73	3.64
14	0.00771	0.48	2.81	0.6	2.95	3.04
16	0.01417	2.44	1.69	1.5	3.18	3.02
17	0.01417	1.09	2.52	2.8	4.75	4.24
19	0.01417	0.73	3.08	1.8	4.11	4.12
20	0.01417	0.65	3.27	1.3	4.06	4.01
21	0.01408	0.32	4.64	0.0	4.62	4.64
22	0.01408	0.31	4.72	0.0	4.65	4.72
23	0.01408	0.30	4.80	0.6	5.02	5.05
24	0.01408	0.29	4.88	0.6	5.05	5.13

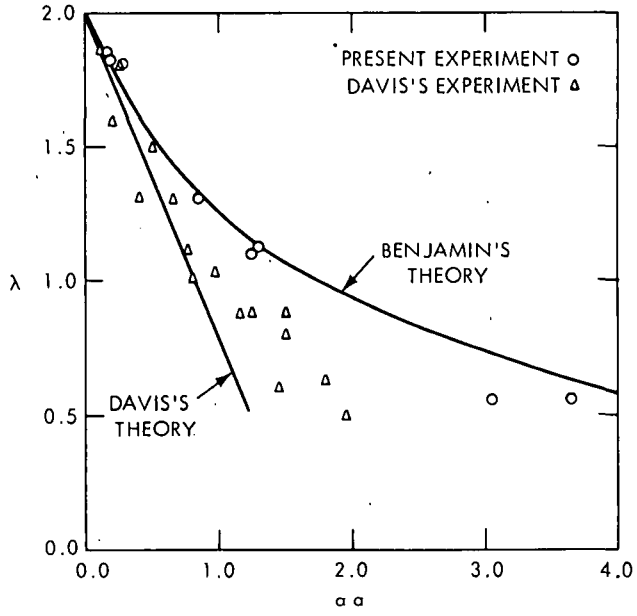

Figure 11. Correlation of the Parameter λ with the Dimensionless Amplitude αa for Observed Solitary Waves and Theoretical Predictions of Benjamin and Davis

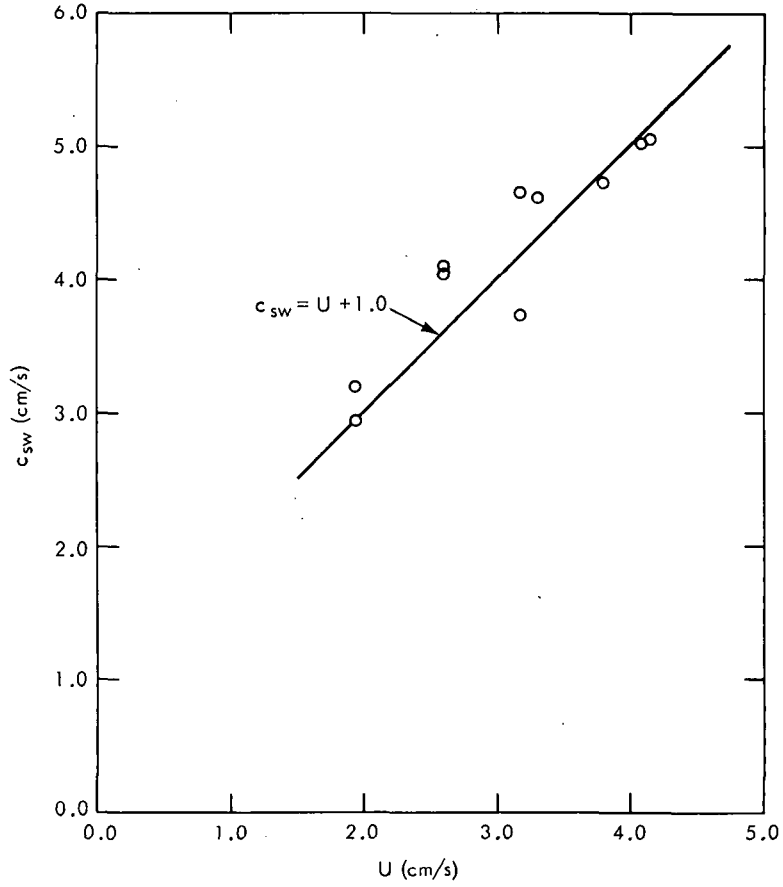

Figure 12. Correlation of Solitary Wave Speed c_{sw} with Plate Speed U

Correlation of Plate Velocity and Wave Speed

A plot of solitary wave speed c_{sw} versus plate speed U appears in figure 12. The correlation between these two quantities is close enough to suggest a contradiction with the above conclusion that the solitary wave is independent of the existence of upstream influence. This writer suggests, however, that the correlation shown in figure 12 is quite indirect: that wave speed c_{sw} depends on the wave amplitude a, which depends on the strength of the starting impulse of the plate and on the speed U for which the towing motor is set when it is switched on.

The results are therefore not as clear as one might wish, but the bulk of the evidence seems to indicate that the initially generated solitary wave and the upstream influence do not interact.

Examination of Upstream Influence

Brunt-Vaisala Frequency

Now, recall from the Introduction the significance to the propagation of internal waves of the Brunt-Vaisala frequency $N = (-g/\rho\ d\rho/dz)^{1/2}$. It was noted that:

(a) For stably stratified fluids, $d\rho/dz \leqslant 0$, so that $N \geqslant 0$.

(b) No internal wave can be propagated with frequency higher than the local value of N.

(c) The direction of propagation of a wave of frequency σ is $\cos^{-1}(\sigma/N)$ from the vertical.

Finally, it was pointed out that one may consider upstream influence to be the propagation of an internal wave having zero frequency, and that the direction of propagation of such a wave would be horizontal.

Figure 13 is a plot of N versus elevation αz for a typical density profile of the type considered in this study. Note that N reaches its maximum at the center line $\alpha z = 0$ and drops off rapidly to zero at short distances above and below the centerline. The significance of this is that any wave having a frequency σ such that $0 < \sigma < N$ would propagate in an increasingly vertical direction as it left the centerline, but could not propagate beyond the elevation at which $\sigma = N$. Thus, such waves would be trapped within the gradient layer and after multiple reflections would eventually die out. The waves with higher frequencies would be reflected more often and would tend to die out faster.

Phase Velocity of the Upstream Influence

Experimental measurement of the propagation speed c_{ui} of upstream influence was not possible in this study due to the presence of the solitary wave. It was not clear where the disturbance caused by the solitary wave ended and where the front of the upstream

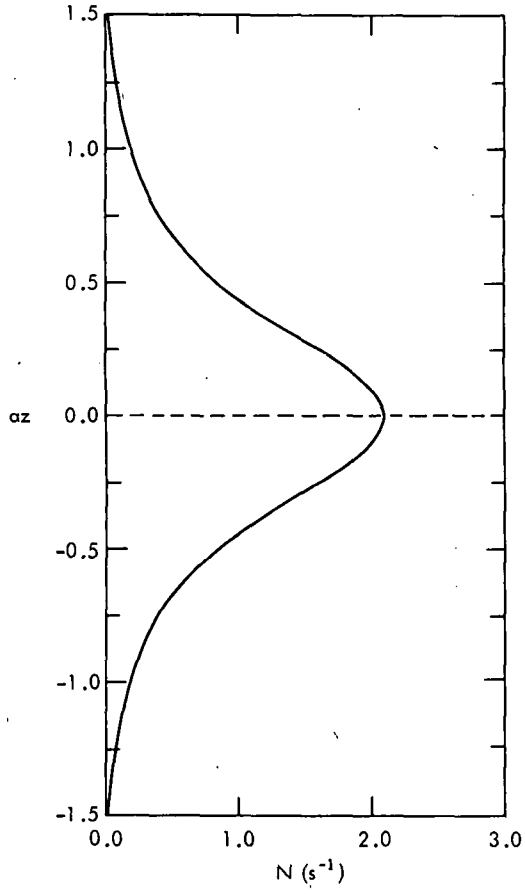

Figure 13. Brunt-Vaisala Frequency N as a Function of Elevation above Centerline in a Region of Sudden Density Variation

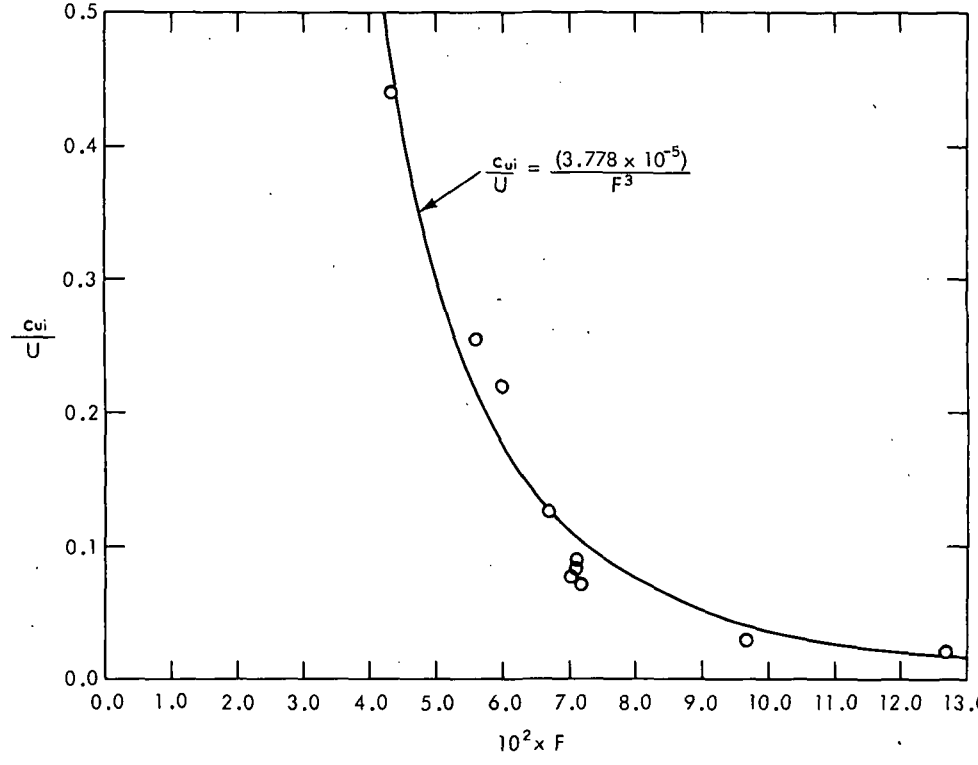

Figure 14. Correlation of Predicted Upstream-influence Propagation Speed c_{ui} with Froude Number F

influence began. Moreover, the velocity profiles were not observed over a time interval long enough to permit experimental evaluation of their variation with time. A phase velocity for the upstream influence could be determined, however, from the results of the numerical study. Since, as will be shown later, the numerical solutions successfully predicted upstream velocity profiles as a function of time and position, the determination of c_{ui} from these solutions is thought to be quite reliable. Table 3 presents these results. In figure 14, c_{ui}/U is plotted as a function of the Froude number $F = U/(g/\alpha)^{1/2}$.

Suggested Relationship Between c_{ui} and Group Velocity of Infinitesimal Internal Waves

The i^{th} component of the group velocity of an infinitesimal internal wave of frequency σ and wave number vector $\vec{k}$ is $(c_g)_i = \partial\sigma/\partial k_i$, i = 1, 2, 3. The relationship $\sigma = \sigma(k_i)$ between frequency and wave number is called the dispersion relation, and is obtained from the analytic solution of an eigenvalue problem formulated from the equations of motion for a stratified fluid with appropriate boundary conditions (see Phillips 1969, pp. 161-165). Phillips points out that for the general case in which the Brunt-Vaisala frequency is an arbitrary function of z, simple analytic solutions to the eigenvalue problem are not possible. For the present study, $N(z) = (g\bar{\omega}\alpha)^{1/2}$ sech αz (see figure 13), and the solution of the eigenvalue problem is such a formidable task that it has not been attempted here. Nevertheless, it is tempting to suggest that the speed c_{ui} is related to the group velocity of infinitesimal internal waves. The existence of such a relationship is suggested by the results of Kao, Pao, and Wei (1972), who found that when a linearly stratified fluid in a channel suddenly begins to discharge into a line sink, a disturbance propagates upstream from the sink with velocity equal to the group velocity of internal gravity waves of zero horizontal wave number. In view of the analogy between rotating and density stratified flows, a relationship between c_{ui} and group velocity is also suggested by the study of Benjamin and Barnard (1964). They found that the motion of a cavity in a rotating fluid induced an upstream disturbance which propagated at the maximum group velocity for infinitesimal traveling waves. Confirmation of the existence of such a relationship for the conditions of this study will await the solution for the dispersion relation.

Comparison of Observed Upstream Influence With Predictions of Janowitz and Experiments of Browand and Winant

The Introduction mentioned the theoretical study by Janowitz (1971) of the slow motion of a vertical flat plate of height 2b in a linearly stratified fluid. This study, whose results are valid when $1/Ri \ll Re \ll 1$, predicts a steady-state, upstream blocking column of length 10^{-2} b (Re · Ri) composed of cells of closed streamlines. The experiments of Browand and Winant (1972) appear to confirm the prediction of a region of recirculating flow upstream.

In the present study, the body speeds were much higher, with Ri = O(1) and $Re \gg 1$. Upstream influence was definitely present, but not in the extreme form of complete blocking. Nevertheless, it is instructive to calculate the slug lengths 10^{-2} b (Re · Ri) for the conditions observed. These are presented in table 4.

Table 3

Propagation Speed of Upstream Influence

Run	Body Speed U (cm/s)	Froude Number F $U/(g/\alpha)^{1/2}$	Solitary Wave Speed c_{sw} (cm/s)	Propagation Speed of Upstream Influence c_{ui} (cm/s)	c_{ui}/U
13	3.18	0.0718	3.73	0.225	0.071
14	1.95	0.0432	2.95	0.857	0.440
16	1.94	0.0968	3.18	0.058	0.030
17	3.80	0.1268	4.75	0.080	0.021
19	2.60	0.0710	4.11	0.216	0.083
20	2.60	0.0670	4.06	0.325	0.125
21	3.31	0.0598	4.62	0.724	0.219
22	3.16	0.0558	4.65	0.800	0.253
23	4.08	0.0709	5.02	0.354	0.087
24	4.15	0.0708	5.05	0.324	0.078

Table 4

Length of Upstream Blocking Column as Predicted by the Janowitz Formula for Present Experiments

Run	13	14	16	17	19	20	21	22	23	24
10^{-2} b (Re · Ri) (cm)	3.0	5.0	48.	11.	11.	10.	4.0	4.0	3.0	3.0

These results confirm that Janowitz's theory is indeed inapplicable to this study, for no recirculating flow of the type described was observed within the predicted distances of the plate. Had such closed streamline flow been present, the oil droplets and dye lines would surely have revealed it.

Influence of the End Wall

Another way in which this study differs from the experiment of Browand and Winant is that it was unnecessary to correct the data for the finite length of the channel. The front of the upstream disturbance was still several meters from the end wall when the velocity profile photographs were taken.

Theoretical and Experimental Results for Upstream Flow Field

The upstream velocity profiles predicted by the numerical study (see section, Theoretical Study) will now be compared with the experimental results. Figures 15 and 16 present the results for two typical experimental runs together with the corresponding theoretical results. Profiles of dimensionless velocity with respect to the plate, u/U, are shown at four upstream locations. Agreement between theory and experiment is excellent in the gradient layer. Theoretical flow velocities in the homogeneous layers are in good qualitative agreement with the experimental, although the predicted velocities are somewhat greater than those actually observed.

Figures 17 and 18 show theoretical and experimental results for the variation of centerline ($z = 0$) velocity with upstream position, αx. Here again, the agreement between theory and experiment is excellent. Shown on the same plots are the predictions for upstream-velocity variation for potential flow. These plots show that the upstream velocity variation is somewhat like potential flow in the immediate vicinity of the plate, but rapidly deviates from this idealization for $\alpha x > 0.5$.

Finally, these experimental results are compared with the theoretical predictions of Janowitz in figure 19, where dimensionless centerline velocity with respect to the plate, u/U, is plotted versus $|x/L^3|^{1/4}$. The quantity L, which Janowitz defines as $L \equiv b/(U\nu/\beta g)^{1/3}$, can be expressed in terms of the parameters used in the present study as follows:

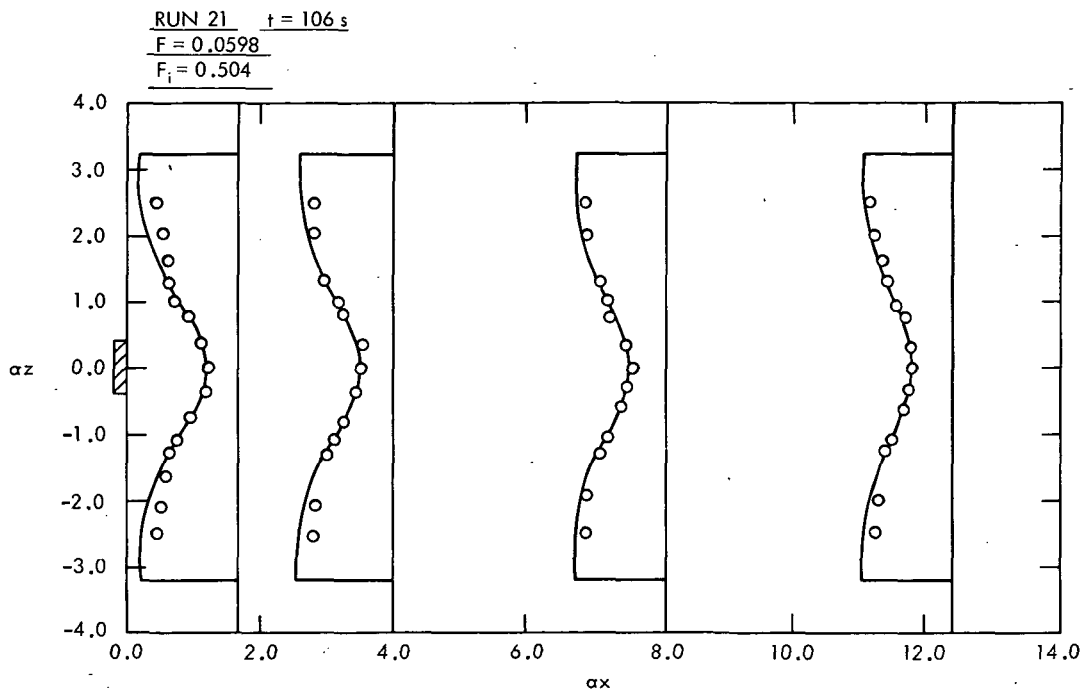

Figure 15. Theoretical and Experimental Results for Upstream Velocity Profiles, Run 21

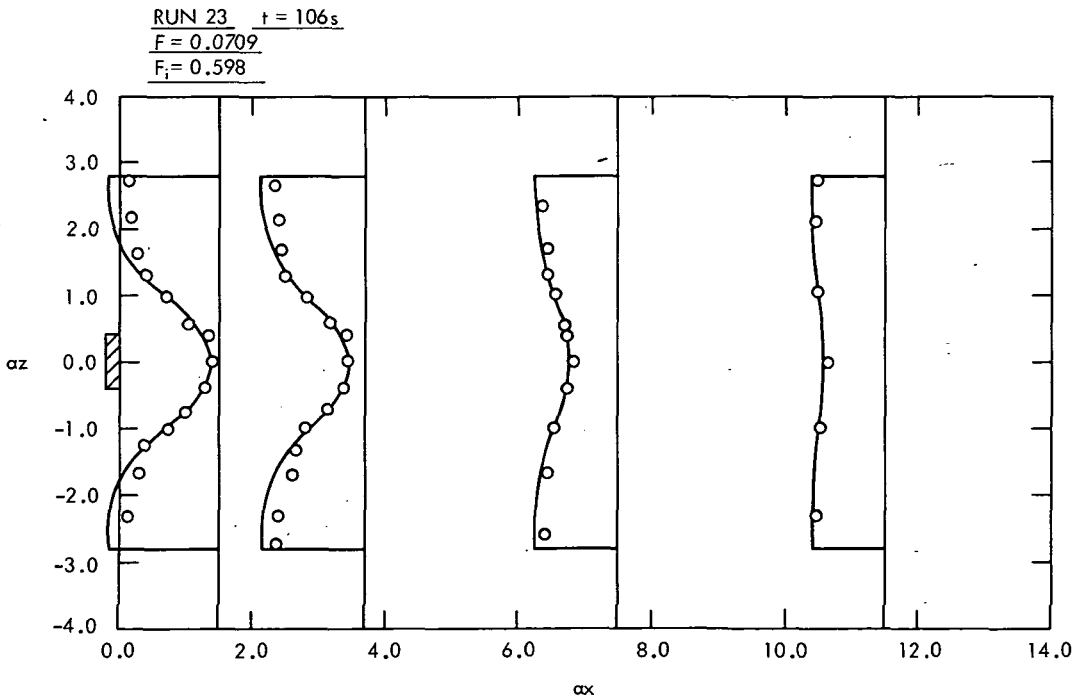

Figure 16. Theoretical and Experimental Results for Upstream Velocity Profiles, Run 23

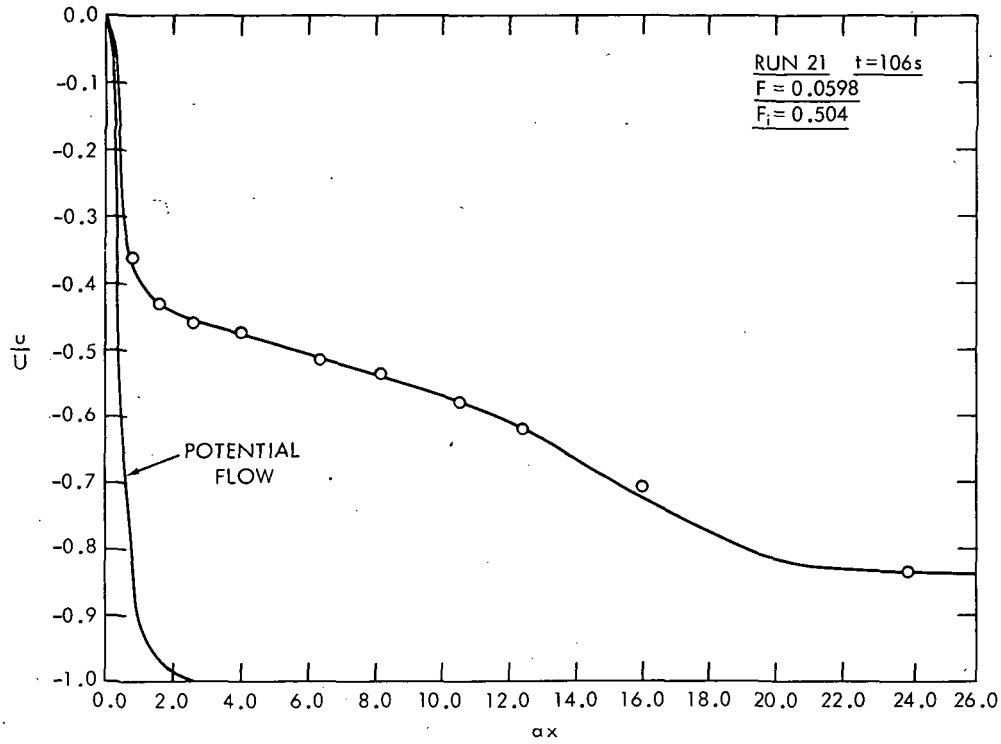

Figure 17. Theoretical and Experimental Results for the Variation of Centerline Velocity with Upstream Position, Run 21

Janowitz considered the density profile

$$\rho = \bar{\rho}(1 - \beta z) \tag{22a}$$

from which

$$\frac{d\rho}{dz} = -\bar{\rho}\beta . \tag{22b}$$

This study has considered

$$\rho = \bar{\rho}(1 - \bar{\omega} \tanh \alpha z) \tag{23a}$$

for which

$$\frac{d\rho}{dz} = -\bar{\rho}\bar{\omega}\alpha \operatorname{sech}^2 \alpha z \tag{23b}$$

or, at z = 0

$$\frac{d\rho}{dz} = -\bar{\rho}\bar{\omega}\alpha . \tag{23c}$$

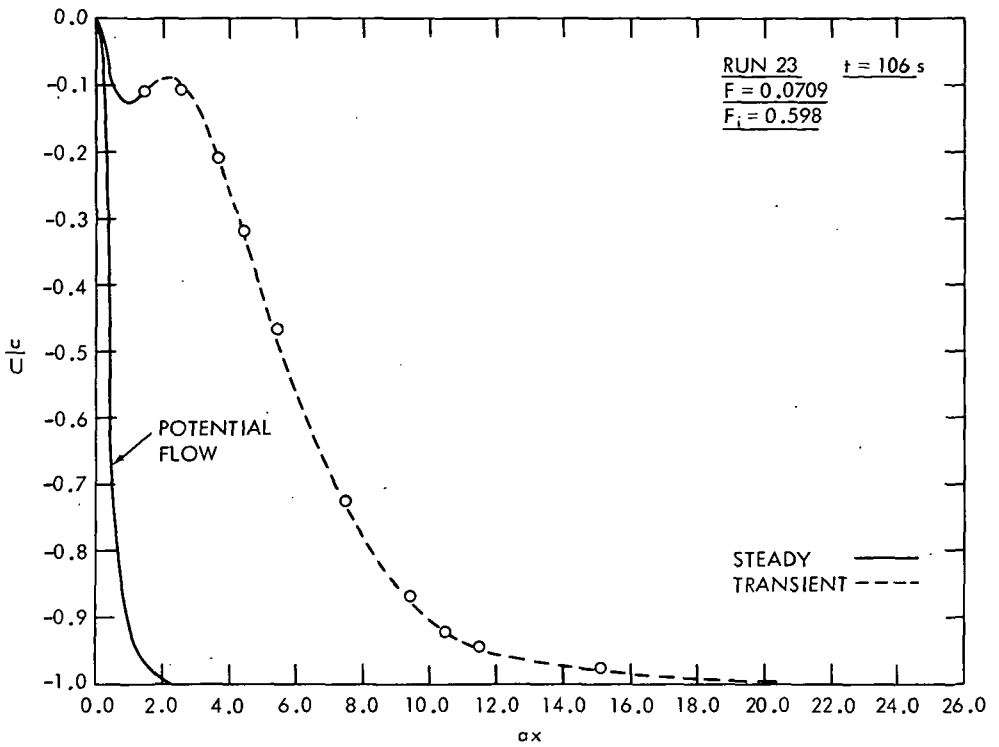

Figure 18. Theoretical and Experimental Results for the Variation of Centerline Velocity with Upstream Position, Run 23

Thus, by analogy between (22b) and (23c), one can define for a plate of height 2b

$$L \equiv b/(U\nu/\bar{\omega}\alpha g)^{1/3} \tag{24}$$

Figure 19 again illustrates that Janowitz's theory, which is formulated for high Richardson number and very low Reynolds number, does not apply to the present experiment. Agreement is particularly poor near the body, where Janowitz's theory predicts the existence of a blocking column with recirculating flow.

Approach to Steady State

In figures 20 and 21 are plotted, for the two runs and at the four upstream stations previously considered, the variation of the theoretical centerline velocity u/U with dimensionless time Uαt. The times during which the experimental data were taken are indicated in the figures. These plots indicate that at the time of the experimental measurements the flow near the body had nearly reached steady state, but that farther upstream it was still quite unsteady.

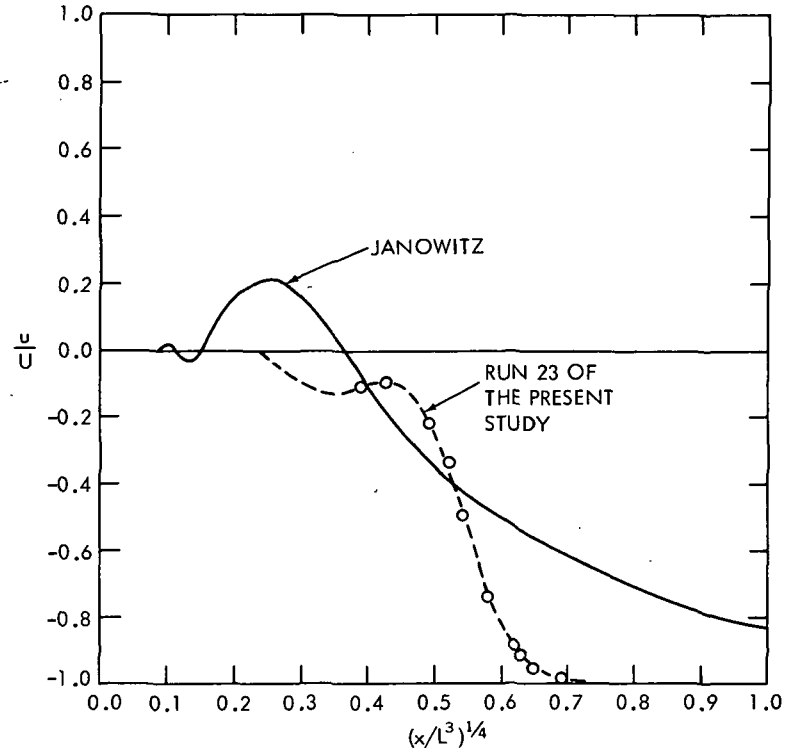

Figure 19. Comparison of Experimental Results for Positional Variation of Centerline Velocity with Janowitz's Theory for Slow-flow Blocking

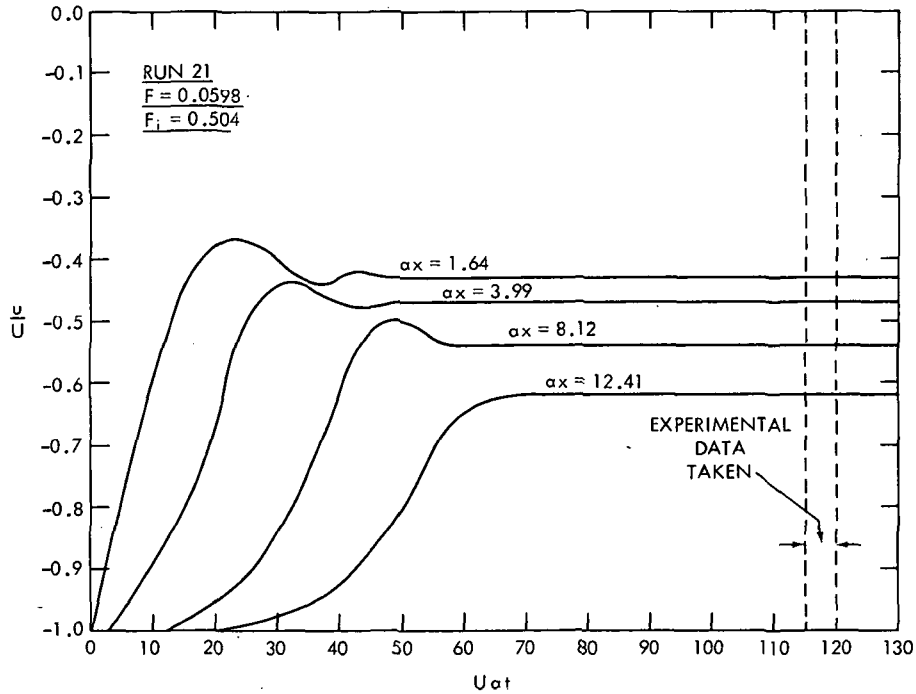

Figure 20. Approach to Steady State. Dimensionless Centerline Velocity as a Function of Dimensionless Time at Four Upstream Locations, Run 21

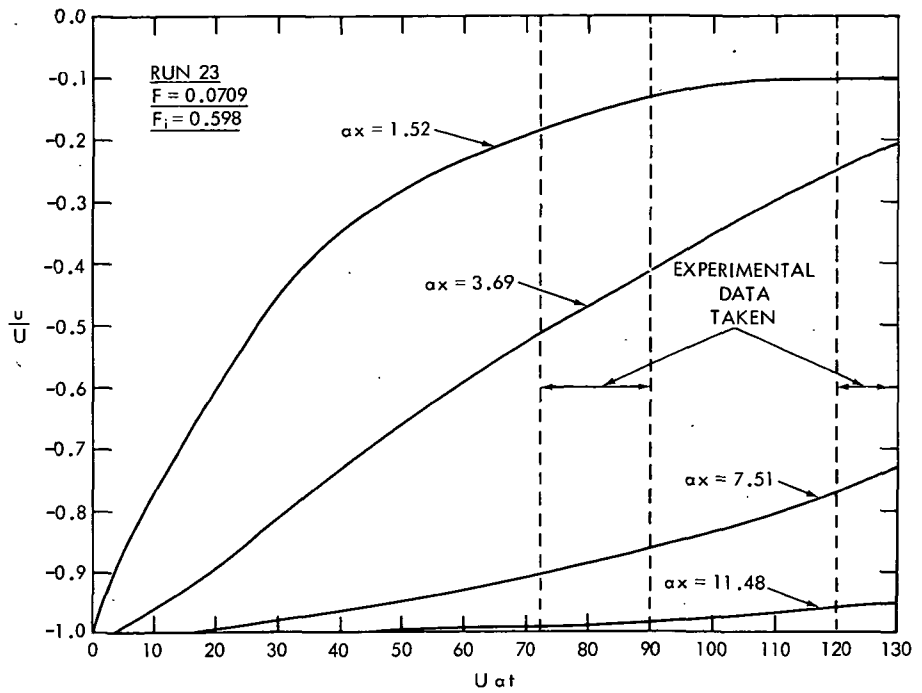

Figure 21. Approach to Steady State. Dimensionless Centerline Velocity as a Function of Dimensionless Time at Four Upstream Locations, Run 23

Relative Importance of Various Terms in the Theoretical Formulation and Conclusions about the Nature of the Observed Upstream Influence

It will be recalled that the formulation presented in the section, Theoretical Study, was made as general as possible. It treated the flow of a diffusive, viscous, non-Boussinesq, stratified fluid about a vertical flat plate. A series of numerical solutions were run on the computer to evaluate the relative importance of various terms in the governing equations and to determine thereby the nature of the observed upstream influence:

(a) When the diffusive term $1/(Sc \cdot Re)\nabla^2 \rho$ was neglected from the formulation, the numerical results for the velocity field were absolutely unchanged. This is not surprising, since, for the conditions of these experiments, Sc = 800, while Re varied from 84 to 1538. Thus, for the conditions of the present study, the flow was nondiffusive.

(b) The Boussinesq approximation resulted in a small but insignificant (1 percent) decrease in the predicted velocities. Evidently, the Boussinesq approximation is a valid assumption for the flow under study.

(c) Neglecting the viscous terms $1/Re\,\nabla^2 \eta$ also resulted in a negligibly small (1 percent) decrease in the predicted velocities. Hence, one concludes that the plate speeds were fast enough that the upstream flow could be regarded as inviscid.

(d) Variation in the Froude number $F = U/(g/\alpha)^{1/2}$, however, had an overwhelming impact on the numerical solution. An increase in F resulted in a dramatic reduction in the length of the predicted region of upstream influence.

From these results one can conclude that the flow under study was governed almost entirely by a balance between *inertial* and *gravitational* forces. This is a significant result, for it means that the observed upstream influence is of an entirely different regime from the slow-flow blocking studied by Janowitz and others. In the case of these very slow flows, a balance exists between the *viscous* and *gravitational* forces.

The effect of the Froude number on the numerical solution is illustrated in figures 22, 23, and 24. Figure 22 shows the predicted variation of centerline velocity with upstream position for F = 0.02, 0.06, 0.10, and 0.20 and for potential flow. This figure shows that as F increases, the upstream influence becomes weaker and the variation of velocity with position approaches that for potential flow. For very small values of F, on the other hand, the upstream solution shows a closed-streamline recirculation region near the body, a result suggestive of the findings of Janowitz. This causes the solution to be somewhat unstable, as is shown clearly in figure 24, where dimensionless velocity at four upstream positions is plotted versus dimensionless time for F = 0.02. This result contrasts with the very stable solution for F = 0.10, as illustrated in figure 23. For intermediate values of F corresponding to the conditions of our experiments, the numerical solutions were quite stable with no evidence of recirculating flow near the body.

Examination of Downstream Flow Field

The photograph presented as figure 25 shows a dye line created by a crystal that happened to drop downstream of the moving plate. The shape of the dye line in the gradient layer shows very clearly the existence of the reverse lee jet previously described.

As mentioned earlier, there were difficulties in obtaining downstream velocity profiles. The optical distortion in the downstream-gradient layer is evident in the figure. Nevertheless, an attempt was made to determine downstream-velocity profiles from the motion of the oil drops that were not swept upstream by the plate. This attempt is summarized in figures 26 and 27. Figure 26 presents profiles of dimensionless velocity with respect to the plate u/U at four downstream locations. Figure 27 shows the variation of centerline velocity with downstream position αx.

The numerical solution, which models a plate of finite thickness, failed to predict the existence of the reverse lee jet. When the numerical model of the plate was shrunk to zero thickness in the x-direction, however, the solution for $U\alpha t < 40$ did indeed show the beginning of the development of a reverse downstream wake. Unfortunately, the singularities at the tips of the infinitesimally thin plate created a disturbance which caused the numerical solution to become noticeably unstable both upstream and downstream for $U\alpha t = 40$ and to become increasingly degenerate with time. The problem of the numerical solution of the equations of motion near mathematically sharp edges has been studied by Lugt and

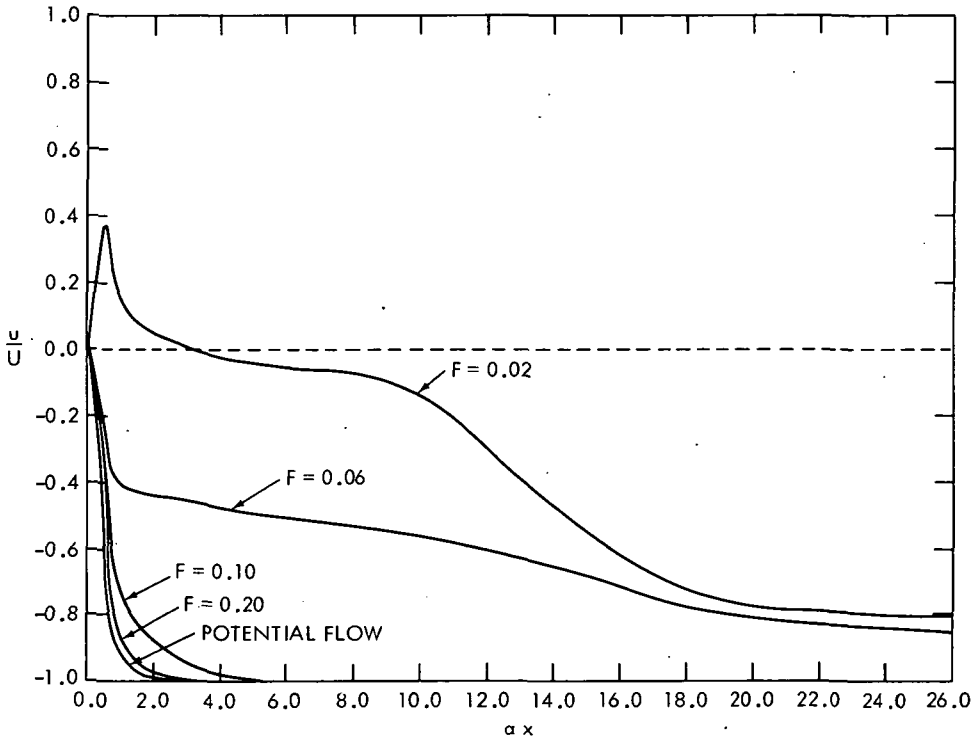

Figure 22. Effect of Froude Number on the Numerical Solution, Showing Variation of Centerline Velocity with Upstream Position

Ohring (1971). They found that they could avoid numerical instability only by manipulating their coordinate system so that the singularity did not coincide with a grid point. This is not a feasible alternative for the geometry of the present study.

Thus, although qualitative prediction of the nature of the downstream flow could be accomplished by numerical modeling of a plate of infinitesimal thickness, that procedure created more problems than it solved.

An Examination of the Numerical Study

In summary, the numerical model successfully predicted the observed flow, including:

(a) The wavelike propagation of the upstream influence to steadily increasing distances in front of the plate

(b) The correct shape and magnitude of upstream velocity profiles.

Moreover, the model permitted identification of the observed upstream influence as the product of a balance between inertial and gravitational forces, thus distinguishing it from the recirculating blocking column produced when viscous and gravitational forces predominate.

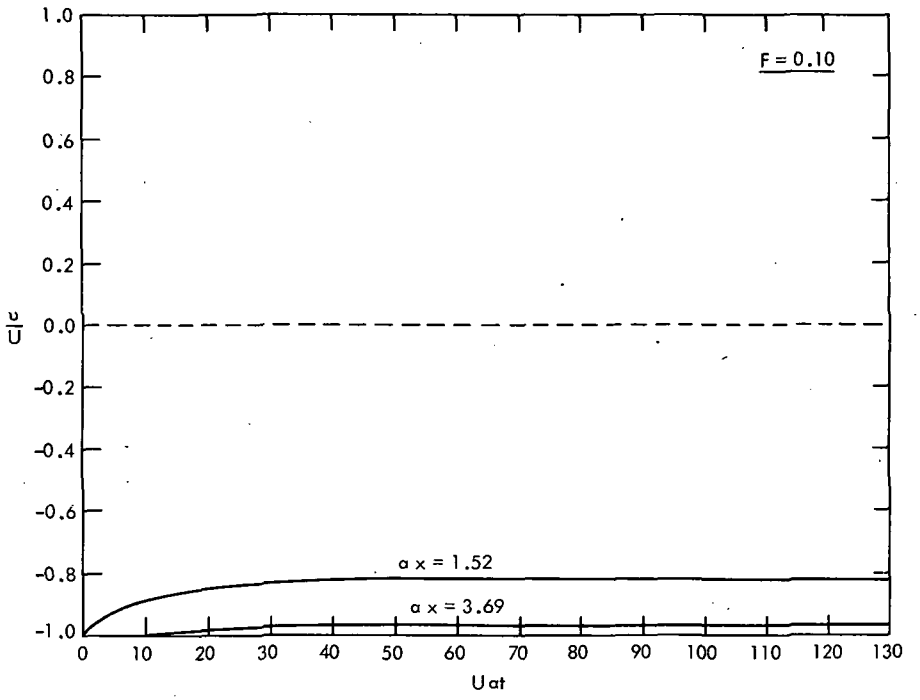

Figure 23. Stable Approach to Steady State for F = 0.10, Showing Dimensionless Centerline Velocity as a Function of Dimensionless Time at Two Upstream Locations

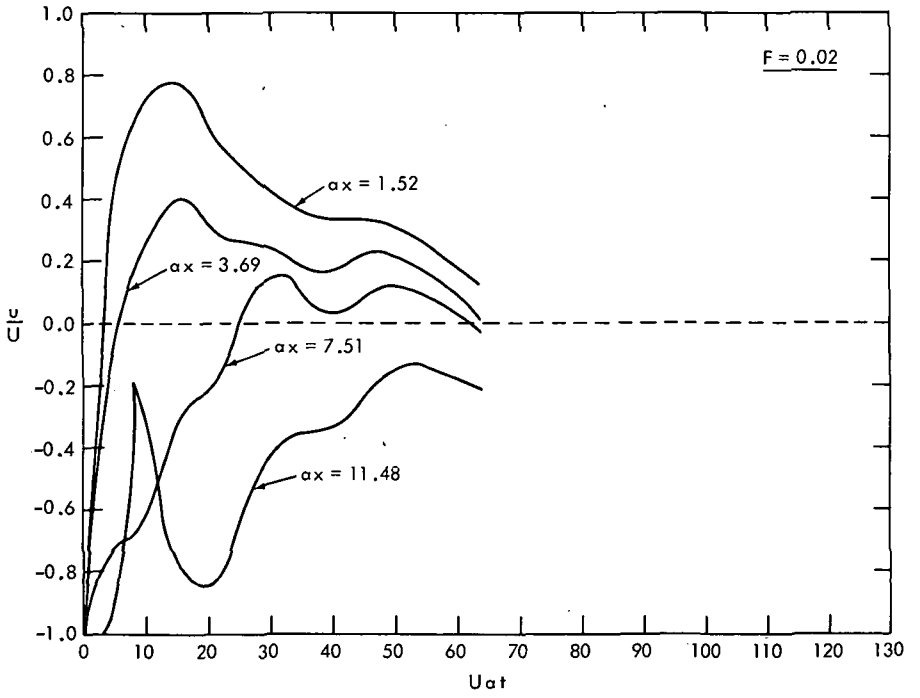

Figure 24. Instability of the Numerical Solution for F = 0.02, Showing Dimensionless Centerline Velocity as a Function of Dimensionless Time at Four Upstream Locations

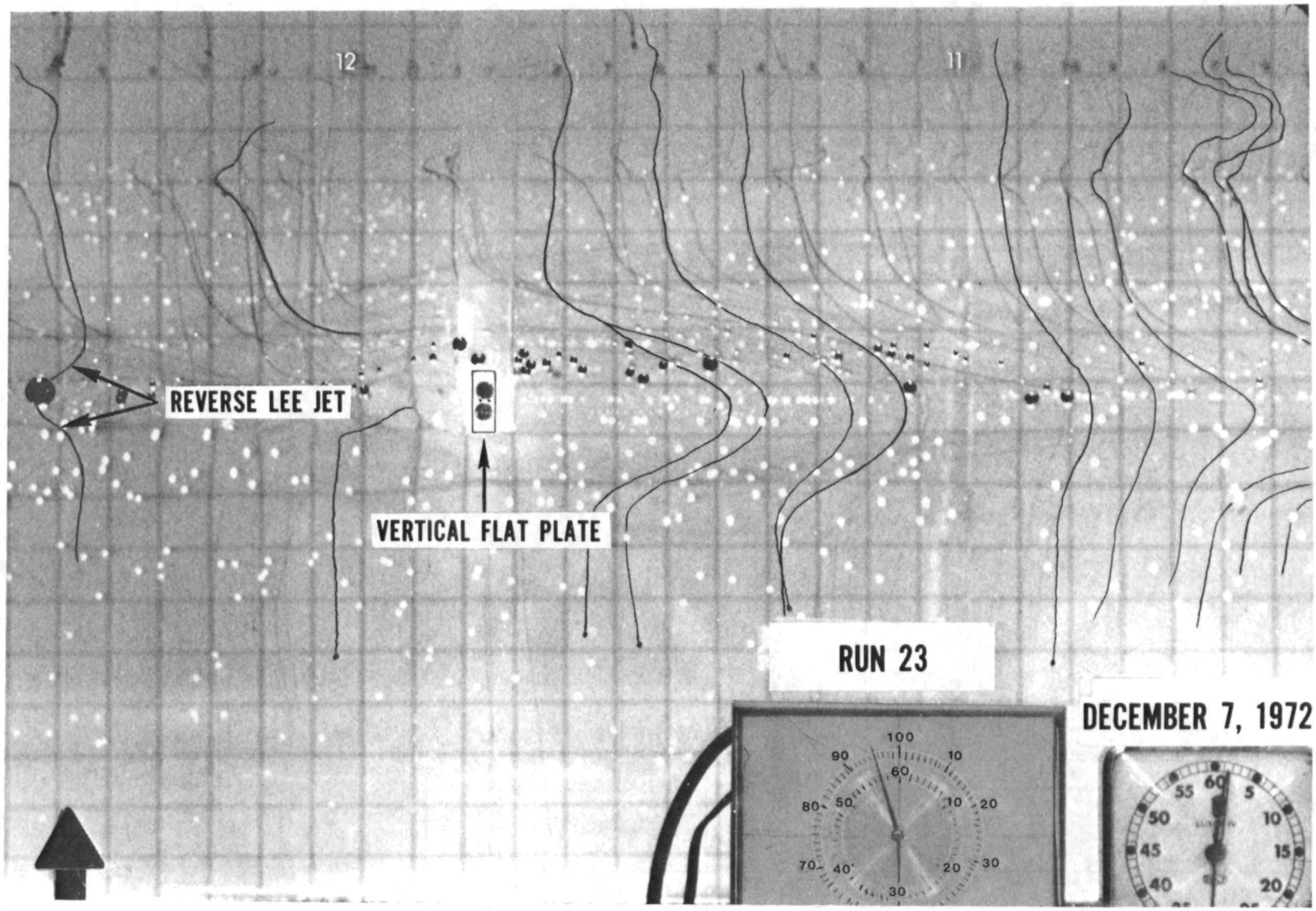

Figure 25. Displacement of a Vertical Dye Line by the Reverse Lee Jet

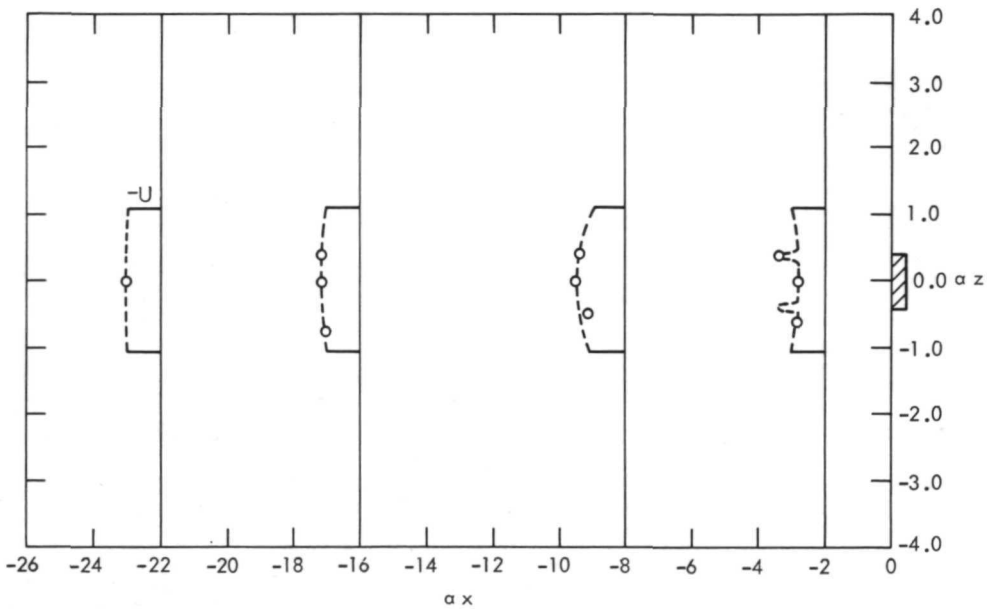

Figure 26. Typical Experimental Results for Downstream Velocity Profiles

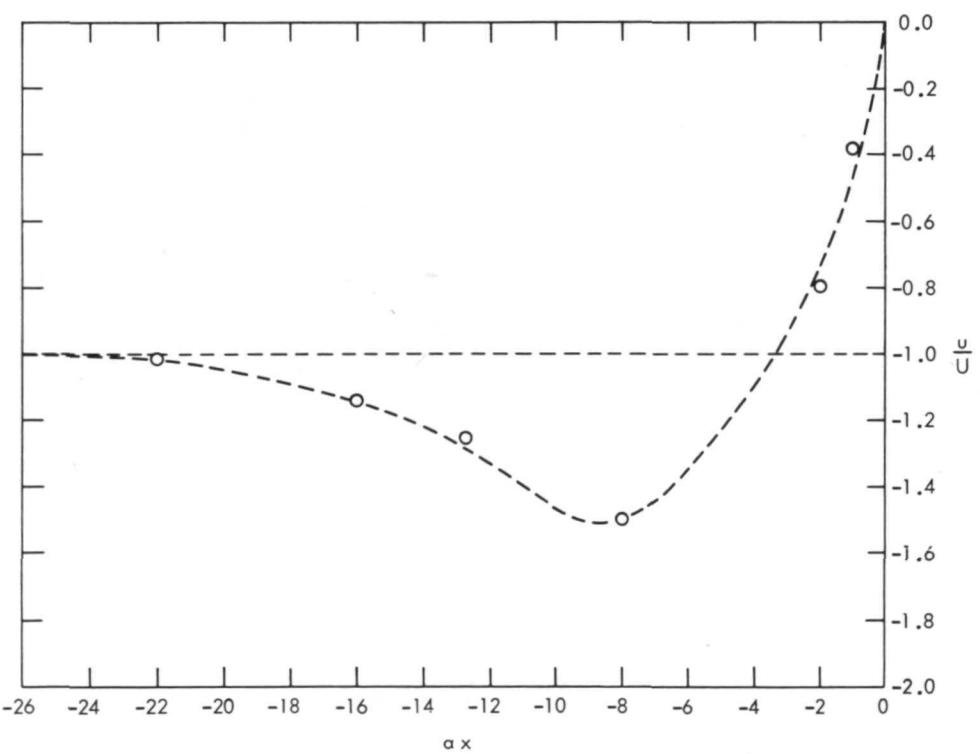

Figure 27. Typical Experimental Results for the Variation of Centerline Velocity with Downstream Position

The numerical model was unsuccessful, however, in predicting the propagation of an internal solitary wave ahead of the upstream influence. Evidently, to successfully predict the generation of such a wave, more work is needed on accurate numerical representation of the impulsive start of the plate.

The model also failed to describe the existence of the reverse lee jet. As mentioned above, this could be accomplished by making the plate infinitesimally thin, but the procedure introduced singularities which eventually destroyed the numerical solution both upstream and downstream.

CONCLUSIONS

Summary of Findings

The significant conclusions of this study are as follows:

(a) The increase during a series of experimental runs of the gradient-layer thickness α^{-1} was very nearly a linear function of the number of transits made through the layer by the vertical flat plate (see figure 5).

(b) The observed upstream influence propagated as an internal wave of zero frequency whose wave speed depended on the Froude number $F = U/(g/\alpha)^{1/2}$.

(c) The behavior of the observed upstream influence can be adequately predicted by a numerical solution of the equations formulated in the section, Theoretical Study. This includes a description of the propagation of the upstream influence to steadily increasing distances from the obstacle, and the prediction of the shape and magnitude of the upstream velocity profiles.

(d) The Boussinesq approximation can properly be used in the formulation of equations to describe the observed upstream influence; moreover, neither mass diffusion nor viscosity are important in the upstream flow.

(e) The upstream influence observed in the present experiments has been identified as the result of a balance between inertial and gravitational forces. Furthermore, no recirculating flow was observed upstream. The observed flow is thus of a different regime from the recirculating blocking column produced in very slow flows where viscous and gravitational forces predominate.

(f) The impulsive start of a vertical flat plate in a region of suddenly varying density will produce an internal solitary wave (Davis and Acrivos 1967; Benjamin 1967). The numerical flow model used in this study, however, fails to predict the generation of this wave.

(g) A reverse lee jet was observed downstream of the moving plate. The mechanism for the formation of the jet is thought to be a buoyancy effect. The present numerical flow model with its plate of finite thickness fails to predict the existence of the lee jet.

Suggestions for Future Research

The dilemma confronted in attempting to predict numerically the existence of the reverse lee jet, without destroying the solution with singularities, suggests that further study is needed in the area of numerical flow modeling in the vicinity of mathematically sharp edges.

Another area needing study is the internal structure of the upstream flow when Re = O(1) so that the inertial and viscous forces are of the same order. Of interest would be the nature of the transition between a recirculating viscous blocking column and a laminar, inertial upstream influence.

Goddard Space Flight Center
National Aeronautics and Space Administration
Greenbelt, Maryland May 1973
502-21-28-01-51

NOMENCLATURE

A	overrelaxation constant
a, c	constants used in the mapping from stretched to real coordinates
a	solitary-wave amplitude
b	half-height of the vertical flat plate
c_g	internal-wave group velocity
c_{sw}^0	propagation speed of an infinitesimal, internal solitary wave
c_{sw}	propagation speed of an internal solitary wave of finite amplitude
c_{ui}	propagation speed of the upstream influence
D	mass diffusion coefficient
F	$U/(g/\alpha)^{1/2}$, Froude number
F_i	$U/(g\,\Delta\rho/\rho\,H)^{1/2}$, or $(1/Ri)^{1/2}$, internal Froude number
g	acceleration of gravity
H	symbol used by Long for total depth of a stratified fluid
i	x-grid index in the finite-difference solution
j	z-grid index in the finite-difference solution
$\vec{k}$	wave number vector of an internal wave
L	$b/(U\nu/\beta g)^{1/3}$, dimensionless parameter used by Janowitz
N	$(-g/\rho\ d\rho/dz)^{1/2}$, Brunt-Vaisala frequency
p	pressure
Re	$U/\alpha\nu$, Reynolds number
Ri	$(N/U\alpha)^2$, Richardson number
s	number of iterations through overrelaxation routine
Sc	ν/D, Schmidt number
t	time
$\tilde{t}$	$U\alpha t$, dimensionless time
u	horizontal fluid velocity with respect to the vertical flat plate
$\tilde{u}$	u/U, dimensionless horizontal velocity

NOMENCLATURE (Continued)

$\bar{u}$	dimensionless horizontal velocity with respect to stretched coordinates
U	velocity of the vertical flat plate with respect to the experimenter
w	vertical fluid velocity with respect to the vertical flat plate
$\tilde{w}$	w/U, dimensionless vertical velocity
$\bar{w}$	dimensionless vertical velocity with respect to stretched coordinates
x, z	Cartesian coordinates
$\tilde{x}, \tilde{z}$	$\alpha x, \alpha z$, dimensionless Cartesian coordinates
$\bar{x}, \bar{z}$	stretched coordinates
α	a parameter of the density profile; α^{-1} is a measure of the gradient-layer thickness
β	$-1/\bar{\rho}\,(d\rho/dz)$, symbol for constant-density gradient used by those investigators who have considered linear density profiles
Δt	finite-difference time increment
Δx	finite-difference x-grid mesh (stretched coordinates)
Δz	finite-difference z-grid mesh (stretched coordinates)
ζ	z component of vorticity
η	y component of vorticity
$\tilde{\eta}$	$\eta/U\alpha$, dimensionless vorticity
λ	$(g/2\alpha c_{sw}^2)\,\ell n\,(\rho_\ell/\rho_u)$, dimensionless parameter used by Davis in his study of internal solitary waves
μ	viscosity
ν	μ/ρ, kinematic viscosity
ξ	x component of vorticity
ρ	fluid density
$\bar{\rho}$	fluid density at the horizontal centerline, z = 0
$\tilde{\rho}$	$\rho/\bar{\rho}$, dimensionless density
ρ_ℓ	density of the homogeneous salt-water layer
ρ_u	density of the homogeneous fresh-water layer
σ	frequency of an internal wave

NOMENCLATURE (Continued)

ψ	stream function defined by $u = \partial\psi/\partial z$, $w = -\partial\psi/\partial x$
$\tilde{\psi}$	$\psi\ \alpha/U$, dimensionless stream function
$\bar{\omega}$	a parameter of the density profile $(\rho_\ell - \rho_u)/(\rho_\ell + \rho_u)$
$\vec{\omega}$	vorticity ($\nabla \times \vec{q} = (\xi, \eta, \zeta)$)

REFERENCES

Benjamin, T. B., and B. J. S. Barnard 1964, "A Study of the Motion of a Cavity in a Rotating Fluid," *J. Fluid Mech.* **19**, pp. 193-209.

Benjamin, T. B. 1967, "Internal Waves of Permanent Form in Fluids of Great Depth," *J. Fluid Mech.* **29**, pp. 559-592.

Benjamin, T. B. 1970, "Upstream Influence," *J. Fluid Mech.* **40**, pp. 49-79.

Bretherton, F. P. 1967, "The Time-Dependent Motion Due to a Cylinder Moving in an Unbounded Rotating or Stratified Fluid," *J. Fluid Mech.* **28**, pp. 545-570.

Browand, F. K., and C. D. Winant 1972, "Blocking Ahead of a Cylinder Moving in a Stratified Fluid: An Experiment," *Geophys. Fluid Dyn.* **4**, pp. 29-53.

Brown, S. N., 1968, "Slow Viscous Flow of a Stratified Fluid Past a Finite Flat Plate," *Proc. Roy. Soc. A.* **306**, pp. 239-256.

Conte, S. D., 1965, *Elementary Numerical Analysis*, New York: McGraw Hill.

Davis, R. E., 1967, *Some Aspects of Wave Motion in Stably Stratified Fluids*, Ph.D. Thesis, Stanford University.

Davis, R. E., and A. Acrivos, 1967, "Solitary Internal Waves in Deep Water," *J. Fluid Mech.* **29**, pp. 593-607.

Debler, W., and J. W. Daily, 1971, *The Towing of Bodies in a Stratified Fluid,* Tech. Rep. EM-71-1, Dept. of Engineering Mechanics, University of Michigan.

Ekman, V. W., 1904, "On Dead Water," *Scientific Results of the Norwegian North Polar Expedition, Pt. XV.*

Graebel, W. P., 1969, "On the Slow Motion of Bodies in Stratified and Rotating Fluids," *Quart. J. Mech. Appl. Math.* **22**, pp. 39-54.

Janowitz, G. S., 1971, "The Slow Transverse Motion of a Flat Plate Through a Non-diffusive Stratified Fluid," *J. Fluid Mech.* **47**, pp. 171-181.

Kao, T. W., H. P. Pao, and S. N. Wei, 1972, "Time-Dependent Behavior of Stratified Flow in a Channel Towards a Line Sink," Paper presented at the International Symposium on Stratified Flows, I.A.H.R., Novosibirsk, U.S.S.R.

Keady, G., 1971, "Upstream Influence in a Two-Fluid System," *J. Fluid Mech.* **49**, pp. 373-384.

Lamb, H., 1932, *Hydrodynamics*, 6th ed. Cambridge University Press (Dover, 1945).

Laws, P., and T. N. Stevenson, 1972, "Measurements of a Laminar Wake in a Confined Stratified Fluid," *J. Fluid Mech.* **54**, pp. 745-748.

Long, R. R., 1953, "Some Aspects of the Flow of Stratified Fluids: I. A Theoretical Investigation," *Tellus* **5**, pp. 42-58.

Long, R. R., 1954, "Some Aspects of the Flow of Stratified Fluids: II. Experiments with a Two-Fluid System," *Tellus* **6**, pp. 97-115.

Long, R. R., 1955, "Some Aspects of the Flow of Stratified Fluids: III. Continuous Density Gradients," *Tellus* **7**, pp. 341-357.

Lugt, H. J., and S. Ohring, 1971, *Laminar Flows Past an Infinitely Thin Disk*, Tech. Note CMD-14-71, Computation and Mathematics Department, Naval Ship Research and Development Center.

McIntyre, M. E., 1972, "On Long's Hypothesis of No Upstream Influence in Uniformly Stratified or Rotating Flow," *J. Fluid Mech.* **52**, pp. 209-243.

Martin, S., and R. R. Long, 1968, "The Slow Motion of a Flat Plate in a Viscous Stratified Fluid," *J. Fluid Mech.* **31**, pp. 669-688.

Pao, Y-H., 1967, *Laminar Flow of a Stably Stratified Fluid Past a Flat Plate*, Boeing Sci. Res. Lab. Document, D 1-82-0488.

Pao, Y-H., 1968, "Laminar Flow of a Stably Stratified Fluid Past a Flat Plate," *J. Fluid Mech.* **34**, pp. 795-808.

Phillips, O. M., 1969, *The Dynamics of the Upper Ocean*, Cambridge: Cambridge University Press.

Stokes, G. G., 1847, "On the Theory of Oscillatory Waves," *Trans. Cambr. Phil. Soc.* **8**, pp. 441-455.

Torrance, K. E., and J. A. Rockett, 1969, "Numerical Study of Natural Convection in an Enclosure With Localized Heating From Below—Creeping Flow to the Onset of Laminar Instability," *J. Fluid Mech.* **36**, pp. 33-54.

APPENDIX 1

TRANSFORMED GOVERNING EQUATIONS

The coordinate transformation (19) applied to the governing equations (20) produces the following transformed system. The continuity equation becomes

$$\frac{\partial \rho}{\partial t} + a(1-\bar{x}^2)\cdot c(1-\bar{z}^2)\left[\frac{\partial}{\partial \bar{x}}(\bar{u}\rho) + \frac{\partial}{\partial \bar{z}}(\bar{w}\rho)\right] \tag{A-1}$$

$$= \frac{1}{Sc\cdot Re}\left\{a^2(1-\bar{x}^2)^2\frac{\partial^2\rho}{\partial \bar{x}^2} - 2a^2\bar{x}(1-\bar{x}^2)\frac{\partial \rho}{\partial \bar{x}} + c^2(1-\bar{z}^2)^2\frac{\partial^2\rho}{\partial \bar{z}^2} - 2c^2\bar{z}(1-\bar{z}^2)\frac{\partial \rho}{\partial \bar{z}}\right\}$$

The transformed momentum equation is

$$c(1-\bar{z}^2)\frac{\partial \rho}{\partial \bar{z}}\left\{c(1-\bar{z}^2)\frac{\partial \bar{u}}{\partial t} + a(1-\bar{x}^2)\cdot c^2(1-\bar{z}^2)^2\frac{\partial}{\partial \bar{x}}(\bar{u}^2)\right.$$

$$\left. + a(1-\bar{x}^2)\cdot c^2(1-\bar{z}^2)\left[(1-\bar{z}^2)\frac{\partial}{\partial \bar{z}}(\bar{u}\,\bar{w}) - 2\bar{u}\,\bar{w}\,\bar{z}\right]\right\}$$

$$- a(1-\bar{x}^2)\frac{\partial \rho}{\partial \bar{x}}\left\{a(1-\bar{x}^2)\frac{\partial \bar{w}}{\partial t} + a^2(1-\bar{x}^2)\cdot c(1-\bar{z}^2)\left[(1-\bar{x}^2)\frac{\partial}{\partial \bar{x}}(\bar{u}\,\bar{w}) - 2\bar{u}\,\bar{w}\,\bar{x}\right]\right.$$

$$\left. + a^2(1-\bar{x}^2)^2\cdot c(1-\bar{z}^2)\frac{\partial}{\partial \bar{z}}(\bar{w}^2)\right\} + \rho\left\{\frac{\partial \eta}{\partial t} + a(1-\bar{x}^2)\cdot c(1-\bar{z}^2)\left[\frac{\partial}{\partial \bar{x}}(\bar{u}\eta) + \frac{\partial}{\partial \bar{z}}(\bar{w}\eta)\right]\right\}$$

$$= a(1-\bar{x}^2)\frac{1}{F^2}\frac{\partial \rho}{\partial \bar{x}} + \frac{1}{Re}\left\{a^2(1-\bar{x}^2)^2\frac{\partial^2\eta}{\partial \bar{x}^2}\right. \tag{A-2}$$

$$\left. - 2a^2\bar{x}(1-\bar{x}^2)\frac{\partial \eta}{\partial \bar{x}} + c^2(1-\bar{z}^2)^2\frac{\partial^2\eta}{\partial \bar{z}^2} - 2c^2\bar{z}(1-\bar{z}^2)\frac{\partial \eta}{\partial \bar{z}}\right\}$$

The velocities are

$$\bar{u} = \frac{\partial \psi}{\partial \bar{z}}, \quad \bar{w} = -\frac{\partial \psi}{\partial \bar{x}} \tag{A3}$$

and the vorticity expressed as the Laplacian of the stream function is

$$\eta = a^2(1-\bar{x}^2)^2\frac{\partial^2\psi}{\partial \bar{x}^2} - 2a^2\bar{x}(1-\bar{x}^2)\frac{\partial \psi}{\partial \bar{x}} + c^2(1-\bar{z}^2)^2\frac{\partial^2\psi}{\partial \bar{z}^2} - 2c^2\bar{z}(1-\bar{z}^2)\frac{\partial \psi}{\partial \bar{z}}. \tag{A4}$$

The transformed boundary conditions for $t > 0$ are

$$\text{as } |\bar{x}|,\ |\bar{z}| \to 1,\ \rho \to \left[1 - \bar{\omega}\ \tanh\left(\frac{1}{c}\ \text{arctanh}\ \bar{z}\right)\right],\quad |\psi| \to \infty \tag{A5}$$

$$\text{and at } \bar{x} = 0,\quad |\bar{z}| \leqslant \tanh c\alpha b, \qquad \frac{\partial \rho}{\partial \bar{x}} = 0 \tag{A6}$$

$$\frac{\partial \psi}{\partial \bar{x}} = 0, \qquad \frac{\partial \psi}{\partial \bar{z}} = 0. \tag{A7}$$

The transformed initial conditions are

$$\rho = \left[1 - \bar{\omega}\ \tanh\left(\frac{1}{c}\ \text{arctanh}\ \bar{z}\right)\right] \quad \text{everywhere at } t = 0 \tag{A8}$$

$$\frac{\partial \psi}{\partial \bar{x}} = \frac{\partial \psi}{\partial \bar{z}} = 0 \quad \text{everywhere at } t = 0 \tag{A9}$$

APPENDIX 2

FINITE-DIFFERENCE FORM OF TRANSFORMED GOVERNING EQUATIONS

The stream function ψ is determined by overrelaxation of (A4) subject to the boundary conditions (A5) and (A7). The overrelaxation scheme is given by

$$\psi_{i,j}^{(s+1)} = \psi_{i,j}^{(s)} + A\,(\psi_{i,j} - \psi_{i,j}^{(s)}) \tag{B1}$$

where i and j are the x and z grid indices, respectively, so that $\psi_{i,j}^{(s+1)}$ is the value computed for the stream function at the grid point (i, j) on the (s+1)*th* iteration. The value of $\psi_{i,j}$ is obtained from the finite-difference form of (A4). If the overrelaxation converges, then as s increases

$$\left(\psi_{i,j} \to \psi_{i,j}^{(s)}\right) \Rightarrow \left(\psi_{i,j}^{(s+1)} \to \psi_{i,j}^{(s)}\right) .$$

A is an overrelaxation constant whose value affects the speed of convergence but not the final result for $\psi_{i,j}^{(s+1)}$. For this study, A was set equal to 1.75. The overrelaxation equation for the stream function is therefore given by

$$\psi_{i,j}^{(s+1)} = (1 - A)\,\psi_{i,j}^{(s)} + \left[0.5\,A \Big/ \left(a^2 (1 - \bar{x}_i^2)^2 + c^2 (1 - \bar{z}_j^2)^2 \left(\frac{\Delta x}{\Delta z}\right)^2 \right)\right] \left[- (\Delta x)^2 \eta_{i,j} \right.$$

$$+ a^2 (1 - \bar{x}_i^2)^2 (\psi_{i+1,j} + \psi_{i-1,j}) \quad - a^2 \bar{x}_i (1 - \bar{x}_i^2) \Delta x (\psi_{i+1,j} - \psi_{i-1,j}) \tag{B2}$$

$$\left. + c^2 (1 - \bar{z}_j^2)^2 \left(\frac{\Delta x}{\Delta z}\right)^2 (\psi_{i,j+1} + \psi_{i,j-1}) \quad - c^2 \bar{z}_j (1 - \bar{z}_j^2) \frac{(\Delta x)^2}{(\Delta z)} (\psi_{i,j+1} - \psi_{i,j-1}) \right]$$

The boundary conditions on ψ at the solid boundary of the obstacle are derived as follows. The $\psi = 0$ streamline is coincident with the horizontal centerline of the flow field except at the obstacle where it bifurcates and follows the contour of the solid boundary. The forward-difference expression for the derivative of a function f at a solid boundary is

$$f'(\bar{x}_i) \approx \frac{1}{2(\Delta x)} \left[-3 f_i + 4 f_{i+1} - f_{i+2}\right] + O\left[(\Delta x)^2\right] \tag{B3a}$$

and the backward-difference expression is

$$f'(\bar{x}_i) \approx \frac{1}{2(\Delta x)} \left[3 f_i - 4 f_{i-1} + f_{i-2}\right] + O\left[(\Delta x)^2\right] \tag{B3b}$$

(Conte 1965, p. 110). The nonslip condition, together with the additional constraint that

$\psi = 0$ along the solid boundary, combines with (B3a) and (B3b) to give the following boundary conditions for ψ.

$$\begin{aligned}
\psi_{M3-1,j} &= \frac{1}{4}\,\psi_{M3-2,j} \qquad j = N3, \ldots, N4 \\
\psi_{M4+1,j} &= \frac{1}{4}\,\psi_{M4+2,j} \qquad j = N3, \ldots, N4 \\
\psi_{i,N3-1} &= \frac{1}{4}\,\psi_{i,N3-2} \qquad i = M3, \ldots, M4 \\
\psi_{i,N4+1} &= \frac{1}{4}\,\psi_{i,N4+2} \qquad i = M3, \ldots, M4
\end{aligned} \tag{B4}$$

where the obstacle is represented as a rectangle contained within the grid lines i = M3 to i = M4 and j = N3 to j = N4. The u and w velocity fields, as given by (A3), become

$$\bar{u}_{i,j} = \frac{\psi_{i,j+1} - \psi_{i,j-1}}{2(\Delta z)}, \qquad \bar{w}_{i,j} = \frac{\psi_{i-1,j} - \psi_{i+1,j}}{2(\Delta x)} \tag{B5}$$

The continuity equation (A1) can be written in finite-difference form as

$$\begin{aligned}
\rho'_{i,j} = \rho_{i,j} + \Delta t \Bigg\{ \frac{1}{Sc \cdot Re} \Bigg[& a^2 (1 - \bar{x}_i^2)^2 \frac{\rho_{i+1,j} - 2\rho_{i,j} + \rho_{i-1,j}}{(\Delta x)^2} \\
& - 2a^2 \bar{x}_i (1 - \bar{x}_i^2) \frac{\rho_{i+1,j} - \rho_{i-1,j}}{2(\Delta x)} + c^2 (1 - \bar{z}_j^2)^2 \frac{\rho_{i,j+1} - 2\rho_{i,j} + \rho_{i,j-1}}{(\Delta z)^2} \\
& - 2c^2 \bar{z}_j (1 - \bar{z}_j^2) \frac{\rho_{i,j+1} - \rho_{i,j-1}}{2(\Delta z)} \Bigg] - a(1 - \bar{x}_i^2) \cdot c(1 - \bar{z}_j^2) \Bigg[\left(\frac{\partial}{\partial \bar{x}} (\bar{u}\rho) \right)_{i,j} \\
& + \left(\frac{\partial}{\partial \bar{z}} (\bar{w}\rho) \right)_{i,j} \Bigg] \Bigg\}
\end{aligned} \tag{B6}$$

where the unprimed variables represent values at t = t and $\rho'_{i,j}$ is the new value of the density at grid point (i, j) and at $t = t + \Delta t$. As mentioned in the section, Theoretical Study, the nonlinear terms $[\partial/\partial\bar{x}\,(\bar{u}\rho)]_{i,j}$ and $[\partial/\partial\bar{z}\,(\bar{\omega}\rho)]_{i,j}$ were evaluated by the "special three-point noncentral difference method" of Torrance and Rockett (1969).

A derivation analogous to that for the boundary conditions on ψ gives the following boundary conditions for ρ.

$$\rho_{M3-1,j} = \frac{3}{4} + \frac{1}{4}\,\rho_{M3-2,j} \qquad j = N3, \ldots, N4$$

$$\rho_{M4+1,j} = \frac{3}{4} + \frac{1}{4}\,\rho_{M4+2,j} \qquad j = N3, \ldots, N4$$

$$\rho_{i,N3-1} = \frac{3}{4} + \frac{1}{4}\,\rho_{i,N3-2} \qquad i = M3, \ldots, M4 \tag{B7}$$

$$\rho_{i,N4+1} = \frac{3}{4} + \frac{1}{4}\,\rho_{i,N4+2} \qquad i = M3, \ldots, M4$$

The momentum equation, which is used to evaluate the change of free stream vorticity with time, can be written in finite-difference form as

$$\begin{aligned}
\eta'_{i,j} = \eta_{i,j} + \Delta t \Bigg\{ & a(1-\bar{x}_i^2)\cdot c(1-\bar{z}_j^2) \left[\left[\frac{\partial}{\partial \bar{x}} (\bar{u}\eta) \right]_{i,j} + \left[\frac{\partial}{\partial \bar{z}} (\bar{w}\eta) \right]_{i,j} \right] \\
& + \frac{1}{\rho} \Bigg[a(1-\bar{x}_i^2)\,\frac{1}{F^2}\,\frac{\rho_{i+1,j}-\rho_{i-1,j}}{2(\Delta x)} + \frac{1}{Re} \Bigg[a^2(1-\bar{x}_i^2)^2\,\frac{\eta_{i+1,j}-2\eta_{i,j}+\eta_{i-1,j}}{(\Delta x)^2} \\
& - 2a^2\bar{x}_i(1-\bar{x}_i^2)\,\frac{\eta_{i+1,j}-\eta_{i-1,j}}{2(\Delta x)} + c^2(1-\bar{z}_j^2)^2\,\frac{\eta_{i,j+1}-2\eta_{i,j}+\eta_{i,j-1}}{(\Delta z)^2} \\
& - 2c^2\bar{z}_j(1-\bar{z}_j^2)\,\frac{\eta_{i,j+1}-\eta_{i,j-1}}{2(\Delta z)} \Bigg] - c(1-\bar{z}_j^2)\,\frac{\rho_{i,j+1}-\rho_{i,j-1}}{2(\Delta z)} \Bigg[c(1-\bar{z}_j^2)\,\frac{\bar{u}'_{i,j}-\bar{u}_{i,j}}{\Delta t} \\
& + a(1-\bar{x}_i^2)\cdot c^2(1-\bar{z}_j^2)^2 \left[\frac{\partial}{\partial \bar{x}} (\bar{u}\,\bar{u}) \right]_{i,j} + a(1-\bar{x}_i^2)\cdot c^2(1-\bar{z}_j^2) \left[(1-\bar{z}_j^2) \left[\frac{\partial}{\partial \bar{z}} (\bar{u}\,\bar{w}) \right]_{i,j} \right. \\
& \left. - 2\bar{u}_{i,j}\bar{w}_{i,j}\bar{z}_j \right] \Bigg] + a(1-\bar{x}_i^2)\,\frac{\rho_{i+1,j}-\rho_{i-1,j}}{2(\Delta x)} \Bigg[a(1-\bar{x}_i^2)\,\frac{\bar{w}'_{i,j}-\bar{w}_{i,j}}{\Delta t} \\
& + a^2(1-\bar{x}_i^2)\cdot c(1-\bar{z}_j^2) \left[(1-\bar{x}_i^2) \left[\frac{\partial}{\partial \bar{x}} (\bar{u}\,\bar{w}) \right]_{i,j} - 2\bar{u}_{i,j}\bar{w}_{i,j}\bar{x}_i \right] \\
& + a^2(1-\bar{x}_i^2)^2\cdot c(1-\bar{z}_j^2) \left[\frac{\partial}{\partial \bar{z}} (\bar{w}\,\bar{w}) \right]_{i,j} \Bigg] \Bigg] \Bigg\}
\end{aligned} \tag{B8}$$

Finally, the vorticity at the solid boundaries is evaluated from $\eta = \nabla^2 \psi$ by taking note of the boundary conditions on ψ and using the forward- and backward-difference expressions for a second derivative at a boundary. These expressions are (Conte 1965, p. 110)

$$f''(\bar{x}_i) \approx \frac{1}{(\Delta x)^2}\left[-f_{i+3} + 4f_{i+2} - 5f_{i+1} + 2f_i\right] + O\left[(\Delta x)^2\right] \qquad \text{(B9a)}$$

$$f''(\bar{x}_i) \approx \frac{1}{(\Delta x)^2}\left[-f_{i-3} + 4f_{i-2} - 5f_{i-1} + 2f_i\right] + O\left[(\Delta x)^2\right] \qquad \text{(B9b)}$$

and the expressions for η at the boundary are

$$\begin{aligned}
\eta_{M3,j} &= a^2(1-\bar{x}_i^2)^2\left(\frac{-\psi_{M3-3,j} + 4\psi_{M3-2,j} - 5\psi_{M3-1,j} + 2\psi_{M3,j}}{(\Delta x)^2}\right), \quad j = N3, \ldots, N4 \\
\eta_{M4,j} &= a^2(1-\bar{x}_i^2)^2\left(\frac{-\psi_{M4+3,j} + 4\psi_{M4+2,j} - 5\psi_{M4+1,j} + 2\psi_{M4,j}}{(\Delta x)^2}\right), \quad j = N3, \ldots, N4 \\
\eta_{i,N3} &= c^2(1-\bar{z}_j^2)^2\left(\frac{-\psi_{i,N3-3} + 4\psi_{i,N3-2} - 5\psi_{i,N3-1} + 2\psi_{i,N3}}{(\Delta z)^2}\right), \quad i = M3, \ldots, M4 \\
\eta_{i,N4} &= c^2(1-\bar{z}_j^2)^2\left(\frac{-\psi_{i,N4+3} + 4\psi_{i,N4+2} - 5\psi_{i,N4+1} + 2\psi_{i,N4}}{(\Delta z)^2}\right), \quad i = M3, \ldots, M4
\end{aligned} \qquad \text{(B10)}$$

APPENDIX 3

COMPUTER PROGRAM

The computer program used to make the theoretical flow predictions for this study is based on the finite difference equations of Appendix 2. It is written in FORTRAN-IV for use on an IBM 360 computer. It uses double precision, and for the present 81 by 41 grid mesh, requires 620 K bytes of storage and 30 to 40 minutes of central processing unit (CPU) time to model a complete experimental run. Most of the CPU time is spent in the overrelaxation step of the computation. The core and CPU time requirements are considerably reduced for coarser grid meshes, but not without some sacrifice in accuracy.

INPUT-DATA FORMAT

Cards 1, 2, 3, and 4 are title cards. A descriptive title can be punched on these cards in columns 1 to 80.

Card 5 contains 12 floating-point data inputs in fields of six columns each:

Col.	1 - 6	DX = Δx = finite-difference x-grid mesh ("stretched" coordinates)
	7 - 12	DZ = Δz = finite-difference z-grid mesh ("stretched" coordinates)
	13 - 18	DT = Δt = dimensionless finite difference time increment
	19 - 24	T = time at start of computation
	25 - 30	F = Froude number = $U/(g/\alpha)^{1/2}$
	31 - 36	Re = Reynolds number = $U/\nu\alpha$
	37 - 42	EPS = (Schmidt number)$^{-1}$ = D/ν
	43 - 48	DAVG = $\bar{\rho}$ = fluid density at z = 0
	49 - 54	OMEG = $\bar{\omega}$ = a parameter of the density profile
	55 - 60	ALPHA = α = a parameter of the density profile
	61 - 66	UBODY = U = velocity of the vertical flat plate with respect to the experimenter
	67 - 72	A = overrelaxation constant

Card 6 contains nine fixed point data inputs, right justified, in fields of six columns each:

Col.	1 - 6	LL = total number of time incrementations to be made during the computation (should be a multiple of 40)

7 - 12 MX = total number of x-grid lines; must be less than or equal to the number of storage locations assigned to X(I) in the DIMENSION statement

13 - 18 M2NEG = downstream thickness of the obstacle in terms of the number of downstream ($x < 0$) grid lines it contains

19 - 24 M2POS = upstream thickness of the obstacle in terms of the number of upstream ($x > 0$) grid lines it contains

25 - 30 NZ = total number of z grid lines; must be less than or equal to the number of storage locations assigned to Z(J) in the DIMENSION statement

31 - 36 MLT1 = 0, if Boussinesq approximation is to be made
= 1, otherwise

37 - 42 MLT2 = 0, if Boussinesq approximation is to be made
= 1, otherwise

43 - 48 MLT3 = 0, if flow is to be assumed inviscid
= 1, otherwise

49 - 54 MLT4 = 0, if flow is to be assumed nondiffusive
= 1, otherwise

Card 7 contains 12 fixed point data inputs, right justified, in fields of six columns each. These input parameters indicate those results which the user has selected to be printed out. If a parameter is zero, the results corresponding to this parameter are not printed out. If the printout is desired, a nonzero integer must be assigned to the parameter. The following list gives each parameter in the order in which it is read in and the result prints out to which it corresponds:

Col. 1 - 6 IPOK – number of iterations K through SUBROUTINE RELAX

7 - 12 IPOP – stream function ψ both initial and at later time

13 - 18 IPOPC – stream function contour elevations

19 - 24 IPODI – initial density profile at a typical cross-section

25 - 30 IPODC – density contour elevations

31 - 36 IPODN – nondimensional density at later time

37 - 42 IPOD – dimensional density at later time

43 - 48 IPOV – vorticity field

49 - 54 IPOUO – nondimensional u-velocity with respect to the obstacle

55 - 60 IPOWO – nondimensional w-velocity with respect to the obstacle

61 - 66 IPOUE – dimensional u-velocity with respect to the experimenter

67 - 72 IPOWE – dimensional w-velocity with respect to the experimenter

COMPUTER PROGRAM LISTING

The following pages present the program listing.

```
C     FLOW ABOUT AN OBSTACLE OF A FLUID WITH A TANH DENSITY PROFILE      MAN   1
C     DAVID A HURDIS                                                    MAN   2
C     NOVEMBER, 1972                                                    MAN   3
      IMPLICIT REAL*8(A-H,O-Z)                                          MAN   4
      DIMENSION IN(80), X(81), XR(81), XRDIM(81), Z(41), ZR(41), ZRDIM(4MAN   5
     11), DT1(81,41), DT2(81,41), DDIM(81,41), DSQD(81,41), VT1(81,41), MAN   6
     2VT2(81,41), DSQV(81,41), U(81,41), UAV(81,41), UOLD(81,41), UR(81,MAN   7
     341), URDIM(81,41), W(81,41), WAV(81,41), WOLD(81,41), WR(81,41), WMAN   8
     4RDIM(81,41), DUUDX(81,41), DWUDZ(81,41), DUWDX(81,41), DWWDZ(81,41MAN   9
     5), DUVDX(81,41), DWVDZ(81,41), DUDDX(81,41), DWDDZ(81,41), BOUS1(8MAN  10
     61,41), BOUS2(81,41), P(81,41), XSEC2(81), ZSEC2(41), H(12,81), PCOMAN  11
     7NT(12), DCONT(12)                                                 MAN  12
C                                                                       MAN  13
C     EQUIVALENCE STATEMENT REDUCES WASTED MEMORY.                      MAN  14
C                                                                       MAN  15
      EQUIVALENCE (UR(1,1),UAV(1,1)), (WR(1,1),WAV(1,1)), (BOUS1(1,1),URMAN  16
     1DIM(1,1)), (BOUS2(1,1),WRDIM(1,1)), (DDIM(1,1),DSQD(1,1),DSQV(1,1)MAN  17
     2), (DUDDX(1,1),DUUDX(1,1),DUWDX(1,1),DUVDX(1,1)), (DWDDZ(1,1),DWUDMAN  18
     3Z(1,1),DWWDZ(1,1),DWVDZ(1,1))                                     MAN  19
      WRITE (6,1020)                                                    MAN  20
C     READ AND WRITE 4 TITLE CARDS                                      MAN  21
      READ (5,1030) IN                                                  MAN  22
      WRITE (6,1030) IN                                                 MAN  23
C     READ AND WRITE INPUT                                              MAN  24
      READ (5,1040) DX,DZ,DT,T,F,RE,EPS,DAVG,OMEG,ALPHA,UBODY,A         MAN  25
      READ (5,1050) LL,MX,M2NEG,M2POS,NZ,MLT1,MLT2,MLT3,MLT4            MAN  26
      CA=ARCTNH(1.0D0)/((1.5D2)*ALPHA)                                  MAN  27
      ALF=ARCTNH(1.0D0)/((2.286D1)*ALPHA)                               MAN  28
      WRITE (6,1060) DX,DZ,DT,T                                         MAN  29
      WRITE (6,1070) F,RE,EPS                                           MAN  30
      WRITE (6,1080) CA,ALF,DAVG,OMEG,ALPHA,UBODY                       MAN  31
      WRITE (6,1090) A,LL,MX,M2NEG,M2POS,NZ                             MAN  32
      WRITE (6,1100) MLT1,MLT2,MLT3,MLT4                                MAN  33
      IF (MLT1) 10,20,30                                                MAN  34
   10 WRITE (6,1110)                                                    MAN  35
      GO TO 1010                                                        MAN  36
```

```
   20 WRITE (6,1120)                                                    MAN  37
      GO TO 40                                                          MAN  38
   30 WRITE (6,1130)                                                    MAN  39
   40 IF (MLT2) 50,60,70                                                MAN  40
   50 WRITE (6,1140)                                                    MAN  41
      GO TO 1010                                                        MAN  42
   60 WRITE (6,1150)                                                    MAN  43
      GO TO 80                                                          MAN  44
   70 WRITE (6,1160)                                                    MAN  45
   80 IF (MLT3) 90,100,110                                              MAN  46
   90 WRITE (6,1170)                                                    MAN  47
      GO TO 1010                                                        MAN  48
  100 WRITE (6,1180)                                                    MAN  49
      GO TO 120                                                         MAN  50
  110 WRITE (6,1190)                                                    MAN  51
  120 IF (MLT4) 130,140,150                                             MAN  52
  130 WRITE (6,1200)                                                    MAN  53
      GO TO 1010                                                        MAN  54
  140 WRITE (6,1210)                                                    MAN  55
      GO TO 160                                                         MAN  56
  150 WRITE (6,1220)                                                    MAN  57
C                                                                       MAN  58
C     READ AND WRITE THE INPUT PARAMETERS WHICH INDICATE THE USER'S     MAN  59
C     SELECTION OF RESULTS TO BE PRINTED OUT.                           MAN  60
  160 READ (5,1230) IPOK,IPOP,IPOPC,IPODI,IPODC,IPODN,IPOD,IPOV,IPOUO,IPMAN  61
     1OWO,IPOUE,IPOWE                                                   MAN  62
      WRITE (6,1240)                                                    MAN  63
      WRITE (6,1250)                                                    MAN  64
      WRITE (6,1260)                                                    MAN  65
      WRITE (6,1270)                                                    MAN  66
      WRITE (6,1280)                                                    MAN  67
      WRITE (6,1290)                                                    MAN  68
      WRITE (6,1300)                                                    MAN  69
      WRITE (6,1240)                                                    MAN  70
      WRITE (6,1310) IPOK                                               MAN  71
      WRITE (6,1320) IPOP                                               MAN  72
```

```
      WRITE (6,1330) IPOPC                                              MAN  73
      WRITE (6,1340) IPODI                                              MAN  74
      WRITE (6,1350) IPODC                                              MAN  75
      WRITE (6,1360) IPODN                                              MAN  76
      WRITE (6,1370) IPOD                                               MAN  77
      WRITE (6,1380) IPOV                                               MAN  78
      WRITE (6,1390) IPOUO                                              MAN  79
      WRITE (6,1400) IPOWO                                              MAN  80
      WRITE (6,1410) IPOUE                                              MAN  81
      WRITE (6,1420) IPOWE                                              MAN  82
C                                                                       MAN  83
C                                                                       MAN  84
C     DOUBLE PRECISION CONSTANTS                                        MAN  85
      D0=0.0D0                                                          MAN  86
      DP25=2.5D-1                                                       MAN  87
      DP5=5.0D-1                                                        MAN  88
      DP75=7.5D-1                                                       MAN  89
      D1=1.0D0                                                          MAN  90
      D2=2.0D0                                                          MAN  91
      D3=3.0D0                                                          MAN  92
      D4=4.0D0                                                          MAN  93
      D5=5.0D0                                                          MAN  94
      D8=8.0D0                                                          MAN  95
C                                                                       MAN  96
C     EVALUATION OF 'STRETCHED' REAL COORDINATES, (XR,ZR) AND           MAN  97
C     OF TRANSFORMED COORDINATES, (X,Z)                                 MAN  98
      M1=MX-1                                                           MAN  99
      M2=(MX+1)/2                                                       MAN 100
      M3=M2-M2NEG                                                       MAN 101
      M4=M2+M2POS                                                       MAN 102
      WRITE (6,1430)                                                    MAN 103
      DO 170 I=1,MX                                                     MAN 104
      X(I)=DX*DFLOAT(I-M2)                                              MAN 105
      XSEC2(I)=D1-X(I)**2                                               MAN 106
      Y=X(I)                                                            MAN 107
      XR(I)=(D1/CA)*ARCTNH(Y)                                           MAN 108
```

```
      XR(1)=(-1.0D5)*ALPHA                                              MAN 109
      XR(MX)=(1.0D5)*ALPHA                                              MAN 110
C     XRDIM=DIMENSIONAL FORM OF XR                                      MAN 111
      XRDIM(I)=XR(I)/ALPHA                                              MAN 112
      WRITE (6,1440) I,X(I),XR(I),XRDIM(I),XSEC2(I)                     MAN 113
  170 CONTINUE                                                          MAN 114
      N1=NZ-1                                                           MAN 115
      N11=N1-1                                                          MAN 116
      N2=(NZ+1)/2                                                       MAN 117
      WRITE (6,1450)                                                    MAN 118
      DO 180 J=1,NZ                                                     MAN 119
      Z(J)=DZ*DFLOAT(J-N2)                                              MAN 120
      ZSEC2(J)=D1-Z(J)**2                                               MAN 121
      Y=Z(J)                                                            MAN 122
      ZR(J)=(D1/ALF)*ARCTNH(Y)                                          MAN 123
      ZR(1)=(-1.0D5)*ALPHA                                              MAN 124
      ZR(NZ)=(1.0D5)*ALPHA                                              MAN 125
C     ZRDIM=DIMENSIONAL FORM OF ZR                                      MAN 126
      ZRDIM(J)=ZR(J)/ALPHA                                              MAN 127
      WRITE (6,1460) J,Z(J),ZR(J),ZRDIM(J),ZSEC2(J)                     MAN 128
  180 CONTINUE                                                          MAN 129
C     DETERMINATION OF GRID AREA OCCUPIED BY OBSTACLE                   MAN 130
      ER=(1.27D0)*ALPHA                                                 MAN 131
      E=DTANH(ALF*ER)                                                   MAN 132
      EGRD=E/DZ                                                         MAN 133
      EGRD1=EGRD+DP5                                                    MAN 134
      EGRD=DFLOAT(IDINT(EGRD))                                          MAN 135
      EGRD1=DFLOAT(IDINT(EGRD1))                                        MAN 136
      IF (EGRD.LT.EGRD1) EGRD=EGRD1                                     MAN 137
      E=EGRD*DZ                                                         MAN 138
      N3=N2-IDINT(EGRD)                                                 MAN 139
      N4=N2+IDINT(EGRD)                                                 MAN 140
      N31=N3-1                                                          MAN 141
      N41=N4+1                                                          MAN 142
```

```
C     FIRST GUESS FOR INITIAL STREAM FUNCTION, P(I,J)                    MAN 143
      DO 190 I=1,MX                                                      MAN 144
      DO 190 J=1,NZ                                                      MAN 145
  190 P(I,J)=-ZR(J)                                                      MAN 146
      DO 220 I=M3,M4                                                     MAN 147
      DO 200 J=N3,N4                                                     MAN 148
  200 P(I,J)=D0                                                          MAN 149
      DO 210 J=1,N31                                                     MAN 150
  210 P(I,J)=((E+Z(J))/(E-D1))*(-ZR(J))                                  MAN 151
      DO 220 J=N41,NZ                                                    MAN 152
  220 P(I,J)=((E-Z(J))/(E-D1))*(-ZR(J))                                  MAN 153
C     OVER-RELAXATION FOR INITIAL STREAM FUNCTION, P(I,J)                MAN 154
      KK=31                                                              MAN 155
      DO 230 I=1,MX                                                      MAN 156
      DO 230 J=1,NZ                                                      MAN 157
C     FLOW IS INITIALLY IRROTATIONAL, HENCE...                           MAN 158
  230 VT1(I,J)=D0                                                        MAN 159
      IF (IPOK.EQ.0.AND.IPOP.EQ.0) GO TO 240                             MAN 160
      WRITE (6,1470)                                                     MAN 161
  240 CONTINUE                                                           MAN 162
      CALL RELAX (A,X,Z,ZR,DX,DZ,CA,ALF,P,VT1,KK,MX,M3,M4,NZ,N3,N4,IPOK)MAN 163
C     PRINT-OUT OF INITIAL TIME                                          MAN 164
      DIMT=T/(ALPHA*UBODY)                                               MAN 165
      IF (IPOP.EQ.0) GO TO 260                                           MAN 166
      WRITE (6,1600) T,DIMT                                              MAN 167
C     WRITE INITIAL STREAM FUNCTION, P(I,J)                              MAN 168
      WRITE (6,1480)                                                     MAN 169
      DO 250 I=1,MX                                                      MAN 170
  250 WRITE (6,1490) I,(P(I,J),J=1,NZ)                                   MAN 171
  260 CONTINUE                                                           MAN 172
C     COMPUTE CONTOUR ELEVATIONS FOR INITIAL STREAMLINES                 MAN 173
      IF (IPOPC.EQ.0) GO TO 320                                          MAN 174
      MESH=5                                                             MAN 175
      KZ=2*MESH+2                                                        MAN 176
      DO 270 K=1,KZ                                                      MAN 177
      PCONT(K)=D0                                                        MAN 178
```

```
      DO 270 I=1,MX                                                    MAN 179
  270 H(K,I)=D0                                                        MAN 180
      NPM=NZ-IDINT((DFLOAT(NZ)-D1)/D8)                                 MAN 181
      PMAX=DFLOAT(IDINT(-D1*P(1,NPM)))                                 MAN 182
      DO 280 J2=1,4                                                    MAN 183
      IF (DABS(P(1,NPM)+PMAX).LT.DP25) GO TO 290                       MAN 184
      PMAX=PMAX+DP25                                                   MAN 185
  280 CONTINUE                                                         MAN 186
  290 DP=PMAX/DFLOAT(MESH)                                             MAN 187
      CALL CONTUR (MX,M3,M4,NZ,N3,N4,MESH,Z,DZ,P,DP,D0,PCONT,H)        MAN 188
C     PUT CONTOUR ELEVATION, H, IN DIMENSIONAL FORM                    MAN 189
      DO 300 K=1,KZ                                                    MAN 190
      DO 300 I=1,MX                                                    MAN 191
      Y=H(K,I)                                                         MAN 192
  300 H(K,I)=(D1/ALF)*ARCTNH(Y)/ALPHA                                  MAN 193
      WRITE (6,1600) T,DIMT                                            MAN 194
C     PRINT-OUT OF CONTOUR ELEVATIONS FOR INITIAL STREAMLINES          MAN 195
      DO 310 K=1,KZ                                                    MAN 196
      WRITE (6,1500) PCONT(K),MX                                       MAN 197
  310 WRITE (6,1510) (H(K,I),I=1,MX)                                   MAN 198
  320 CONTINUE                                                         MAN 199
C     INITIAL SOLUTION FOR DENSITY FIELD.  DT1=DENSITY AT OLD TIME, AND MAN 200
C     DT2=DENSITY AT NEW TIME                                          MAN 201
      DO 330 I=1,MX                                                    MAN 202
      DO 330 J=2,N1                                                    MAN 203
  330 DT1(I,J)=D1-OMEG*DTANH(ZR(J))                                    MAN 204
      DO 340 I=1,MX                                                    MAN 205
      DT1(I,1)=DT1(I,2)                                                MAN 206
  340 DT1(I,NZ)=DT1(I,N1)                                              MAN 207
      DO 350 I=1,MX                                                    MAN 208
      DO 350 J=1,NZ                                                    MAN 209
      DT2(I,J)=DT1(I,J)                                                MAN 210
  350 CONTINUE                                                         MAN 211
```

```
C     CALCULATION AND PRINT-OUT OF INITIAL DIMENSIONAL DENSITY FIELD AT MAN 212
C     A TYPICAL CROSS-SECTION.                                          MAN 213
      IF (IPODI.EQ.0) GO TO 370                                         MAN 214
      WRITE (6,1470)                                                    MAN 215
      WRITE (6,1600) T,DIMT                                             MAN 216
      WRITE (6,1520)                                                    MAN 217
      WRITE (6,1530)                                                    MAN 218
      DO 360 J=1,NZ                                                     MAN 219
      J1=NZ+1-J                                                         MAN 220
      DDIM(2,J1)=DT1(2,J1)*DAVG                                         MAN 221
  360 WRITE (6,1540) J1,DDIM(2,J1)                                      MAN 222
  370 CONTINUE                                                          MAN 223
C     COMPUTE CONTOUR ELEVATIONS FOR INITIAL LINES OF CONSTANT DENSITY  MAN 224
      IF (IPODC.EQ.0) GO TO 410                                         MAN 225
      MESH=5                                                            MAN 226
      KZ=2*MESH+2                                                       MAN 227
      DO 380 K=1,KZ                                                     MAN 228
      DCONT(K)=D0                                                       MAN 229
      DO 380 I=1,MX                                                     MAN 230
  380 H(K,I)=D0                                                         MAN 231
      DD=(DT1(1,7)-D1)/DFLOAT(MESH)                                     MAN 232
      CALL CONTUR (MX,M3,M4,NZ,N3,N4,MESH,Z,DZ,DT1,DD,D1,DCONT,H)       MAN 233
C     PUT CONTOUR ELEVATION, H, IN DIMENSIONAL FORM                     MAN 234
      DO 390 K=1,KZ                                                     MAN 235
      DO 390 I=1,MX                                                     MAN 236
      Y=H(K,I)                                                          MAN 237
  390 H(K,I)=(D1/ALF)*ARCTNH(Y)/ALPHA                                   MAN 238
      WRITE (6,1600) T,DIMT                                             MAN 239
```

```
C     PRINT-OUT OF CONTOUR ELEVATIONS FOR INITIAL LINES OF                MAN 240
C     CONSTANT DENSITY                                                    MAN 241
      DO 400 K=1,KZ                                                       MAN 242
      WRITE (6,1550) DCONT(K),MX                                          MAN 243
  400 WRITE (6,1560) (H(K,I),I=1,MX)                                      MAN 244
  410 CONTINUE                                                            MAN 245
C     INITIAL SOLUTION FOR VORTICITY FIELD.  VT1=VORTICITY AT OLD TIME,   MAN 246
C     AND VT2=VORTICITY AT NEW TIME                                       MAN 247
      DO 420 I=1,MX                                                       MAN 248
      DO 420 J=1,NZ                                                       MAN 249
      VT2(I,J)=VT1(I,J)                                                   MAN 250
  420 CONTINUE                                                            MAN 251
C     INITIAL SOLUTION FOR VELOCITY FIELD.  UOLD=DP/DZ  WOLD=-DP/DX       MAN 252
      DO 430 I=2,M1                                                       MAN 253
      DO 430 J=3,N11                                                      MAN 254
      UOLD(I,J)=(P(I,J+1)-P(I,J-1))/(D2*DZ)                               MAN 255
      WOLD(I,J)=(P(I-1,J)-P(I+1,J))/(D2*DX)                               MAN 256
  430 CONTINUE                                                            MAN 257
      DO 440 I=1,MX                                                       MAN 258
      WOLD(I,1)=D0                                                        MAN 259
      WOLD(I,2)=D0                                                        MAN 260
      WOLD(I,NZ)=D0                                                       MAN 261
  440 WOLD(I,N1)=D0                                                       MAN 262
      DO 450 J=3,N11                                                      MAN 263
      UOLD(MX,J)=(P(MX,J+1)-P(MX,J-1))/(D2*DZ)                            MAN 264
      WOLD(MX,J)=WOLD(M1,J)                                               MAN 265
      UOLD(1,J)=(P(1,J+1)-P(1,J-1))/(D2*DZ)                               MAN 266
  450 WOLD(1,J)=WOLD(2,J)                                                 MAN 267
      DO 460 I=1,MX                                                       MAN 268
      UOLD(I,2)=(ZSEC2(3)/ZSEC2(2))*UOLD(I,3)                             MAN 269
  460 UOLD(I,N1)=(ZSEC2(N11)/ZSEC2(N1))*UOLD(I,N11)                       MAN 270
C     SET VELOCITY WITHIN REGION OCCUPIED BY SOLID BODY EQUAL TO ZERO.    MAN 271
      DO 470 I=M3,M4                                                      MAN 272
      DO 470 J=N3,N4                                                      MAN 273
      UOLD(I,J)=D0                                                        MAN 274
  470 WOLD(I,J)=D0                                                        MAN 275
```

```
C     CALCULATION AND PRINT-OUT OF INITIAL DIMENSIONAL U VELOCITY WITH  MAN 276
C     RESPECT TO THE EXPERIMENTER                                       MAN 277
      IF (IPOUE.EQ.0) GO TO 510                                         MAN 278
      DO 480 I=1,MX                                                     MAN 279
      DO 480 J=2,N1                                                     MAN 280
  480 URDIM(I,J)=((ALF*ZSEC2(J)*UOLD(I,J))*UBODY)+UBODY                 MAN 281
      DO 490 I=1,MX                                                     MAN 282
      URDIM(I,1)=D0                                                     MAN 283
  490 URDIM(I,NZ)=D0                                                    MAN 284
      WRITE (6,1470)                                                    MAN 285
      WRITE (6,1600) T,DIMT                                             MAN 286
      WRITE (6,1570)                                                    MAN 287
      DO 500 I=1,MX                                                     MAN 288
  500 WRITE (6,1690) I,(URDIM(I,J),J=1,NZ)                              MAN 289
  510 CONTINUE                                                          MAN 290
C     START OF TIME INCREMENTATION OUTER DO LOOP                        MAN 291
      LI=40                                                             MAN 292
      IF (IPOK.EQ.0) GO TO 520                                          MAN 293
      WRITE (6,1580)                                                    MAN 294
  520 CONTINUE                                                          MAN 295
      DO 1000 L=1,LL                                                    MAN 296
      T=T+DT                                                            MAN 297
C     EVALUATION OF VELOCITY FIELD.  U=DP/DZ  W=-DP/DX                  MAN 298
      DO 530 I=2,M1                                                     MAN 299
      DO 530 J=3,N11                                                    MAN 300
      U(I,J)=(P(I,J+1)-P(I,J-1))/(D2*DZ)                                MAN 301
      W(I,J)=(P(I-1,J)-P(I+1,J))/(D2*DX)                                MAN 302
  530 CONTINUE                                                          MAN 303
      DO 540 I=1,MX                                                     MAN 304
      W(I,1)=D0                                                         MAN 305
      W(I,2)=D0                                                         MAN 306
      W(I,NZ)=D0                                                        MAN 307
  540 W(I,N1)=D0                                                        MAN 308
      DO 550 J=3,N11                                                    MAN 309
      U(MX,J)=(P(MX,J+1)-P(MX,J-1))/(D2*DZ)                             MAN 310
      W(MX,J)=W(M1,J)                                                   MAN 311
      U(1,J)=(P(1,J+1)-P(1,J-1))/(D2*DZ)                                MAN 312
  550 W(1,J)=W(2,J)                                                     MAN 313
```

```
      DO 560 I=1,MX                                                    MAN 314
      U(I,2)=(ZSEC2(3)/ZSEC2(2))*U(I,3)                                MAN 315
  560 U(I,N1)=(ZSEC2(N11)/ZSEC2(N1))*U(I,N11)                          MAN 316
C     SET VELOCITY WITHIN REGION OCCUPIED BY SOLID BODY EQUAL TO ZERO.  MAN 317
      DO 570 I=M3,M4                                                   MAN 318
      DO 570 J=N3,N4                                                   MAN 319
      U(I,J)=D0                                                        MAN 320
  570 W(I,J)=D0                                                        MAN 321
C     EVALUATION OF NON-LINEAR CONVECTIVE TERMS IS BY THE SPECIAL      MAN 322
C     THREE-POINT NON-CENTRAL DIFFERENCES METHOD.                      MAN 323
C     NOMENCLATURE...                                                  MAN 324
C     DUUDX = D(U**2)/DX            VELOCITY                           MAN 325
C     DWUDZ = D(W*U)/DZ             VELOCITY                           MAN 326
C     DUWDX = D(U*W)/DX             VELOCITY                           MAN 327
C     DWWDZ = D(W**2)/DZ            VELOCITY                           MAN 328
C     DUVDX =D(U*VT1)/DX            VORTICITY                          MAN 329
C     DWVDZ = D(W*VT1)/DZ           VORTICITY                          MAN 330
C     DUDDX = D(U*DT1)/DX           DENSITY                            MAN 331
C     DWDDZ = D(W*DT1)/DZ           DENSITY                            MAN 332
      DO 580 I=1,M1                                                    MAN 333
      DO 580 J=2,N11                                                   MAN 334
      UAV(I,J)=(U(I+1,J)+U(I,J))/D2                                    MAN 335
  580 WAV(I,J)=(W(I,J+1)+W(I,J))/D2                                    MAN 336
      DO 590 I=2,M1                                                    MAN 337
      DO 590 J=3,N11                                                   MAN 338
      CALL NONLIN (DUDDX,UAV,DT1,DX,DWDDZ,WAV,DT1,DZ,I,J)              MAN 339
  590 CONTINUE                                                         MAN 340
C     TIME ADVANCEMENT OF DENSITY                                      MAN 341
      DO 600 I=2,M1                                                    MAN 342
      DO 600 J=3,N11                                                   MAN 343
      CALL DELSQR (DSQD,CA,X,DT1,DX,ALF,Z,DZ,I,J)                      MAN 344
      DT2(I,J)=DT1(I,J)+DT*(-CA*XSEC2(I)*ALF*ZSEC2(J)*(DUDDX(I,J)+DWDDZ(MAN 345
     1I,J))+(EPS/RE)*DSQD(I,J)*DFLOAT(MLT4))                           MAN 346
  600 CONTINUE                                                         MAN 347
```

```
      DO 610 J=3,N11                                                    MAN 348
      DT2(1,J)=DT2(2,J)                                                 MAN 349
      DT2(MX,J)=DT2(M1,J)                                               MAN 350
  610 CONTINUE                                                          MAN 351
C     DENSITY BOUNDARY CONDITION AT OBSTACLE...DT2=1.00; D(DT2)/DN=0.   MAN 352
      DO 620 I=M3,M4                                                    MAN 353
      DO 620 J=N3,N4                                                    MAN 354
  620 DT2(I,J)=D1                                                       MAN 355
      DO 630 I=M3,M4                                                    MAN 356
      DT2(I,N3-1)=DP75+DP25*DT2(I,N3-2)                                 MAN 357
  630 DT2(I,N4+1)=DP75+DP25*DT2(I,N4+2)                                 MAN 358
      DO 640 J=N3,N4                                                    MAN 359
      DT2(M3-1,J)=DP75+DP25*DT2(M3-2,J)                                 MAN 360
  640 DT2(M4+1,J)=DP75+DP25*DT2(M4+2,J)                                 MAN 361
C     TIME ADVANCEMENT OF VORTICITY                                     MAN 362
      DO 650 I=2,M1                                                     MAN 363
      DO 650 J=3,N11                                                    MAN 364
      CALL NONLIN (DUUDX,UAV,U,DX,DWUDZ,WAV,U,DZ,I,J)                   MAN 365
      C1=ALF*ZSEC2(J)                                                   MAN 366
      C2=C1                                                             MAN 367
      C3=CA*XSEC2(I)*C1*C1                                              MAN 368
      C4=C3/ZSEC2(J)                                                    MAN 369
      BOUS1(I,J)=C1*((DT1(I,J+1)-DT1(I,J-1))/(D2*DZ))*(C2*(U(I,J)-UOLD(IMAN 370
     1,J))/DT+C3*DUUDX(I,J)+C4*(ZSEC2(J)*DWUDZ(I,J)-D2*U(I,J)*W(I,J)*Z(JMAN 371
     2)))                                                               MAN 372
      CALL NONLIN (DUWDX,UAV,W,DX,DWWDZ,WAV,W,DZ,I,J)                   MAN 373
      C1=-CA*XSEC2(I)                                                   MAN 374
      C2=-C1                                                            MAN 375
      C3=CA*C2*ALF*ZSEC2(J)                                             MAN 376
      C4=C3*XSEC2(I)                                                    MAN 377
      BOUS2(I,J)=C1*((DT1(I+1,J)-DT1(I-1,J))/(D2*DX))*(C2*(W(I,J)-WOLD(IMAN 378
     1,J))/DT+C3*(XSEC2(I)*DUWDX(I,J)-D2*U(I,J)*W(I,J)*X(I))+C4*DWWDZ(I,MAN 379
     2J))                                                               MAN 380
      CALL NONLIN (DUVDX,UAV,VT1,DX,DWVDZ,WAV,VT1,DZ,I,J)               MAN 381
      CALL DELSQR (DSQV,CA,X,VT1,DX,ALF,Z,DZ,I,J)                       MAN 382
```

```
      VT2(I,J)=VT1(I,J)+DT*(-CA*XSEC2(I)*ALF*ZSEC2(J)*(DUVDX(I,J)+DWVDZ(MAN 383
     1I,J))+(D1/DT1(I,J))*(-DFLOAT(MLT1)*BOUS1(I,J)-DFLOAT(MLT2)*BOUS2(IMAN 384
     2,J)+(CA/(F*F))*XSEC2(I)*(DT1(I+1,J)-DT1(I-1,J))/(D2*DX)+(D1/RE)*DFMAN 385
     3LOAT(MLT3)*DSQV(I,J)))                                            MAN 386
  650 CONTINUE                                                          MAN 387
      DO 660 J=3,N11                                                    MAN 388
      VT2(1,J)=VT2(2,J)                                                 MAN 389
      VT2(MX,J)=VT2(M1,J)                                               MAN 390
  660 CONTINUE                                                          MAN 391
      DO 670 I=1,MX                                                     MAN 392
  670 VT2(I,N2)=D0                                                      MAN 393
C     VORTICITY BOUNDARY CONDITION AT OBSTACLE                          MAN 394
      DO 680 I=M3,M4                                                    MAN 395
      VT2(I,N3)=((ALF*ZSEC2(N3)/DZ)**2)*(-P(I,N3-3)+D4*P(I,N3-2)-D5*P(I,MAN 396
     1N3-1)+D2*P(I,N3))                                                 MAN 397
  680 VT2(I,N4)=((ALF*ZSEC2(N4)/DZ)**2)*(-P(I,N4+3)+D4*P(I,N4+2)-D5*P(I,MAN 398
     1N4+1)+D2*P(I,N4))                                                 MAN 399
      DO 690 J=N3,N4                                                    MAN 400
      VT2(M3,J)=((CA*XSEC2(M3)/DX)**2)*(-P(M3-3,J)+D4*P(M3-2,J)-D5*P(M3-MAN 401
     11,J)+D2*P(M3,J))                                                  MAN 402
  690 VT2(M4,J)=((CA*XSEC2(M4)/DX)**2)*(-P(M4+3,J)+D4*P(M4+2,J)-D5*P(M4+MAN 403
     11,J)+D2*P(M4,J))                                                  MAN 404
C     OVER-RELAXATION FOR STREAM FUNCTION, P(I,J)                       MAN 405
      KK=11                                                             MAN 406
      CALL RELAX (A,X,Z,ZR,DX,DZ,CA,ALF,P,VT1,KK,MX,M3,M4,NZ,N3,N4,IPOK)MAN 407
C     CONVERT NEW TIME VARIABLE TO OLD                                  MAN 408
      DO 700 I=1,MX                                                     MAN 409
      DO 700 J=1,NZ                                                     MAN 410
      DT1(I,J)=DT2(I,J)                                                 MAN 411
      VT1(I,J)=VT2(I,J)                                                 MAN 412
      UOLD(I,J)=U(I,J)                                                  MAN 413
      WOLD(I,J)=W(I,J)                                                  MAN 414
  700 CONTINUE                                                          MAN 415
```

```
C     CHECK NUMBER OF ITERATIONS, L, THROUGH TIME INCREMENTATION DO LOOPMAN 416
C     IF L=LI, PRINT OUT RESULTS, INCREMENT LI, AND REPEAT THE        MAN 417
C     TIME INCREMENTATION AND PERIODIC PRINT-OUT UNTIL L=LI=LL.       MAN 418
      IF (L-LI) 1000,710,710                                          MAN 419
  710 LI=LI+40                                                        MAN 420
C     CALCULATION OF DIMENSIONAL TIME                                 MAN 421
      DIMT=T/(ALPHA*UBODY)                                            MAN 422
C                                                                     MAN 423
C     PRINT-OUT OF RESULTS                                            MAN 424
C                                                                     MAN 425
C                                                                     MAN 426
      IF (IPODN.EQ.0) GO TO 730                                       MAN 427
      WRITE (6,1590)                                                  MAN 428
      WRITE (6,1600) T,DIMT                                           MAN 429
C     PRINT-OUT NON-DIMENSIONAL DENSITY FIELD                         MAN 430
      WRITE (6,1610)                                                  MAN 431
      DO 720 I=1,MX                                                   MAN 432
  720 WRITE (6,1620) I,(DT2(I,J),J=1,NZ)                              MAN 433
  730 CONTINUE                                                        MAN 434
C     CALCULATE AND PRINT-OUT DIMENSIONAL DENSITY FIELD               MAN 435
      IF (IPOD.EQ.0) GO TO 760                                        MAN 436
      DO 740 I=1,MX                                                   MAN 437
      DO 740 J=1,NZ                                                   MAN 438
  740 DDIM(I,J)=DT2(I,J)*DAVG                                         MAN 439
      WRITE (6,1590)                                                  MAN 440
      WRITE (6,1600) T,DIMT                                           MAN 441
      WRITE (6,1630)                                                  MAN 442
      DO 750 I=1,MX                                                   MAN 443
  750 WRITE (6,1620) I,(DDIM(I,J),J=1,NZ)                             MAN 444
  760 CONTINUE                                                        MAN 445
C     PRINT-OUT NON-DIMENSIONAL VORTICITY FIELD                       MAN 446
      IF (IPOV.EQ.0) GO TO 780                                        MAN 447
      WRITE (6,1590)                                                  MAN 448
      WRITE (6,1600) T,DIMT                                           MAN 449
      WRITE (6,1640)                                                  MAN 450
```

```
      DO 770 I=1,MX                                                    MAN 451
  770 WRITE (6,1650) I,(VT2(I,J),J=1,NZ)                               MAN 452
  780 CONTINUE                                                         MAN 453
C     PRINT-OUT NON-DIMENSIONAL STREAM FUNCTION                        MAN 454
      IF (IPOP.EQ.0) GO TO 800                                         MAN 455
      WRITE (6,1590)                                                   MAN 456
      WRITE (6,1600) T,DIMT                                            MAN 457
      WRITE (6,1660)                                                   MAN 458
      DO 790 I=1,MX                                                    MAN 459
  790 WRITE (6,1670) I,(P(I,J),J=1,NZ)                                 MAN 460
  800 CONTINUE                                                         MAN 461
C     REFER THE CALCULATED VELOCITIES TO THE 'REAL' COORDINATE SYSTEM  MAN 462
      DO 810 I=1,MX                                                    MAN 463
      DO 810 J=2,N1                                                    MAN 464
      UR(I,J)=ALF*ZSEC2(J)*U(I,J)                                      MAN 465
      WR(I,J)=CA*XSEC2(I)*W(I,J)                                       MAN 466
  810 CONTINUE                                                         MAN 467
      DO 820 I=1,MX                                                    MAN 468
      UR(I,1)=-D1                                                      MAN 469
      UR(I,NZ)=-D1                                                     MAN 470
      WR(I,1)=D0                                                       MAN 471
      WR(I,NZ)=D0                                                      MAN 472
  820 CONTINUE                                                         MAN 473
C     PRINT-OUT NON-DIMENSIONAL VELOCITY FIELD                         MAN 474
      IF (IPOUO.EQ.0) GO TO 840                                        MAN 475
      WRITE (6,1590)                                                   MAN 476
      WRITE (6,1600) T,DIMT                                            MAN 477
      WRITE (6,1680)                                                   MAN 478
      DO 830 I=1,MX                                                    MAN 479
  830 WRITE (6,1690) I,(UR(I,J),J=1,NZ)                                MAN 480
  840 CONTINUE                                                         MAN 481
      IF (IPOWO.EQ.0) GO TO 860                                        MAN 482
      WRITE (6,1590)                                                   MAN 483
      WRITE (6,1600) T,DIMT                                            MAN 484
      WRITE (6,1700)                                                   MAN 485
```

```
      DO 850 I=1,MX                                                    MAN 486
  850 WRITE (6,1690) I,(WR(I,J),J=1,NZ)                                MAN 487
  860 CONTINUE                                                         MAN 488
C     CALCULATE AND PRINT-OUT DIMENSIONAL VELOCITIES WITH RESPECT TO   MAN 489
C     AN OBSERVER WHO SEES THE OBSTACLE MOVING IN THE +X-DIRECTION     MAN 490
C     WITH VELOCITY EQUAL TO UBODY.  (I.E., THE VELOCITIES ARE MADE    MAN 491
C     DIMENSIONAL AND A GALILEAN TRANSFORMATION OF THE U VELOCITY IS   MAN 492
C     MADE.)                                                           MAN 493
      DO 870 I=1,MX                                                    MAN 494
      DO 870 J=1,NZ                                                    MAN 495
      URDIM(I,J)=(UR(I,J)*UBODY)+UBODY                                 MAN 496
  870 WRDIM(I,J)=WR(I,J)*UBODY                                         MAN 497
      IF (IPOUE.EQ.0) GO TO 890                                        MAN 498
      WRITE (6,1590)                                                   MAN 499
      WRITE (6,1600) T,DIMT                                            MAN 500
      WRITE (6,1710)                                                   MAN 501
      DO 880 I=1,MX                                                    MAN 502
  880 WRITE (6,1690) I,(URDIM(I,J),J=1,NZ)                             MAN 503
  890 CONTINUE                                                         MAN 504
      IF (IPOWE.EQ.0) GO TO 910                                        MAN 505
      WRITE (6,1590)                                                   MAN 506
      WRITE (6,1600) T,DIMT                                            MAN 507
      WRITE (6,1720)                                                   MAN 508
      DO 900 I=1,MX                                                    MAN 509
  900 WRITE (6,1690) I,(WRDIM(I,J),J=1,NZ)                             MAN 510
  910 CONTINUE                                                         MAN 511
C     COMPUTE COUTOUR ELEVATIONS FOR STREAMLINES                       MAN 512
      IF (IPOPC.EQ.0) GO TO 950                                        MAN 513
      MESH=5                                                           MAN 514
      KZ=2*MESH+2                                                      MAN 515
      DO 920 K=1,KZ                                                    MAN 516
      PCONT(K)=D0                                                      MAN 517
      DO 920 I=1,MX                                                    MAN 518
  920 H(K,I)=D0                                                        MAN 519
      CALL CONTUR (MX,M3,M4,NZ,N3,N4,MESH,Z,DZ,P,DP,D0,PCONT,H)        MAN 520
```

```
C     PUT CONTOUR ELEVATION, H, IN DIMENSIONAL FORM                    MAN 521
      DO 930 K=1,KZ                                                    MAN 522
      DO 930 I=1,MX                                                    MAN 523
      Y=H(K,I)                                                         MAN 524
  930 H(K,I)=(D1/ALF)*ARCTNH(Y)/ALPHA                                  MAN 525
      WRITE (6,1600) T,DIMT                                            MAN 526
C     PRINT-OUT OF CONTOUR ELEVATIONS FOR STREAMLINES                  MAN 527
      DO 940 K=1,KZ                                                    MAN 528
      WRITE (6,1730) PCONT(K),MX                                       MAN 529
  940 WRITE (6,1740) (H(K,I),I=1,MX)                                   MAN 530
  950 CONTINUE                                                         MAN 531
C     COMPUTE CONTOUR ELEVATIONS FOR LINES OF CONSTANT DENSITY         MAN 532
      IF (IPODC.EQ.0) GO TO 990                                        MAN 533
      MESH=5                                                           MAN 534
      KZ=2*MESH+2                                                      MAN 535
      DO 960 K=1,KZ                                                    MAN 536
      DCONT(K)=D0                                                      MAN 537
      DO 960 I=1,MX                                                    MAN 538
  960 H(K,I)=D0                                                        MAN 539
      CALL CONTUR (MX,M3,M4,NZ,N3,N4,MESH,Z,DZ,DT2,DD,D1,DCONT,H)      MAN 540
C     PUT CONTOUR ELEVATION, H, IN DIMENSIONAL FORM                    MAN 541
      DO 970 K=1,KZ                                                    MAN 542
      DO 970 I=1,MX                                                    MAN 543
      Y=H(K,I)                                                         MAN 544
  970 H(K,I)=(D1/ALF)*ARCTNH(Y)/ALPHA                                  MAN 545
      WRITE (6,1600) T,DIMT                                            MAN 546
C     PRINT-OUT OF CONTOUR ELEVATIONS FOR LINES OF CONSTANT DENSITY    MAN 547
      DO 980 K=1,KZ                                                    MAN 548
      WRITE (6,1750) DCONT(K),MX                                       MAN 549
  980 WRITE (6,1760) (H(K,I),I=1,MX)                                   MAN 550
  990 CONTINUE                                                         MAN 551
 1000 CONTINUE                                                         MAN 552
 1010 STOP                                                             MAN 553
C                                                                      MAN 554
 1020 FORMAT (1H1)                                                     MAN 555
 1030 FORMAT (20A4/,20A4/,20A4/,20A4)                                  MAN 556
```

```
1040 FORMAT (4F6.3,F6.5,F6.1,F6.5,F6.4,F6.5,3F6.2)                              MAN 557
1050 FORMAT (9I6)                                                               MAN 558
1060 FORMAT ('0DX= ',F6.3,'  DZ= ',F6.3,'  DT= ',F6.3,'  T= ',F6.3)             MAN 559
1070 FORMAT ('0F= ',F8.5,'  RE= ',F6.1,'  EPS= ',F8.5)                          MAN 560
1080 FORMAT ('0CA= ',F6.3,'  ALF= ',F6.3,'  DAVG= ',F6.4,'  OMEG=',F8.5MAN 561
     1,'  ALPHA= ',F6.2,,'  UBODY= ',F6.2)                                      MAN 562
1090 FORMAT ('0A= ',F6.2,'   LL= ',I6,'   MX= ',I6,'    M2NEG= ',I6,'  MAN 563
     1 M2POS= ',I6,'   NZ= ',16)                                               MAN 564
1100 FORMAT ('0MLT1= ',I5,'  MLT2= ',I5,'  MLT3= ',I5,'  MLT4= ',I5)           MAN 565
1110 FORMAT ('0INPUT DATA IS IN ERROR.  MLT1 CANNOT BE NEGATIVE')              MAN 566
1120 FORMAT ('0SINCE MLT1=0, FIRST BOUSSINESQ TERM WILL BE NEGLECTED')         MAN 567
1130 FORMAT ('0SINCE MLT1=1, FIRST BOUSSINESQ TERM WILL BE INCLUDED')          MAN 568
1140 FORMAT ('0INPUT DATA IS IN ERROR.  MLT2 CANNOT BE NEGATIVE')              MAN 569
1150 FORMAT ('0SINCE MLT2=0, SECOND BOUSSINESQ TERM WILL BE NEGLECTED')MAN 570
1160 FORMAT ('0SINCE MLT2=1, SECOND BOUSSINESQ TERM WILL BE INCLUDED')         MAN 571
1170 FORMAT ('0INPUT DATA IS IN ERROR.  MLT3 CANNOT BE NEGATIVE')              MAN 572
1180 FORMAT ('0SINCE MLT3=0, VORTICITY DIFFUSION TERM WILL BE NEGLECTEDMAN 573
     1')                                                                       MAN 574
1190 FORMAT ('0SINCE MLT3=1, VORTICITY DIFFUSION TERM WILL BE INCLUDED'MAN 575
     1)                                                                        MAN 576
1200 FORMAT ('0INPUT DATA IS IN ERROR.  MLT4 CANNOT BE NEGATIVE')              MAN 577
1210 FORMAT ('0SINCE MLT4=0, DENSITY DIFFUSION TERM WILL BE NEGLECTED')MAN 578
1220 FORMAT ('0SINCE MLT4=1, DENSITY DIFFUSION TERM WILL BE INCLUDED')         MAN 579
1230 FORMAT (12I6)                                                              MAN 580
1240 FORMAT (1H0)                                                               MAN 581
1250 FORMAT ('0THE FOLLOWING INPUT PARAMETERS INDICATE THOSE RESULTS WHMAN 582
     1ICH THE USER HAS SELECTED TO BE PRINTED OUT.')                           MAN 583
1260 FORMAT ('0THE 12 PARAMETERS ARE READ FROM THE INPUT CARD AS INTEGEMAN 584
     1RS IN 12 FIELDS OF 6 COLUMNS EACH.')                                     MAN 585
1270 FORMAT ('0IF A PARAMETER = 0, (I.E., BLANK OR 0 ON THE INPUT CARD)MAN 586
     1, THE RESULTS CORRESPONDING TO THIS PARAMETER')                          MAN 587
1280 FORMAT ('0ARE  N O T  PRINTED OUT.  IF THE PRINT-OUT IS DESIRED, AMAN 588
     1 NON-ZERO INTEGER MUST BE ASSIGNED TO THE PARAMETER.')                   MAN 589
1290 FORMAT ('0THE FOLLOWING LIST GIVES EACH PARAMETER IN THE ORDER IN MAN 590
     1WHICH IT IS READ IN, THE RESULT PRINT-OUT(S)')                           MAN 591
```

```
1300 FORMAT ('0TO WHICH IT CORRESPONDS, AND THE VALUE CHOSEN FOR IT FORMAN 592
    1  T H I S  RUN.')                                                  MAN 593
1310 FORMAT ('0IPOK -- NUMBER OF ITERATIONS, K, THROUGH SUBROUTINE RELAMAN 594
    1X ----- IPOK=',I3)                                                MAN 595
1320 FORMAT ('0IPOP -- STREAM FUNCTION, P, BOTH INITIAL AND AT LATER TIMAN 596
    1ME ---- IPOP=',I3)                                                MAN 597
1330 FORMAT ('0IPOPC -- STREAM FUNCTION CONTOUR ELEVATIONS ------------MAN 598
    1------- IPOPC=',I2)                                               MAN 599
1340 FORMAT ('0IPODI -- INITIAL DENSITY PROFILE AT A TYPICAL CROSS SECTMAN 600
    1ION --- IPODI=',I2)                                               MAN 601
1350 FORMAT ('0IPODC -- DENSITY CONTOUR ELEVATIONS --------------------MAN 602
    1------- IPODC=',I2)                                               MAN 603
1360 FORMAT ('0IPODN -- NON-DIMENSIONAL DENSITY AT LATER TIME ---------MAN 604
    1------- IPODN=',I2)                                               MAN 605
1370 FORMAT ('0IPOD -- DIMENSIONAL DENSITY AT LATER TIME --------------MAN 606
    1------- IPOD=',I3)                                                MAN 607
1380 FORMAT ('0IPOV -- VORTICITY FIELD --------------------------------MAN 608
    1------- IPOV=',I3)                                                MAN 609
1390 FORMAT ('0IPOUO -- NON-DIMENSIONAL U VELOCITY WITH RESPECT TO OBSTMAN 610
    1ACLE -- IPOUO=',I2)                                               MAN 611
1400 FORMAT ('0IPOWO -- NON-DIMENSIONAL W VELOCITY WITH RESPECT TO OBSTMAN 612
    1ACLE -- IPOWO=',I2)                                               MAN 613
1410 FORMAT ('0IPOUE -- DIMENSIONAL U VELOCITY WITH RESPECT TO EXPERIMEMAN 614
    1NTER -- IPOUE=',I2)                                               MAN 615
1420 FORMAT ('0IPOWE -- DIMENSIONAL W VELOCITY WITH RESPECT TO EXPERIMEMAN 616
    1NTER -- IPOWE=',I2)                                               MAN 617
1430 FORMAT (1H1)                                                      MAN 618
1440 FORMAT (' I= ',I3,'  X= ',F7.4,'  XR= ',F10.2,'  XRDIM= ',F10.2,' MAN 619
    1CM.',/    (1.-X(I)**2)= ',F7.4)                                   MAN 620
1450 FORMAT (1H1)                                                      MAN 621
1460 FORMAT (' J= ',I3,'  Z= ',F7.4,'  ZR= ',F10.2,'  ZRDIM= ',F10.2,' MAN 622
    1CM.',/    (1.-Z(J)**2)= ',F7.4)                                   MAN 623
1470 FORMAT (1H1)                                                      MAN 624
1480 FORMAT ('0INITIAL NON-DIMENSIONAL STREAM FUNCTION')               MAN 625
1490 FORMAT (' I=',I3/,(8F15.3))                                       MAN 626
1500 FORMAT ('0CONTOUR ELEVATIONS IN CENTIMETERS FOR THE INITIAL STREAMMAN 627
    1LINE P=',F6.2,', FOR I=1,',I3,'.')                                MAN 628
```

```
 1510 FORMAT (1H0,(8F15.2))                                                    MAN 629
 1520 FORMAT ('0INITIAL DIMENSIONAL DENSITY FIELD AT A TYPICAL CROSS-SECMAN 630
     1TION, (GM./CU. CM.)')                                                   MAN 631
 1530 FORMAT (1H0)                                                            MAN 632
 1540 FORMAT (' J= ',I3,F10.4)                                                MAN 633
 1550 FORMAT ('0CONTOUR ELEVATIONS IN CENTIMETERS FOR THE DT1=',F6.4,' IMAN 634
     1NITIAL LINE OF CONSTANT NON-DIMENSIONAL DENSITY    I=1,',I2,'.')       MAN 635
 1560 FORMAT (1H0,(8F15.2))                                                   MAN 636
 1570 FORMAT ('0INITIAL DIMENSIONAL U VELOCITY WITH RESPECT TO THE EXPERMAN 637
     1IMENTER, (CM./SEC.)')                                                   MAN 638
 1580 FORMAT (1H1)                                                            MAN 639
 1590 FORMAT (1H1)                                                            MAN 640
 1600 FORMAT ('0NON-DIMENSIONAL TIME= ',F7.3,'  DIMENSIONAL TIME= ',F7.3MAN 641
     1,' SECONDS')                                                            MAN 642
 1610 FORMAT ('0NON-DIMENSIONAL DENSITY FIELD')                               MAN 643
 1620 FORMAT (' I=',I3/,(8F15.4))                                             MAN 644
 1630 FORMAT ('0DIMENSIONAL DENSITY FIELD, (GM./CU. CM.)')                    MAN 645
 1640 FORMAT ('0NON-DIMENSIONAL VORTICITY FIELD')                             MAN 646
 1650 FORMAT (' I=',I3/,(8F15.3))                                             MAN 647
 1660 FORMAT ('0NON-DIMENSIONAL STREAM FUNCTION')                             MAN 648
 1670 FORMAT (' I=',I3/,(8F15.3))                                             MAN 649
 1680 FORMAT ('0NON-DIMENSIONAL U VELOCITY WITH RESPECT TO THE OBSTACLE'MAN 650
     1)                                                                       MAN 651
 1690 FORMAT (' I=',I3/,(8F15.2))                                             MAN 652
 1700 FORMAT ('0NON-DIMENSIONAL W VELOCITY WITH RESPECT TO THE OBSTACLE'MAN 653
     1)                                                                       MAN 654
 1710 FORMAT ('0DIMENSIONAL U VELOCITY WITH RESPECT TO THE EXPERIMENTER,MAN 655
     1 (CM./SEC.)')                                                          MAN 656
 1720 FORMAT ('0DIMENSIONAL W VELOCITY WITH RESPECT TO THE EXPERIMENTER,MAN 657
     1 (CM./SEC.)')                                                          MAN 658
 1730 FORMAT ('0CONTOUR ELEVATIONS IN CENTIMETERS FOR THE P=',F6.2,' STRMAN 659
     1EAMLINE;   I=1,',I3,'.')                                               MAN 660
 1740 FORMAT (1H0,(8F15.2))                                                   MAN 661
 1750 FORMAT ('0CONTOUR ELEVATIONS IN CENTIMETERS FOR THE DT2=',F6.4,' LMAN 662
     1INE OF CONSTANT NON-DIMENSIONAL DENSITY;   I=1,',I3,'.')                MAN 663
 1760 FORMAT (1H0,(8F15.2))                                                   MAN 664
      END                                                                     MAN 665-
```

```
      SUBROUTINE RELAX (A,X,Z,ZR,DX,DZ,CA,ALF,P,ETA,KK,MX,M3,M4,NZ,N3,N4RLX    1
     1,IPOK)                                                            RLX    2
      IMPLICIT REAL*8(A-H,O-Z)                                          RLX    3
      DIMENSION X(MX), Z(NZ), ZR(NZ), P(MX,NZ), PA(81,41), ETA(MX,NZ)   RLX    4
      D0=0.0D0                                                          RLX    5
      D4=4.0D0                                                          RLX    6
      M1=MX-1                                                           RLX    7
      M31=M3-1                                                          RLX    8
      M32=M3-2                                                          RLX    9
      M41=M4+1                                                          RLX   10
      M42=M4+2                                                          RLX   11
      N1=NZ-1                                                           RLX   12
      N11=N1-1                                                          RLX   13
      N2=(NZ+1)/2                                                       RLX   14
      N21=N2+1                                                          RLX   15
      N42=N4+2                                                          RLX   16
      DO 150 K=1,150                                                    RLX   17
      DO 10 I=1,MX                                                      RLX   18
   10 P(I,N2)=D0                                                        RLX   19
      DO 20 I=M3,M4                                                     RLX   20
      DO 20 J=N3,N4                                                     RLX   21
   20 P(I,J)=D0                                                         RLX   22
      DO 30 I=M3,M4                                                     RLX   23
      P(I,N3-1)=P(I,N3-2)/D4                                            RLX   24
   30 P(I,N4+1)=P(I,N4+2)/D4                                            RLX   25
      DO 40 J=N3,N4                                                     RLX   26
      P(M3-1,J)=P(M3-2,J)/D4                                            RLX   27
   40 P(M4+1,J)=P(M4+2,J)/D4                                            RLX   28
      DO 50 I=1,MX                                                      RLX   29
      P(I,1)=-ZR(1)                                                     RLX   30
      P(I,2)=-ZR(2)                                                     RLX   31
      P(I,N1)=-ZR(N1)                                                   RLX   32
   50 P(I,NZ)=-ZR(NZ)                                                   RLX   33
      DO 60 I=2,M32                                                     RLX   34
      DO 60 J=N21,N11                                                   RLX   35
      CALL PSI (A,I,J,P,X,Z,CA,DX,DZ,ALF,ETA)                           RLX   36
```

```
   60 CONTINUE                                                          RLX  37
      DO 70 I=M31,M41                                                   RLX  38
      DO 70 J=N42,N11                                                   RLX  39
      CALL PSI (A,I,J,P,X,Z,CA,DX,DZ,ALF,ETA)                           RLX  40
   70 CONTINUE                                                          RLX  41
      DO 80 I=M42,M1                                                    RLX  42
      DO 80 J=N21,N11                                                   RLX  43
      CALL PSI (A,I,J,P,X,Z,CA,DX,DZ,ALF,ETA)                           RLX  44
   80 CONTINUE                                                          RLX  45
C     TEST FOR CONVERGENCE                                              RLX  46
      IF (K-KK) 150,90,110                                              RLX  47
   90 DO 100 I=1,MX                                                     RLX  48
      DO 100 J=N2,NZ                                                    RLX  49
  100 PA(I,J)=P(I,J)                                                    RLX  50
      GO TO 150                                                         RLX  51
  110 DO 120 I=1,MX                                                     RLX  52
      DO 120 J=N2,NZ                                                    RLX  53
      IF (DABS(P(I,J)-PA(I,J))-0.0005) 120,120,140                      RLX  54
  120 CONTINUE                                                          RLX  55
C     TAKING ADVANTAGE OF SYMMETRY ABOUT THE HORIZONTAL CENTER LINE     RLX  56
      DO 130 I=1,MX                                                     RLX  57
      DO 130 J=2,N2                                                     RLX  58
  130 P(I,N2-J+1)=-P(I,N2+J-1)                                          RLX  59
      IF (IPOK.EQ.0) GO TO 160                                          RLX  60
      WRITE (6,170) K                                                   RLX  61
      GO TO 160                                                         RLX  62
  140 KK=KK+10                                                          RLX  63
  150 CONTINUE                                                          RLX  64
      WRITE (6,180) K                                                   RLX  65
  160 CONTINUE                                                          RLX  66
      RETURN                                                            RLX  67
C                                                                       RLX  68
  170 FORMAT (' K= ',I3)                                                RLX  69
  180 FORMAT ('0THE OVER-RELAXATION DOES NOT CONVERGE.  K=',I3)         RLX  70
      END                                                               RLX  71-
```

```
      SUBROUTINE PSI (A,I,J,P,X,Z,CA,DX,DZ,ALF,ETA)                      PSI    1
      IMPLICIT REAL*8(A-H,O-Z)                                           PSI    2
      DIMENSION X(81), XSEC2(81), Z(41), ZSEC2(41), P(81,41), ETA(81,41)PSI    3
      D=DX/DZ                                                            PSI    4
      DP5=5.0D-1                                                         PSI    5
      D1=1.0D0                                                           PSI    6
      XSEC2(I)=D1-X(I)**2                                                PSI    7
      ZSEC2(J)=D1-Z(J)**2                                                PSI    8
      C1=DP5*A/(((CA*XSEC2(I))**2)+((ALF*ZSEC2(J)*D)**2))                PSI    9
      C2=-DX*DX                                                          PSI   10
      C3=(CA*XSEC2(I))**2                                                PSI   11
      C4=-CA*CA*X(I)*XSEC2(I)*DX                                         PSI   12
      C5=(ALF*ZSEC2(J)*D)**2                                             PSI   13
      C6=-ALF*ALF*Z(J)*ZSEC2(J)*DX*DX/DZ                                 PSI   14
      P(I,J)=(D1-A)*P(I,J)+C1*(C2*ETA(I,J)+C3*(P(I+1,J)+P(I-1,J))+C4*(P(PSI   15
     1I+1,J)-P(I-1,J))+C5*(P(I,J+1)+P(I,J-1))+C6*(P(I,J+1)-P(I,J-1)))    PSI   16
      RETURN                                                             PSI   17
      END                                                                PSI   18-
```

```
      SUBROUTINE NONLIN (DDX,AV1,FN1,DX,DDZ,AV2,FN2,DZ,I,J)                NLN   1
      IMPLICIT REAL*8(A-H,O-Z)                                             NLN   2
      DIMENSION DDX(81,41), AV1(81,41), FN1(81,41), DDZ(81,41), AV2(81,4NLN   3
     11), FN2(81,41)                                                       NLN   4
      D0=0.0D0                                                             NLN   5
      IF (AV1(I,J).GE.D0.AND.AV1(I-1,J).GE.D0) GO TO 10                    NLN   6
      IF (AV1(I,J).LT.D0.AND.AV1(I-1,J).LT.D0) GO TO 20                    NLN   7
      IF (AV1(I,J).GE.D0.AND.AV1(I-1,J).LT.D0) GO TO 30                    NLN   8
      DDX(I,J)=(AV1(I,J)*FN1(I+1,J)-AV1(I-1,J)*FN1(I-1,J))/DX              NLN   9
      GO TO 40                                                             NLN  10
   10 DDX(I,J)=(AV1(I,J)*FN1(I,J)-AV1(I-1,J)*FN1(I-1,J))/DX                NLN  11
      GO TO 40                                                             NLN  12
   20 DDX(I,J)=(AV1(I,J)*FN1(I+1,J)-AV1(I-1,J)*FN1(I,J))/DX                NLN  13
      GO TO 40                                                             NLN  14
   30 DDX(I,J)=(AV1(I,J)*FN1(I,J)-AV1(I-1,J)*FN1(I,J))/DX                  NLN  15
   40 IF (AV2(I,J).GE.D0.AND.AV2(I,J-1).GE.D0) GO TO 50                    NLN  16
      IF (AV2(I,J).LT.D0.AND.AV2(I,J-1).LT.D0) GO TO 60                    NLN  17
      IF (AV2(I,J).GE.D0.AND.AV2(I,J-1).LT.D0) GO TO 70                    NLN  18
      DDZ(I,J)=(AV2(I,J)*FN2(I,J+1)-AV2(I,J-1)*FN2(I,J-1))/DZ              NLN  19
      GO TO 80                                                             NLN  20
   50 DDZ(I,J)=(AV2(I,J)*FN2(I,J)-AV2(I,J-1)*FN2(I,J-1))/DZ                NLN  21
      GO TO 80                                                             NLN  22
   60 DDZ(I,J)=(AV2(I,J)*FN2(I,J+1)-AV2(I,J-1)*FN2(I,J))/DZ                NLN  23
      GO TO 80                                                             NLN  24
   70 DDZ(I,J)=(AV2(I,J)*FN2(I,J)-AV2(I,J-1)*FN2(I,J))/DZ                  NLN  25
   80 RETURN                                                               NLN  26
      END                                                                  NLN  27-
```

```
      SUBROUTINE DELSQR (DSQFN,CA,X,FN,DX,ALF,Z,DZ,I,J)                 DSQ    1
      IMPLICIT REAL*8(A-H,O-Z)                                          DSQ    2
      DIMENSION X(81), XSEC2(81), Z(41), ZSEC2(41), DSQFN(81,41), FN(81,DSQ    3
     141)                                                               DSQ    4
      D1=1.0D0                                                          DSQ    5
      D2=2.0D0                                                          DSQ    6
      XSEC2(I)=D1-X(I)**2                                               DSQ    7
      ZSEC2(J)=D1-Z(J)**2                                               DSQ    8
      C1=(CA*XSEC2(I))**2                                               DSQ    9
      C2=-D2*CA*CA*X(I)*XSEC2(I)                                        DSQ   10
      C3=(ALF*ZSEC2(J))**2                                              DSQ   11
      C4=-D2*ALF*ALF*Z(J)*ZSEC2(J)                                      DSQ   12
      DSQFN(I,J)=C1*(FN(I+1,J)-D2*FN(I,J)+FN(I-1,J))/(DX*DX)+C2*(FN(I+1,DSQ   13
     1J)-FN(I-1,J))/(D2*DX)+C3*(FN(I,J+1)-D2*FN(I,J)+FN(I,J-1))/(DZ*DZ)+DSQ   14
     2C4*(FN(I,J+1)-FN(I,J-1))/(D2*DZ)                                  DSQ   15
      RETURN                                                            DSQ   16
      END                                                               DSQ   17-
```

```
      SUBROUTINE CONTUR (MX,M3,M4,NZ,N3,N4,MESH,Z,DZ,F,DF,FAV,FCONT,H)  CON    1
      IMPLICIT REAL*8(A-H,O-Z)                                          CON    2
      DIMENSION Z(NZ), F(MX,NZ), FCONT(12), DFDZ(81,41), DDFDZ(81,41), HCON    3
     1(12,81)                                                           CON    4
C     CARRIAGE CONTROL                                                  CON    5
      WRITE (6,240)                                                     CON    6
C     DOUBLE PRECISION CONSTANTS                                        CON    7
      D0=0.0D0                                                          CON    8
      D1=1.0D0                                                          CON    9
      D2=2.0D0                                                          CON   10
      D3=3.0D0                                                          CON   11
      D4=4.0D0                                                          CON   12
      D5=5.0D0                                                          CON   13
C     COMPUTE DELIMITERS                                                CON   14
      M31=M3-1                                                          CON   15
      M41=M4+1                                                          CON   16
      N1=NZ-1                                                           CON   17
      N11=N1-1                                                          CON   18
C     COMPUTE 1ST AND 2ND DERIVATIVES OF F WITH RESPECT TO Z            CON   19
      DO 10 I=1,MX                                                      CON   20
      DO 10 J=3,N11                                                     CON   21
      DFDZ(I,J)=(F(I,J+1)-F(I,J-1))/(D2*DZ)                             CON   22
   10 DDFDZ(I,J)=(F(I,J+1)-D2*F(I,J)+F(I,J-1))/(DZ*DZ)                  CON   23
C     DERIVATIVES AT UPPER AND LOWER BOUNDARIES OF OBSTACLE             CON   24
      DO 20 I=M3,M4                                                     CON   25
C     BACKWARD DIFFERENCE AT LOWER BOUNDARY, J=N3                       CON   26
      DFDZ(I,N3)=(D3*F(I,N3)-D4*F(I,N3-1)+F(I,N3-2))/(D2*DZ)            CON   27
      DDFDZ(I,N3)=(-F(I,N3-3)+D4*F(I,N3-2)-D5*F(I,N3-1)+D2*F(I,N3))/(DZ*CON   28
     1DZ)                                                               CON   29
C     FORWARD DIFFERENCE AT UPPER BOUNDARY, J=N4                        CON   30
      DFDZ(I,N4)=(-D3*F(I,N4)+D4*F(I,N4+1)-F(I,N4+2))/(D2*DZ)           CON   31
   20 DDFDZ(I,N4)=(-F(I,N4+3)+D4*F(I,N4+2)-D5*F(I,N4+1)+D2*F(I,N4))/(DZ*CON   32
     1DZ)                                                               CON   33
C     COMPUTATION OF THE VALUES OF F FOR WHICH THE CONTOUR ELEVATIONS   CON   34
C     ARE TO BE DETERMINED                                              CON   35
      KZ=2*MESH+2                                                       CON   36
```

```
C       K3=CENTER LINE AND LOWER BOUNDARY OF OBSTACLE                          CON  37
        K3=KZ/2                                                                CON  38
C       K4=CENTER LINE AND UPPER BOUNDARY OF OBSTACLE                          CON  39
        K4=K3+1                                                                CON  40
        DO 30 K=1,K3                                                           CON  41
   30   FCONT(K)=FAV+DF*(K3-K)                                                 CON  42
        DO 40 K=K4,KZ                                                          CON  43
   40   FCONT(K)=FAV+DF*(K4-K)                                                 CON  44
C       EVALUATION OF THE CONTOUR ELEVATION OF F(I,J)=FCONT(K) FOR             CON  45
C       K=1,KZ AND I=1,MX.                                                     CON  46
C                                                                              CON  47
        DO 50 I=1,M31                                                          CON  48
        H(K3,I)=D0                                                             CON  49
   50   H(K4,I)=D0                                                             CON  50
        DO 60 I=M3,M4                                                          CON  51
        H(K3,I)=Z(N3)                                                          CON  52
   60   H(K4,I)=Z(N4)                                                          CON  53
        DO 70 I=M41,MX                                                         CON  54
        H(K3,I)=D0                                                             CON  55
   70   H(K4,I)=D0                                                             CON  56
C                                                                              CON  57
        DO 220 K=1,KZ                                                          CON  58
        IF (K.EQ.K3.OR.K.EQ.K4) GO TO 220                                      CON  59
        DO 220 I=1,MX                                                          CON  60
        DO 80 J=2,N1                                                           CON  61
        IF (F(I,J).GE.FCONT(K)) GO TO 80                                       CON  62
        GO TO 90                                                               CON  63
   80   CONTINUE                                                               CON  64
   90   J=J-1                                                                  CON  65
        IF (F(I,J).NE.FCONT(K)) GO TO 100                                      CON  66
        H(K,I)=Z(J)                                                            CON  67
        GO TO 220                                                              CON  68
C       TO AVOID USING THE DERIVATIVES AT J=2, SPECIAL TREATMENT IS GIVEN      CON  69
C       TO THIS CASE.                                                          CON  70
```

```
  100 IF (J.EQ.2) GO TO 190                                                    CON  71
      DISCR=DFDZ(I,J)**2-D2*DDFDZ(I,J)*(F(I,J)-FCONT(K))                       CON  72
      IF (DISCR.GE.D0) GO TO 110                                               CON  73
      WRITE (6,250) I,J,K,FAV                                                  CON  74
      WRITE (6,260) FCONT(K),F(I,J),DFDZ(I,J),DDFDZ(I,J),DISCR                 CON  75
      GO TO 230                                                                CON  76
  110 IF (DABS(DDFDZ(I,J)).GE.1.0D-7) GO TO 120                                CON  77
      H(K,I)=Z(J)+(FCONT(K)-F(I,J))/DFDZ(I,J)                                  CON  78
      GO TO 220                                                                CON  79
  120 ROOT1=(D1/DDFDZ(I,J))*(-DFDZ(I,J)+DSQRT(DISCR))                          CON  80
      ROOT2=(D1/DDFDZ(I,J))*(-DFDZ(I,J)-DSQRT(DISCR))                          CON  81
C     DETERMINE WHICH ROOT MAKES PHYSICAL SENSE.                               CON  82
      CHEK1=1.0D3                                                              CON  83
      CHEK2=1.0D3                                                              CON  84
      IF (ROOT1.GE.D0.AND.ROOT1.LT.DZ) CHEK1=ROOT1                             CON  85
      IF (ROOT2.GE.D0.AND.ROOT2.LT.DZ) CHEK2=ROOT2                             CON  86
  130 IF (CHEK1.EQ.ROOT1.AND.CHEK2.EQ.ROOT2) GO TO 140                         CON  87
      GO TO 150                                                                CON  88
  140 IF (ROOT1.NE.ROOT2) GO TO 160                                            CON  89
      GO TO 170                                                                CON  90
  150 IF (CHEK1.EQ.ROOT1.AND.CHEK2.EQ.1.0D3) GO TO 170                         CON  91
      IF (CHEK1.EQ.1.0D3.AND.CHEK2.EQ.ROOT2) GO TO 180                         CON  92
  160 WRITE (6,270)                                                            CON  93
      WRITE (6,280) I,J,K,FAV                                                  CON  94
      WRITE (6,290) ROOT1,ROOT2                                                CON  95
  170 H(K,I)=Z(J)+ROOT1                                                        CON  96
      GO TO 220                                                                CON  97
  180 H(K,I)=Z(J)+ROOT2                                                        CON  98
      GO TO 220                                                                CON  99
  190 J=3                                                                      CON 100
      DISCR=DFDZ(I,J)**2-D2*DDFDZ(I,J)*(F(I,J)-FCONT(K))                       CON 101
      IF (DISCR.GE.D0) GO TO 200                                               CON 102
      WRITE (6,250) I,J,K,FAV                                                  CON 103
      WRITE (6,260) FCONT(K),F(I,J),DFDZ(I,J),DDFDZ(I,J),DISCR                 CON 104
      GO TO 230                                                                CON 105
  200 IF (DABS(DDFDZ(I,J)).GE.1.0D-7) GO TO 210                                CON 106
      H(K,I)=Z(J)+(FCONT(K)-F(I,J))/DFDZ(I,J)                                  CON 107
      GO TO 220                                                                CON 108
```

```
  210 ROOT1=(D1/DDFDZ(I,J))*(-DFDZ(I,J)+DSQRT(DISCR))                    CON 109
      ROOT2=(D1/DDFDZ(I,J))*(-DFDZ(I,J)-DSQRT(DISCR))                    CON 110
C     DETERMINE WHICH ROOT MAKES PHYSICAL SENSE                          CON 111
      CHEK1=1.0D3                                                        CON 112
      CHEK2=1.0D3                                                        CON 113
      IF (ROOT1.LE.D0.AND.DABS(ROOT1).LT.DZ) CHEK1=ROOT1                 CON 114
      IF (ROOT2.LE.D0.AND.DABS(ROOT2).LT.DZ) CHEK2=ROOT2                 CON 115
      GO TO 130                                                          CON 116
  220 CONTINUE                                                           CON 117
  230 RETURN                                                             CON 118
C                                                                        CON 119
  240 FORMAT (1H1)                                                       CON 120
  250 FORMAT ('0DISCRIMINANT IN SUBROUTINE CONTUR LESS THAN ZERO FOR I='CON 121
     1,I3,', J=',I3,', AND K=',I3,' WITH FAV=',F7.4)                     CON 122
  260 FORMAT ('0FCONT=',F7.4,'  F=',F7.4,'  DFDZ=',F8.4,'  DDFDZ=',F8.4,CON 123
     1'  DISCR=',F7.2)                                                   CON 124
  270 FORMAT ('0IN SUBROUTINE CONTUR, ROOT1 AND ROOT2 ARE BOTH PHYSICALLCON 125
     1Y POSSIBLE SOLUTIONS WHEN...')                                     CON 126
  280 FORMAT ('0I=',I3,', J=',I3,', AND K=',I3,' WITH FAV=',F7.4)        CON 127
  290 FORMAT ('0ROOT1=',F7.5,'  ROOT2=',F7.5,'  ....,SO BEWARE!')        CON 128
      END                                                                CON 129-
```

```
      FUNCTION ARCTNH (Y)                                          ATH    1
      IMPLICIT REAL*8(A-H,O-Z)                                     ATH    2
      ARCTNH=0.0D0                                                 ATH    3
      TERM=0.000                                                   ATH    4
      DO 10 N=1,1000                                               ATH    5
      TERM=TERM+(1.0D0)                                            ATH    6
      ATNH=(Y**(2*N-1))/(2.*TERM-1.0D0)                            ATH    7
      IF (DABS(ATNH).LE.(1.0D-13)) GO TO 20                        ATH    8
      ARCTNH=ARCTNH+ATNH                                           ATH    9
   10 CONTINUE                                                     ATH   10
   20 RETURN                                                       ATH   11
      END                                                          ATH   12-
```

"The aeronautical and space activities of the United States shall be conducted so as to contribute . . . to the expansion of human knowledge of phenomena in the atmosphere and space. The Administration shall provide for the widest practicable and appropriate dissemination of information concerning its activities and the results thereof."

—NATIONAL AERONAUTICS AND SPACE ACT OF 1958

NASA SCIENTIFIC AND TECHNICAL PUBLICATIONS

TECHNICAL REPORTS: Scientific and technical information considered important, complete, and a lasting contribution to existing knowledge.

TECHNICAL NOTES: Information less broad in scope but nevertheless of importance as a contribution to existing knowledge.

TECHNICAL MEMORANDUMS: Information receiving limited distribution because of preliminary data, security classification, or other reasons. Also includes conference proceedings with either limited or unlimited distribution.

CONTRACTOR REPORTS: Scientific and technical information generated under a NASA contract or grant and considered an important contribution to existing knowledge.

TECHNICAL TRANSLATIONS: Information published in a foreign language considered to merit NASA distribution in English.

SPECIAL PUBLICATIONS: Information derived from or of value to NASA activities. Publications include final reports of major projects, monographs, data compilations, handbooks, sourcebooks, and special bibliographies.

TECHNOLOGY UTILIZATION PUBLICATIONS: Information on technology used by NASA that may be of particular interest in commercial and other non-aerospace applications. Publications include Tech Briefs, Technology Utilization Reports and Technology Surveys.

Details on the availability of these publications may be obtained from:

SCIENTIFIC AND TECHNICAL INFORMATION OFFICE

NATIONAL AERONAUTICS AND SPACE ADMINISTRATION

Washington, D.C. 20546